

**New pH Sensitive Sensor Materials. Luminescent Fiber-
Optic Dual Sensors for Non-Invasive and Simultaneous
Measurement of pH and pO₂ (Dissolved Oxygen) in
Biological Systems.**

DISSERTATION ZUR ERLANGUNG DES
DOKTORGRADES DER NATURWISSENSCHAFTEN

(Dr. rer. nat)

DER FAKULTÄT CHEMIE UND PHARMAZIE
DER UNIVERSITÄT REGENSBURG



vorgelegt von

Anna S. Kocincová

(geb. Vasylevska)

aus Odessa (Ukraine)

Mai 2007

Diese Doktorarbeit entstand in der Zeit von Februar 2004 bis Mai 2007 am Institut für Analytische Chemie, Chemo- und Biosensorik an der Universität Regensburg.

Die Arbeit wurde angeleitet von Prof. Dr. Otto S. Wolfbeis.

Promotionsgesuch eingereicht am 23.04.2007

Kolloquiumstermin: 21.05.2007

Prüfungsausschuß:	Vorsitzender:	Prof. Dr. B. Dick
	Erstgutachter:	Prof. Dr. O. S. Wolfbeis
	Zweitgutachter:	Prof. Dr. D. Belder
	Drittprüfer:	Prof. Dr. A. Göpferich

Danksagung

Mein erster Dank gilt **Prof. Dr. Wolfbeis** für die Vergabe der interessanten Themen, für sein Interesse am Fortgang dieser Arbeit, sowie für die sehr guten Arbeitsbedingungen am Lehrstuhl.

Ein besonderes Dankeschön geht an **Dr. Christian Krause** (PreSens Precision GmbH), der mir unermüdlich die Grundlagen der optischen Sensorik beibrachte und für die problemlose Bereitstellung von Chemikalien und Messgeräten. Danke auch trotz seiner knapp bemessenen Zeit für die zahlreichen Diskussionen über meine angehäuften Schwierigkeiten.

Ein weiteres großes Dankeschön geht an **Dr. Alexander Karasyov** (Active Motif Chromeon GmbH), der immer ein kompetenter Ansprechpartner für alle Fragen zur Synthese von optischen pH-Sensoren war. Ich bedanke mich auch für die Hilfe an meinen ersten Tagen in Deutschland und für die Diskussionen fernab der Chemie.

Dr. Sergey Borisov (Technische Universität Graz) möchte ich für sein Interesse an meiner Arbeit danken, der immer Zeit für meine häufigen Nachfragen zur optischen Sensorik hatte und gern versuchte, zu schwierigen Situationen die Lösung zu finden. Ich bedanke mich auch für die lustige Zusammenarbeit und für seinen Trost bei bisweilen misslungenen Experimenten.

Ganz herzlich möchte ich **Dr. Sarina Arain** (PreSens Precision GmbH) danken für die Ermöglichung der Bakterienversuche und den Umgang mit dem SDR. Außerdem danke ich Sarina und **Dr. Claudia Schröder** für die sehr sehr schöne gemeinsame Laborzeit und für die ständige Hilfe im Alltag.

Weiterhin bedanke ich mich ganz herzlich bei den derzeitigen Mitgliedern unseres Institutes, insbesondere **Matthias Stich, Doris Burger, Petra Suchomel, Martin Link, Christian Spangler, Corinna Spangler, Gisela Hierlmeier, Stefan Nagl und Dr. Michael Schäferling** für die wissenschaftlichen und nichtwissenschaftlichen Diskussionen und die sehr gute Atmosphäre am Lehrstuhl.

Ein herzlicher Dank geht an die gute Seele des Lehrstuhls, **Edeltraud Schmid**, die mit ihrem unermüdlichen Einsatz den Lehrstuhl mit stets guter Laune und großartigem Organisationstalent am Laufen hält.

Dem Bundesministerium für Bildung und Forschung (BMBF) danke ich für die finanzielle Unterstützung während dieser Arbeit.

Abschließend möchte ich mich bei meiner Familie bedanken:

Besonderen Dank an meine Eltern **Sergej** und **Praskovja Vasilevskie** und Schwester **Natalia** für den Glauben an mich und ferne Unterstützung in schlechten und guten Zeiten. (Особая благодарность моим родителям Сергею и Прасковьи Василевским, а также моей сестре Наталии за веру в мои силы и моральную поддержку не только в лучшие, но и в трудные времена).

Und ganz besonders herzlich möchte ich mich bei meinem Mann **Mgr. LLM Jaroslav Kocinec** bedanken, der mir immer Ruhe und Kraft gegeben hat. „Zu zweit war und ist alles immer halb so schwer und doppelt so schön.“

Table of Contents

CHAPTER 1

Progress in Microsensing of pH and pO₂.....1

1.1 Motivation.....1

1.2 State of the Art of Optical Sensing of pH, pO₂, and of Dual pH/pO₂ Sensing.....3

1.2.1 pH Sensors.....3

1.2.2 pO₂ Sensors.....4

1.2.3 pH/pO₂ Dual Sensors.....6

1.2.4 pH/pO₂ Dual Microsensors.....7

1.3 Referencing Methods for Measurements of Luminescent Optical Sensors.....8

1.3.1 Referencing via Ratiometric Measurements.....8

1.3.2 The Frequency Domain Dual Lifetime Referencing (DLR) and Modified Dual Lifetime Referencing (m-DLR).....10

1.4 References.....15

CHAPTER 2

Novel Coumarin-Based Fluorescent pH Indicators, Probes and Membranes Covering a Broad pH Range.....28

2.1 Introduction.....28

2.2 Experimental.....30

2.2.1 Materials.....30

2.2.2 Synthesis.....30

2.2.3 Preparation of the pH-Sensitive Sensor Beads and Sensor Membranes.....32

2.2.4 Preparation of the Ratiometric Sensing Material.....35

2.2.5 Preparation of the Mixed-Indicator pH Sensitive Sensor

Membrane.....	35
2.2.6 Instruments and Measurements.....	35
2.3 Results and Discussion.....	37
2.3.1 Spectral Properties of the pH Indicators in Solution.....	37
2.3.2 Photostability of the pH Indicators.....	42
2.3.3 pH-Sensitive Membranes	43
2.4 Conclusion.....	47
2.5 References.....	48
 CHAPTER 3	
Dual Lifetime Referenced Sensor Membranes for Fiber Optic Determination of pH Using Microbeads and Nanoparticles.....	54
3.1 Introduction.....	54
3.2 Material and Methods.....	56
3.2.1 Chemicals.....	56
3.2.2 Apparatus.....	56
3.2.3 Buffer Preparation.....	57
3.2.4 Covalent Immobilization of the Indicators on Polymer Beads.....	58
3.2.5 Membrane Preparation.....	58
3.2.6. Dual Lifetime Referencing Frequency-Domain (DLR) Method.....	59
3.3 Results and Discussion.....	60
3.3.1 Choice of Materials.....	60
3.3.2 Sensor Characteristics.....	61
3.3.3. DLR-Referenced pH Membranes.....	64
3.4 Conclusion.....	69
3.5 References.....	70

CHAPTER 4

Indicator-Loaded Permeation-Selective Microbeads for Use in Fiber Optic Simultaneous Sensing of pH and Dissolved Oxygen.....73

4.1 Introduction.....	73
4.2 Experimental.....	75
4.2.1 Materials and Reagents.....	75
4.2.2 pH Meter.....	76
4.2.3 Buffer Preparation.....	76
4.2.4 Preparation of Sensor Beads and Sensor Membranes.....	77
4.2.4.1 <i>Preparation of the Oxygen-Sensitive Microbeads SB-1 and the Sensor Membrane SM-1.....</i>	78
4.2.4.2 <i>Preparation of the Oxygen-Sensitive Microbeads SB-2 and SB-3 and the Sensor Membranes SM-2 and SM-3.....</i>	78
4.2.4.3 <i>Preparation of the pH-Sensitive Microbeads SB-4 and SB-5 and the Sensor Membranes SM-4 and SM-5.....</i>	79
4.2.4.4 <i>Preparation of Dually Sensing Materials DS-1, DS-2 and DS-3.....</i>	79
4.2.5 Measurements.....	80
4.3 Results and Discussion.....	81
4.3.1 Choice of Materials.....	81
4.3.2 Response of the pH Sensor Materials SM-4 and SM-5.....	85
4.3.3 Response of the Oxygen Sensor Membranes.....	89
4.3.3.1 <i>Oxygen-Sensitive Probe SM-1.....</i>	89
4.3.3.2 <i>Oxygen-Sensitive Probe SM-2.....</i>	91
4.3.3.3 <i>Oxygen-Sensitive Probe SM-3.....</i>	93
4.3.4 Response of the Dual Sensor in the Intensity Mode.....	95
4.3.5 Response of the Dual Sensor to pH in the Frequency Domain.....	99
4.3.6 Response of the Dual Sensor to Oxygen in the Frequency Domain.....	101
4.3.7 Sensor Homogeneity.....	102
4.3.8 Validation.....	103
4.4 Conclusion.....	104
4.5 References.....	105

CHAPTER 5

Fiber Optic Microsensor for Simultaneous Sensing of Oxygen and pH..... 110

5.1 Introduction..... 110

5.2 Experimental..... 112

5.2.1 Materials..... 112

5.2.2 Preparation of the Microsensor..... 112

5.2.3 Components of the Optical System for Dual Sensing of O₂/pH..... 113

5.2.4 Response Curve..... 114

5.2.5 Experimental Data Fitting..... 114

5.3 Results and Discussion..... 114

5.3.1 Choice of Materials..... 114

5.3.2 Spectroscopy and Optoelectronic System..... 116

5.3.3 Response of the Sensor..... 117

5.3.4 Response Times..... 120

5.3.5 Photostability..... 120

5.3.6 Validation..... 121

5.4 Conclusion..... 122

5.5 References..... 122

CHAPTER 6

Simultaneous Non-invasive Monitoring of Dissolved Oxygen and pH During Bacterial Growth in 24-well Microplates..... 126

6.1 Introduction..... 126

6.2 Experimental..... 128

6.2.1 Preparation of the Dually-Sensing Material..... 128

6.2.2 Instrumentation..... 129

6.2.3 Calibration of the Dual Sensor..... 130

6.2.4 Bacterial Cultivation – Preculture and Growth Experiments..... 131

6.3 Results and Discussion.....	132
6.3.1 Calibration of Dual Sensor Membrane at 25 °C and at 37 °C.....	132
6.3.2 Calibration Function for Oxygen.....	135
6.3.3 Bacteria Fermentation in Microbioreactors.....	136
6.4 Conclusion.....	138
6.5 References.....	139
 CHAPTER 7	
Summary.....	142
 CHAPTER 8	
Zusammenfassung.....	144
 CHAPTER 9	
Abbreviations, Acronyms and Symbols.....	146
 CHAPTER 10	
Curriculum Vitae.....	148
 CHAPTER 11	
List of Publications.....	150

Chapter 1

Progress in Microsensing of pH and pO₂

1.1 Motivation

pH (latin: *pondus hydrogenii*) and pO₂ (oxygen partial pressure) are often determined analytical parameters in research and industry. The monitoring of pH and pO₂ as quality parameters is used in clinical diagnostics of blood (blood gas analysis)¹⁻³, body fluids⁴⁻¹¹ and respiration activity¹² for assessing the status of critical patients. In the food industry a control of pH and pO₂ is needed as indication of the quality of drinking water^{13,14}, the freshness of food¹⁵⁻¹⁹ and the sterility of food and beverage²⁰⁻²². Knowing pH and oxygen concentration is also essential in seawater analysis^{23,24} and in marine research²⁵⁻²⁷.

Additionally, pH is one important control factor in industrial waste water treatment and acidity of rain²⁸⁻³¹. Furthermore, oxygen and pH are two important parameters in biotechnology for process control in bioreactors during fermentation of microorganisms³²⁻³⁷. Although optical sensing of dissolved oxygen³⁸⁻⁴² and pH^{38,43} in microplates has recently been demonstrated, no realistic system for simultaneous monitoring of both parameters was proposed so far. Several systems do allow for simultaneous measurements of dissolved oxygen and pH in a single microbioreactor, but can hardly be applied to high-throughput bioprocessing due to the complicity of the microbioreactor, sensing element or detection system^{44,45}.

Electrochemical sensors are the established tools for pH and oxygen measurements. However, glass electrodes are limited to single-point measurements and are not suitable for obtaining information on pH distribution. Moreover, electrodes are bulky and invasive, and potentially create the risk of electric shock during *in vivo* measurements.

Optical sensors offer a promising alternative. The chemical, physical, mechanical and optical properties of the sensor can be varied by the combination of indicator and polymer^{46,47}. The varying of analyte concentration results in change of spectral properties of indicators. Absorbance, reflectance or luminescence is parameters usually used for optical analyte determination. Most optical luminescent sensors and probes usually use either luminescence intensity^{27,48-50} or luminescence decay time⁵¹⁻⁵⁶ as the analytical information.

Simultaneous and continuous detection of two or more parameters is also a field of growing interest in chemical optical sensor development. Optical dual sensors have weighty advantages in contrast to single sensors since they:

1. enable simultaneous monitoring of two parameters at one point (very important for the highly spatial resolution measurement in tissue and isolated organs);
2. make possible the improvement of precision of measurements due to temperature compensation in a sensor layer (in case of dual sensors pH/T, CO₂/T etc.);
3. allow for reduction of measurement errors (e. g. gradient of temperature);
4. provide smaller influence on measurement systems due to reduced number of sensors;
5. make possible straightforward miniaturization of the sensor due to reduced number of sensors, the analytes sensitive “cocktail” being fixed on the tip of an optic fiber (diameter of one fiber-optic microsensor is 140 μm or even lower (~ 40 μm) for the pulled fibers).

The aim of this work was to synthesize and characterize new luminescent probes suitable for preparation of pH sensors for various ranges of pH. For optimization of sensor properties different polymers supports were used onto which the indicators were immobilized. In addition to development and characterization of single optical sensors, this work presents the development of planar sensors and microsensor for non-invasive simultaneous monitoring of two parameters (pH and pO₂). The dual sensor was successfully applied for the simultaneous measurement of pH and pO₂ in fermentation processes of bacteria *Pseudomonas Putida* and *E. Coli* in microbioreactors.

1.2 State of the Art of Optical Sensing of pH, pO₂, and of Dual pH/pO₂ Sensing

1.2.1 pH Sensors

The increased interest in development of optical sensors was observed in the last two decades. This is strongly connected with progress of optical technology. For the selective analyte recognition and signal transduction optical sensors comprise development of the fibers, detection systems (photodiodes, CCD-chips, photomultiplier tubes) and light sources (lasers, lamps and light emitting diodes). In the case of optical pH sensors the indicator is absorbed, immobilized or entrapped in polymer matrix which can be used then in various formats including planar sensor spots⁵⁷ or fiber-optic sensors⁵⁸. The first type of single pH sensor developed in the 70s years was a pH test stripe based on the absorption of pH indicator covalently immobilized on the cellulose matrix. In 1980 Peterson⁵⁹ presented the first optical pH sensor. The sensor made use of the absorbance dye phenol red and was applied for evaluation of blood pH in-vivo and in-vitro. The dye was immobilized into polystyrene microspheres. Lately mostly used absorbance-based pH indicators were phenol red, bromothymol blue and other⁶⁰⁻⁶⁴. In 1982 Saari⁶⁵ reported the first fluorescence-based pH sensor where fluoresceinamin was covalently immobilized on cellulose.

The most frequently used pH indicators are 8-hydroxypyrene-1,3,6-trisulfonic acid sodium salt (HPTS), carboxyfluorescein derivatives (e.g. mono-, dichlorocarboxyfluorescein), seminaaphthorhodafluor (SNARF) and hydroxycoumarins⁶⁶⁻⁷⁰. The important criteria for the choice of pH indicator for preparation of optical pH sensing material are 1) excitation in the range between 405 and 550 nm; 2) emission of indicator in the range from 550 to 700 nm; 3) large Stokes shift; 4) pK_a value, suitable for a particular application; 5) high quantum yield; 6) high photostability and 7) no cross-sensitivity to ionic strength (IS). Existing pH indicators can not meet all of these criteria; for example, carboxyfluorescein has only moderate photostability, the pK_a value of HPTS is strongly dependent on ionic strength of sensing solution, and most coumarins are excitable in the range from 300 to 400 nm. Against all the odds a majority of optical pH sensors are based on fluorescence, because of high sensitivity of the resulting sensor and relative simple instrumental set-up.

The properties of polymer matrix have strong influence on the characteristics of the pH optical sensor. To minimize the effect of ionic strength on the pK_a value of indicator

Wolfbeis and Offenbacher⁷¹ presented a pH sensor based on a single indicator with different surface chemistry. In a first sensor type, the indicator is embedded in an uncharged micro-environment. This sensor is highly sensitive to changes in ionic strength. In a second sensor type, the indicator is placed in a highly charged environment. This sensor is less sensitive towards changes of ionic strength. Other polymer matrices include ion-exchangers^{72,73}, hydrophobic plasticized PVC⁷⁴, sol-gels⁷⁵⁻⁷⁷ or hydrogels⁷⁸ and were often used as polymer matrix in optical pH sensors. However, the slow response time is severe disadvantage for majority of these polymers. Moreover, the characteristics of pH sensor based on the plasticized PVC membrane can easily change following a plasticizer leaching from the membrane.

The most widely employed pH sensor polymers are cellulose derivatives and hydrogels because of their excellent mechanical properties, stability at various pH's and temperatures⁷⁹ and high permeability to water, ions and dissolved gases. The polyurethane-based^{80,81} or pHEMA-based hydrogels⁸² are characterized by excellent water uptake (and thus swelling) and good compatibility with biological materials.

1.2.2 pO₂ Sensors

Oxygen is one of the most important chemical species. In many research fields determination of oxygen levels is required. In environmental analysis continuous measurement are essential to monitor oxygen levels continuously in the atmosphere and in the water. In the medical field, oxygen levels in exhaled air or in the blood of a patient are the key physiological parameters. Such parameters should ideally be monitored continuously. The measurement of oxygen is also essential in industries that utilize metabolizing organisms and in biotechnology that utilize plants and microbes for producing drugs such as antibiotics and anticancer drugs. Several methods were used, including those which are based on titration⁸³, amperometry⁸⁴, chemiluminescence⁸⁵ and thermoluminescence⁸⁶. Winkler titration⁸³ has been employed as the standard method for the measurement of oxygen. The development of Clark-type electrodes provided a revolutionary technique for the oxygen control and was used as conventional method. Oxygen measurement using Clark cells is based on reduction of oxygen at the cathode. Therefore, the limited diffusion of oxygen through the film is the factor that can change the diffusion resistance, such as fouling of the film, or a change in flow conditions in the testing fluid, can cause errors. Also electrical interference can affect such cells and if electrodes consume most oxygen they can generate misleading data. Thus, there is a big

interest in the development of new techniques for oxygen detection and the optical oxygen sensors are one of the best alternatives in this area.

Optical oxygen sensors are inexpensive, simple to use and easily miniaturized, do not produce electrical shock or consume oxygen. More recent optical sensors based on quenching of photoluminescence usually measure the luminescence intensity^{87,88} or lifetime⁸⁹ of a metal organic dye immobilized in a polymer film that varies with changing of concentration of the analyte. Also, the relatively long phosphorescence lifetime of the indicator dyes allows for the use of less sophisticated measurements instrumentation.

The properties of sensing films are strongly depended on the properties of polymer matrices. Oxygen permeability, non-polarity for providing mechanically and chemically stable matrix are important requirements for the choice of polymers. Thus, the most useful polymer matrices for preparation of oxygen sensitive membrane that meet these requirements are silicon rubbers⁹⁰, organic glassy polymers (polystyrene, polymethyl methacrylate, polyvinyl chloride)⁹¹⁻⁹³, cellulose derivatives⁹⁴ or fluoropolymers such as polytrifluoroethyl methacrylate⁹⁵. Compared to other organic polymers the silicone rubbers have the highest oxygen permeability, which leads to high quenching efficiency⁹⁶. The indicators, however, tend to aggregate in silicone rubbers, which render this matrixes unsuitable for prolonged use (unless an indicator is immobilized in beads, which are then dispersed in silicone⁹⁷). Sol-gel polymers are viable polymers for preparation of optical oxygen sensors^{98,99}. Modification of these polymers allows for reducing of long response time and prevents leaching indicator from the matrix¹⁰⁰. Organically-modified silica (ormosil) is a typical example¹⁰⁰.

The organometallic compounds are viable probes for oxygen sensing. High quantum yield, long lifetimes, high molar absorbance, photostability, compatibility with low-price excitation light source (LED, laser diode) are important aspects in the choice of indicator. Most widely used oxygen sensitive luminophore can be classified into two categories. One is the polypyridyl complexes of transition metal Ru²⁺ (or Os²⁺, Ir³⁺) with ligands such as 2,2'-bipyridyl, 1,10-phenanthroline or 4,7-diphenyl-1,10-phenanthroline. These complexes possess high quantum yields, relatively long luminescence lifetime under nitrogen saturated conditions (~ μs) and large Stokes shifts of approximately 150 nm, and can be excited in the blue region of the spectrum^{47,101-103}. In general, transition metal polypyridine complexes are ionic dyes and thus are insoluble in organic polymers. They can be incorporated into non-polar sensor polymer matrix in the form of lipophilic ion pair with ions such as 3-(trimethylsilyl)-1-propanesulfonate or tetraphenylborate^{104,105}. The other group includes the metalloporphyrines. Particularly, Pt²⁺ and Pd²⁺ porphyrins are used as oxygen sensitive probes.

The lipophilic complexes of Pt²⁺ and Pd²⁺ with ligands such as octaethylporphyrin¹⁰⁶, octaethylporphyrin ketones^{92,107} or fluorinated porphyrin such as tetrakis(pentafluorophenyl)porphyrin (TFPP)¹⁰⁸ display strong phosphorescence with high quantum yields (0.1 - 0.5) at room temperature, long decay time (40 – 1000 μ s), excellent photostability of sensing materials (in case of TFPP) and possibility to excite the sensor membrane in the near UV and in the visible range of spectrum.

Thus, the right choice of luminophore and polymer as sensor matrix makes possible to tune sensitivity of the oxygen sensors, but also to achieve good compatibility with pH indicators in dual sensors.

1.2.3 pH/pO₂ Dual Sensors

The number and variety of different optical sensors for simultaneous sensing of two or more parameters today is large and growing quickly. Monitoring of multiply analytes is often required in clinical, biological and environmental systems. During the last 20 years some optical multisensors were developed for controlling parameters such as glucose-oxygen¹⁰⁹⁻¹¹¹, glucose-pH¹¹², pH-oxygen^{113,114}, pH-CO₂¹¹⁵, oxygen-CO₂¹¹⁶, oxygen-temperature^{117,118} etc. Most of them found applications in biotechnology by bioprocess control or in medicine (blood analysis). “Multianalyte” sensors comprise either several single-analyte sensors, each with its own detector (array sensors), or a sensor bundle with a single detector employing an elaborate switching procedure to address each sensor in the bundle^{119,120}. The in vivo use such of this sensor bundles is limited because of their large size. Simultaneous measurement of pH, CO₂ and O₂ is also a long-standing goal of industrial – analytical chemists for process control. The assessment of fermentation performance is determined presently by measuring such parameters as temperature, gas composition, pH and optical density¹²¹. The ability of measuring simultaneously and at the same position pH and O₂ would provide better process control and a greater understanding of the chemical dynamics within the reactor. At present, only a very limited number of dual sensor systems can provide such measurement¹²²⁻¹²⁴.

Fiber optic sensors are prepared by immobilizing indicators onto optical fibers¹²⁵ or by immobilizing on a solid support, enveloped by a membrane permeable to gas or ions and attached to the end of an optical fiber³². Two different concepts for the sensor membrane composition have been used. Firstly, double-layer sensor membranes are known, where the sensor chemistry for each of the two analytes is immobilized into separate polymer matrices and both sensor layers are coated with each other¹²⁶. The second type of sensor membrane is a

hybrid membrane where the sensor chemistry of both analytes is immobilized in the same single-layer polymer matrix¹²⁷. The indicators change their optical properties by interacting with specific analytes. Optical oxygen sensing is based on fluorescence quenching by molecular oxygen, while pH sensing is based on the interdependence of optical properties with respect to the equilibrium between the acidic and basic form of a reagent resulting from pH changing in the medium. These, in turn, may be monitored by changes in fluorescence intensity or light absorption.

Due to the nature of a biotechnological process, continuous monitoring is strongly preferred over discontinuous analytical methods. At present, electrodes are mainly being used as sensors for measuring the parameters such as pH and pO₂¹²⁸. One can mention the main advantages of the optrodes make optical sensors a promising alternative compared to most commercially available electrodes: they can be sterilized (autoclaved); they produce no clogging of the membrane with biomass (unlike electrode membranes¹²⁹); then can be used immediately after calibration, whereas the electrodes have to be kept filled with electrolyte solution; they consist of organic polymer layers and therefore are much easier to handle and cheaper than glass electrodes.

1.2.4 pH/pO₂ Dual Microsensors

In biological and environmental samples the measurement of chemical parameters with high spatial resolution becomes more and more of interest. The knowledge of their microscale distribution is of importance to understand the function and regulation in complex living systems. Microsensors (i.e., sensors of < 200 µm diameter) enable an almost non-invasive measurement of the chemical conditions in intact biological systems. They can be placed inside the body using a protective housing such as a steel needle, and still will remain only minimally invasive⁵⁵.

Numerous electrochemical and fiber optic microsensors have been described for the detection of chemical parameters such as glucose¹³⁰⁻¹³², oxygen^{133,134}, sulfide¹³⁵, pH¹³⁶⁻¹³⁸, nitrate^{139,140} or nitrous oxide¹⁴¹. A disadvantage that limits a more frequent use of microelectrodes is their time-consuming fabrication and high cost. In contrast, are simple to design and therefore offer an interesting alternative for chemical sensing with high spatial resolution.

Optical microsensors – also referred to as micro-optodes – were recently introduced in the field of biotechnology and aquatic biology and are much easier to fabricate than micro-

electrodes¹⁴². Important biological phenomena, including calcium regulation¹⁴³, chemotaxis¹⁴⁴, neuronal activity¹⁴⁵, and cell growth and division^{146,147}, and tissue oxygenation^{148,149} are highly dependent on such parameters as pH, oxygen and temperature. The optode technique offers a way for simultaneous determination of various relevant chemical and physical parameters with a single microsensor. The development of suitable microsensors for simultaneous monitoring of more than one parameter is difficult. Ji et al.¹⁵⁰ have introduced a fiber-optic microsensor for intracellular pH and [Ca²⁺] measurement. The sensing chemistry was immobilized to the distal end of optical fibers with a core size of 50 μm . The concentration of the Ca²⁺ and pH in a sample solution are determined by spectral processing of the fluorescence sensing signals. Also the dual microoptodes for determination of dissolved oxygen and temperature was described⁵⁵. This sensor found application in aquatic microbiology since. The sensor chemistry is deposited onto the tip of a tapered optical fiber.

1.3 Referencing Methods for Measurements of Luminescent Optical Sensors

Ratiometric (dual-wavelength) measurements are a preferable method compared to single-intensity based measurements, since the ratio of fluorescence intensities at two wavelengths is independent on the total concentration of the dye, photobleaching, fluctuations of the light source intensity or the detector sensitivity.

1.3.1 Referencing via Ratiometric Measurements

If two forms of pH indicators in basic and acidic conditions are fluorescent, the ratio of emission intensities of these forms can be used as an analytical signal. The most popular fluorescent ratiometric pH indicators are 8-hydroxypyrene-1,3,6-trisulfonate (HPTS), fluorescein derivatives (carboxyfluorescein, carboxynaphthofluorescein and etc.), SNARF and SNAFL. Three different methods for ratiometric measurements depending on the spectral characteristics of the indicator are possible:

- single emission and dual excitation wavelength;
- single excitation and dual emission wavelength (this principle was used for pH indicator described in Chapter 2 and is shown in Fig. 1.1);
- and dual excitation and dual emission wavelength.

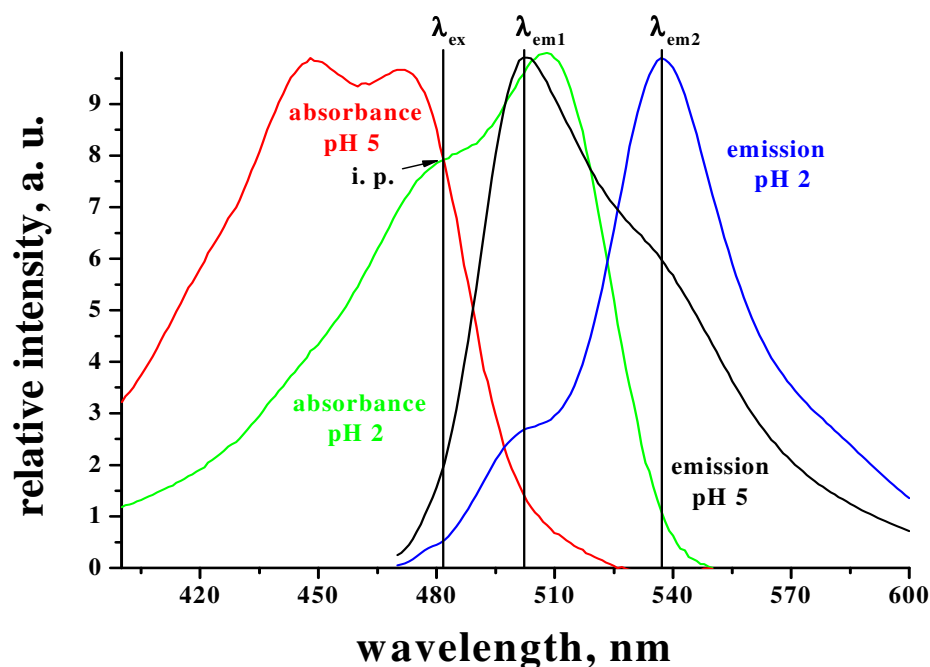


Figure 1.1 A typical example of ratiometric approach where excitation is preformed at isosbestic point (i. p.) and dual emission is monitored at two different wavelengths.

If only one form (protonated or deprotonated) of a pH indicator is fluorescent, a reference (pH independent dye) for ratiometric measurements can be used. This for both dyes alternatively, composition, however, requires overlapping emission spectra, but different excitation bands or overlapping excitation and different emission bands, in order to achieve efficient separation of the emission or excitation intensities (Fig. 1.2). In Chapter 4 the systems excitable with one light source, but having dual emission are described.

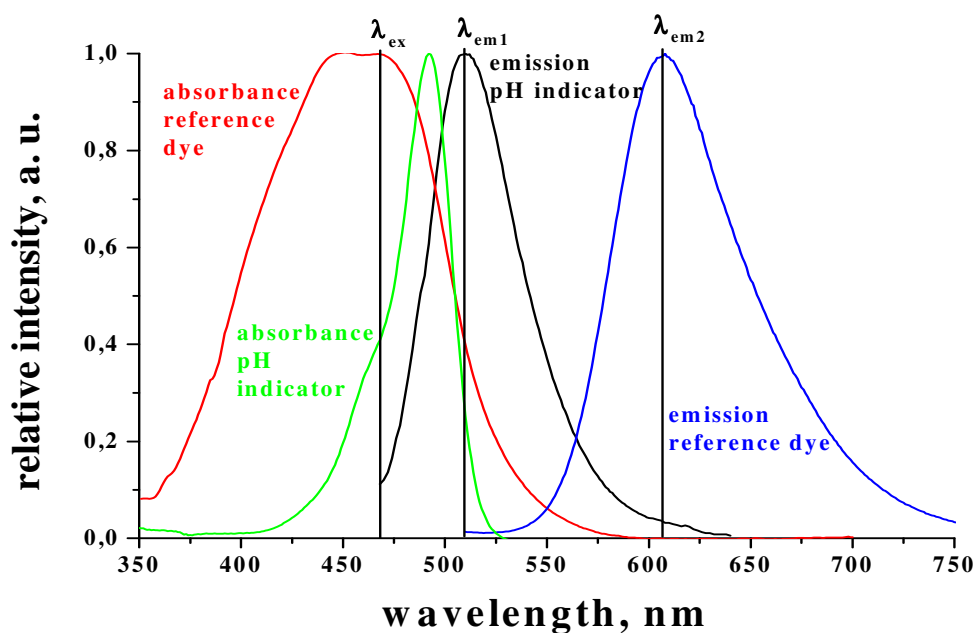


Figure 1.2 A typical example of ratiometric approach in which excitation of indicator/reference dye system is performed at a single wavelength and emission of both is monitored at two different wavelengths.

1.3.2 The Frequency Domain Dual Lifetime Referencing (DLR) and Modified Dual Lifetime Referencing (m-DLR)

The frequency domain method¹⁵¹ is a technique that allows precise determination of decay time with unsophisticated equipment that is easy to miniaturize. In the frequency domain method an indicator is excited by sinusoidally modulated light. Depending on its decay time, the luminescence of the indicator has the same waveform but is phase-shifted at a given frequency f . The decay time (τ) can be determined via the phase shift Φ according to:

$$\tau = \frac{\tan \Phi}{2 \cdot \pi \cdot f_{\text{mod}}} \quad (1.1)$$

where f_{mod} is the modulation frequency of the excitation light and τ is the luminescent decay time defined as the average time the molecule remains in the excited state before it returns to the ground state.

Phase modulation technique is most often employed for determination of relatively long decay times (in the order of micro- and milliseconds, which is a case for certain luminescent probe). Unfortunately, the equipment becomes more complicated, bulky, and

costly for determination of short decay times (in the order of nanoseconds) which is typical for most indicators for which a high-frequency (MHz range) modulation is a must.

In the dual lifetime referencing (DLR) technique^{152,153} the fluorescence of an indicator is referenced against the long-lived luminescence of a standard and thus is converted into phase shift information. In this scheme it is mandatory that the absorption and emission spectra of both indicators overlap in order to allow (1) simultaneous excitation with one light source, and (2) simultaneous detection of luminescence. The reference dye is usually immobilized in nanobeads of a gas-impermeable polymer such as polyacrylonitrile (PAN)¹⁵⁴ to avoid quenching by oxygen. The modulation frequency of the excitation light is adapted to the lifetime of the long-lived reference. As a result, the fluorescence signal of the short-lived indicator follows the modulated excitation light without phase delay, while the modulated reference luminescence displays a phase-shift and at the same time undergoes demodulation (i.e., decrease of the emission amplitude)^{155,156}, which increases at higher modulation frequencies.

The phase shift Φ_m of the overall luminescence depends only on the ratio of intensities of the reference luminophore and the indicator dye (Fig. 1.3). The reference luminophore gives a constant background signal (ref), and the fluorescence signal of the indicator (ind) depends on the analyte concentration. This results in high amplitude in its unquenched state (case A) and low amplitude if is quenched by analyte (case B). Therefore, the overall phase shift Φ_m directly reflects the intensity of the indicator dye and, consequently, the analyte concentration. The modulation frequency is adjusted to the decay time of the reference dye with its long decay time.

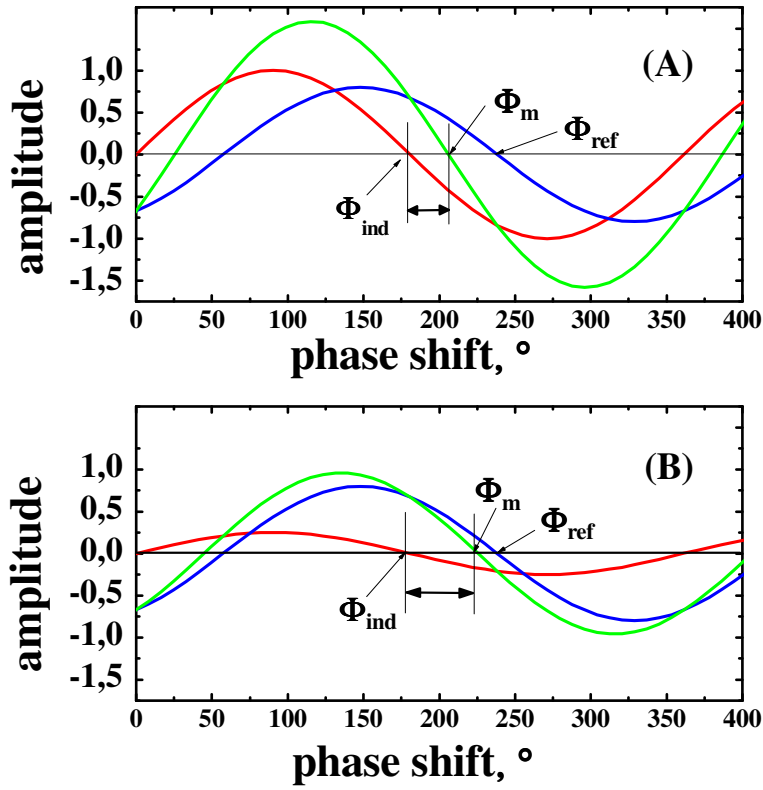


Figure 1.3 The DLR schema. Phase shift of the overall luminescence (Φ_m), the reference (Φ_{ref}), and the indicator (Φ_{ind}). (A) fluorescence of indicator in its unquenched state, (B) fluorescence of the indicator in the quenched state.

Equation 1.2 results in a linear relation between phase angle Φ_m and the ratio of A_{ind}/A_{ref} , because the phase angle of the reference luminophore Φ_{ref} was assumed to be constant. Therefore, the phase angle of the overall signal can be taken as a referenced measure for the pH-dependent amplitude of the indicator.

$$\cot \Phi_m = \cot \Phi_{ref} + \frac{1}{\sin \Phi_{ref}} \cdot \frac{A_{ind}}{A_{ref}} \quad (1.2)$$

The response functions for the DLR-based sensors are frequency dependent, i.e., the dependence of the phase shift Φ on analyte concentration $[A]$ is represented by a different function if the modulation frequency f is changed ($\Phi = F_1([A])$ at f_1 and $\Phi = F_2([A])$ at f_2). This can be used for designing dual sensors, i.e., sensors capable of simultaneous detection of two analytes.

When applying the DLR technique to dual sensing, the long-lived luminescent (e.g., oxygen) indicator also acts as a reference for a short-lived fluorescent (e.g., pH indicator) so that the observed phase shift depends on the concentration of both analytes: $\Phi = F_1([A_1], [A_2])$ at f_l . The method is referred to as a “modified dual lifetime referencing method” (m-DLR). Obviously, it is not possible to separate the information about the concentration of the analytes if the measurement is performed at one frequency. However, if calibration is performed at two frequencies (which are close to the optimal modulation frequency of a long-lived indicator), unambiguous signal separation becomes possible.

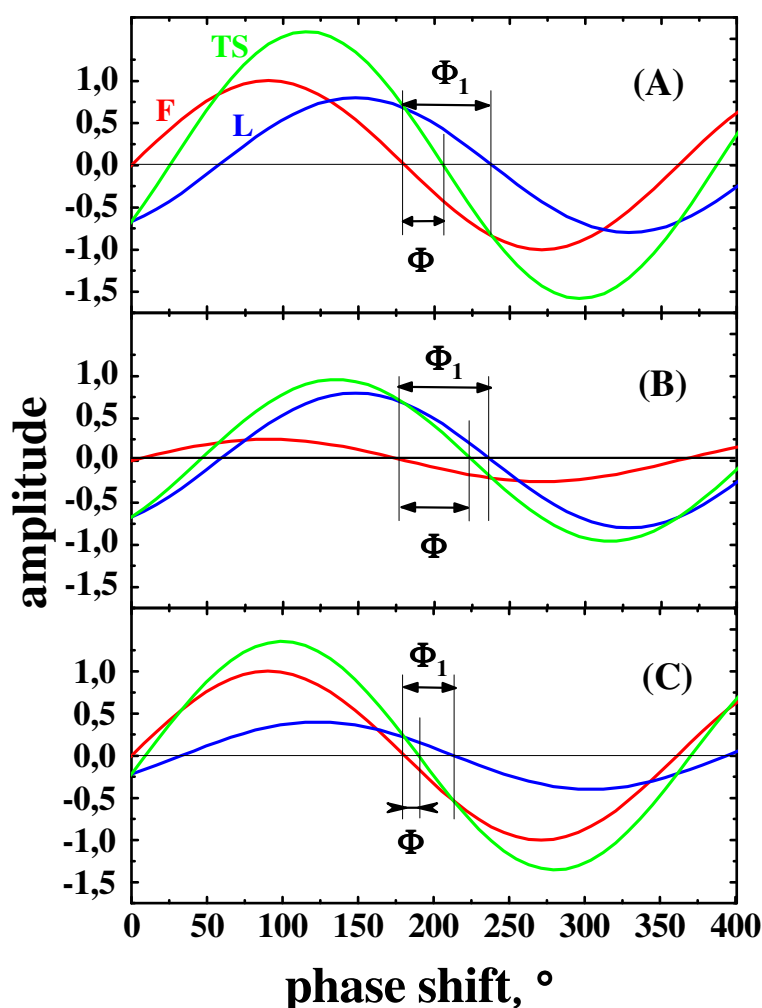


Figure 1.4 Schematic representation of the modified frequency-domain DLR method for three situations. Phase are shown for a fluorescent indicator (F; virtually identical to those of the light source); for a long-lived luminescent luminophore (L); and for the total signal resulting from a mixture of the two (TS). In panel (A), both indicators are in the absence of any analytes. In (B), the fluorescence intensity of the short-lived indicator is reduced by an analyte. In (C), the emission of the long-lived indicator is partially quenched.

A schematic of the m-DLR method operating in the frequency domain is presented in Fig. 1.4. The excitation light is sinusoidally modulated, and so is the emission of the indicators. At low modulation frequencies (i.e., in the kHz range) the signal of the fluorescent indicator remains unaltered (i.e., the phase shift Φ is almost zero). On the other side, the emission of the long-lived luminescent indicator (μ s decay time) is phase shifted. The phase shift Φ_1 increases with the decay time of the long-lived luminophore.

In the conventional DLR method the long-lived luminophore does not respond to any analyte, but serves only as an inert reference for the short-lived fluorescence. The overall phase shift Φ is thus an average value and can vary between almost zero and Φ_1 (the phase shift of the long-decaying reference). This value can be fine-tuned by varying the ratio of both dyes. When a fluorescent indicator responds to the analyte of interest (pH, CO₂, ions, etc.) the fluorescence intensity changes (Fig. 1.4B). A decrease in fluorescence intensity, for example, corresponds to an increase in overall phase shift. Thus, fluorescence intensity is converted into phase shift information.

Like in the conventional DLR method, the m-DLR scheme also makes use of a long-lived reference luminophore. It is, however, not inert and, in fact, acts as a second indicator dye. As a result, its shift is not constant anymore but responds to the second analyte (oxygen or temperature). This is illustrated in Fig. 1.4C. At higher oxygen concentrations, for example, the phase shift Φ_1 decreases as the result of quenching (reduction of decay time), and so does luminescence intensity of the indicator. Consequently, the overall phase shift decreases too.

The following equation originally was derived¹⁵⁷ for the compensation of background fluorescence. It also allows the calculation of the decay time of a long-lived indicator in the presence of a fluorescent one, by measurement of the phase shifts at two different modulation frequencies:

$$\tau = \frac{1}{2\pi} \left(\frac{\left\{ f_1^2 - f_2^2 \pm \left[f_2^2 - f_1^2 - 4(\cot \Phi_2 \cdot f_2 \cdot f_1^2 - \cot \Phi_1 \cdot f_1 \cdot f_2^2) \cdot (\cot \Phi_2 \cdot f_2 - \cot \Phi_1 \cdot f_1) \right]^{\frac{1}{2}} \right\}}{2(\cot \Phi_2 \cdot f_2 \cdot f_1^2 - \cot \Phi_1 \cdot f_1 \cdot f_2^2)} \right) \quad (1.3)$$

where Φ_1 and Φ_2 are the phase shifts at modulation frequencies f_1 and f_2 . This equation can also be used to calculate the decay time of the long-lived indicator (and consequently the concentration of the second analyte) in m-DLR based dual sensors. Once this parameter is

known, the concentration of the first analyte can be calculated as well. This will be demonstrated experimentally in Chapter 4.

Similar to the conventional DLR scheme, photobleaching of the indicators results in a shift of the response curves. While photodecomposition of a fluorescent indicator affects the determination of one analyte only, photo-degradation of the long-lived luminophore will affect both. Thus, in the case of photo-degradation of the indicators or poisoning of the sensor the need of recalibration arises.

The homogeneity of the sensor material is critical if the sensing material is used in the form of particles. Low homogeneity implies a shift of response curves for different spots of the material and therefore results in a bias in accuracy. However, the main advantage of the microbead approach consists in the excellent photostability of the materials because any singlet oxygen produced by the oxygen indicator cannot easily deteriorate the fluorescent indicator in another bead.

The modified DLR method can be also applied in the time domain measurements¹⁵⁸. Schroeder et al. have presented a planar optical dual sensor for simultaneous determination of pH and pO₂. The sensor membrane was fabricated by dissolving the two indicators (a lipophilic fluorescein derivate as pH indicator and PtTFPP as oxygen indicator) in a single hydrogel polymer matrix. The scheme involves the time-resolved acquisition of images in three windows during a series of square-shaped excitation pulses. Therefore, an iteration procedure is necessary to calculate pH and pO₂ values from the raw data of the dual sensors.

In summary, the m-DLR method is promising for multi-analyte measurement because of a relatively simple set-up, and the possibility of sensor miniaturization.

1.4 References

1. Kojima S, Suzuki H **A micro sensing system for blood gas analysis**. Chem. Sensors **2003**, 19, 25-27
2. Badonnel Y, Crance JP, Bertrand JM, Panek E **Determination of pH, carbon dioxide tension, and oxygen tension by micromethods**. Pharmacien Biologiste (Paris) **1969**, 6(61), 149-154
3. Jeevarajan A S, Vani S, Tazlor T D, Anderson M M **Continuous pH monitoring in a perfused bioreactor system using an optical pH sensor**. Biotechnol. Bioeng. **2002**, 78, 467-473

4. Mekhail K, Khacho M, Gunaratnam L, Lee S **Oxygen sensing by H⁺. Implications for HIF and hypoxic cell memory.** *Cell Cycle* **2004**, 3, 1027-1029
5. Meruva R K, Meyerhoff M E **Catheter-type sensor for potentiometric monitoring of oxygen, pH and carbon dioxide.** *Biosens. Bioelectron.* **1998**, 13, 201-212
6. Durham R M, Weigelt J A **Monitoring gastric pH levels.** *Surgery, gynecology & obstetrics* **1989**, 169(1), 14-16
7. Grant S A, Bettencourt K, Krulevitch P, Hamilton J, Glass R **In vitro and in vivo measurements of fiber optic and electrochemical sensors to monitor brain tissue pH.** *Sens. Actuators B* **2001**, B72(2), 174-179
8. Posch H E, Leiner M J P, Wolfbeis O S **Towards a gastric pH-sensor: an optrode for the pH 0-7 range.** *Fresenius J. Anal. Chem.* **1989**, 334(2), 162-165
9. Ganter M, Zollinger A **Continuous intravascular blood gas monitoring: development, current techniques, and clinical use of a commercial device.** *Brit. J. Anaesth.* **2003**, 91(3), 397-407
10. Lin C Y **A simple glass-electrode system for the determination of pH of blood and other biological fluids with temperature control.** *J. Scientific Instruments*, **1944**, 21-32
11. Kristensen M **Continuous intragastric pH determination. I. pH of the gastric juice determined in situ and following aspiration** *Den. Acta Medica Scand.*, **1965**, 177(4), 415-425
12. Kolle C, Gruber W, Trettnak W, Biebornik K, Dolezal C, Reininger F, O'Leary P **Fast optochemical sensor for continuous monitoring of oxygen in breath-gas analysis.** *Sens. Actuators B* **1997**, 38, 141-149
13. Canete F, Rios A, Luque de Castro M D, Valcarcel M **Determination of analytical parameters in drinking water by flow injection analysis. Part 1. Simultaneous determination of pH, alkalinity and total ionic concentration.** *Analyst* **1987**, 112, 263-266
14. Preininger C, Klimant I, Wolfbeis O S **Optical fiber sensor for biological oxygen demand.** *Anal. Chem.* **1994**, 66, 1841-1846
15. John G T, Goelling D, Klimant I, Schneider H, Heinzle E **pH-sensing 96-well microtitre plates for the characterization of acid production by dairy starter cultures.** *J. Dairy Res.* **2003**, 70, 327-333
16. Marshall A J, Blyth J, Davidson C A B, Lowe C R **pH-sensitive holographic sensors.** *Anal. Chem.* **2003**, 75, 4423-4431

17. Papkovsky D B, Papkovskaya N, Smyth A, Kerry J, Ogurtsov V I **Phosphorescent sensor approach for non-destructive measurement of oxygen in packaged foods: optimization of disposable oxygen sensors and their characterization over a wide temperature range.** *Anal. Lett.* **2000**, 33, 1755-1777
18. O'Mahony F C, O'Riordan T C, Papkovskaya N, Kerry J P, Papkovsky D B **Non-destructive assessment of oxygen levels in industrial modified atmosphere packaged cheddar cheese.** *Food Control.* **2006**, 17, 286-292
19. Young O A, Thomson R D, Merhtens V G, Loeffen M P F **Industrial application to cattle of a method for the early determination of meat ultimate pH.** *Meat Sci.* **2004**, 67, 107-112
20. John G T, Goelling D, Klimant I, Schneider H, Heinzle E **pH – sensing 96-well microtitre plates for the characterisation of acid production by dairy starter cultures.** *J. Dairy Res.* **2003**, 70, 327-333
21. Dybko A, Wroblewski W, Rozniecka E, Pozniakb K, Maciejewski J, Romaniuk R, Brzozka Z **Assessment of water quality based on the multiparameter fiber optic probe.** *Sens. Actuators B* **1998**, 51, 208-213
22. Mills A **Oxygen indicators and intelligent inks for packaging food.** *Chem. Soc. Rev.* **2005**, 34, 1003-1011
23. Schroeder C, Weidgans B M, Klimant I **pH Fluorosensors for use in marine systems.** *Analyst* **2005**, 130, 907-916
24. Bellerby R G, Olsen A, Johannessen T, Croot P A **high precision spectrophotometric method for on-line shipboard seawater pH measurements: the automated marine pH sensor (AMpS).** *Talanta* **2002**, 56, 61-69
25. Klimant I, Meyer V, Kuhl M **Fiber-optic oxygen microsensors, a new tool in aquatic biology.** *J. Limnol. and Oceanogr.* **1995**, 40, 1159-1165
26. Gouin J F, Baros F, Birot D, Andre J C **A fiber-optic oxygen sensor for oceanography.** *Sens. Actuators, B* **1997**, 39, 401-406
27. Neurauter G, Klimant I, Wolfbeis O S **Fiber-optic microsensor for high resolution pCO₂ sensing in marine environment.** *Fresenius J. Anal. Chem.* **2000**, 366, 481-487
28. Brennan C J, Peden M E **Theory and practice in the electrometric determination of pH in precipitation.** *Atmos. Environ.* **1987**, 21(4), 901ff
29. Marinenko G, Koch W F **A critical review of measurement practices for the determination of pH and acidity of atmospheric precipitation.** *Environment Int.*, **1984**, 10(4), 315-319

30. Bourilkov J, Belz M, Boyle W, Grattan K **Electrical pH control in aqueous solutions.** Proc. SPIE **1999**, 3538, 268-277
31. Tang T B **Toward a miniature wireless integrated multisensor microsystem for industrial and biomedical applications.** IEEE Sensors Journal **2002**, 2, 628-635
32. Kostov Y, Harms P, Randers-Eichhorn L, Rao R **Low-cost microbioreactor for high-throughput bioprocessing.** Biotechnol. Bioeng. 2001, 72, 346-352
33. Maharbiz M M, Holtz W J, Howe R T, Keasling J D **Microbioreactor arrays with parametric control for high-throughput experimentation.** Biotechnol. Bioeng. **2004**, 85(4), 376-381
34. Harms P, Kostov Y, Rao G **Bioprocess monitoring.** Current opinion in Biotechnology, **2002**, 13, 124-127
35. Celik E, Calik P **Bioprocess parameters and oxygen transfer characteristics in β -Lactamase production by *Bacillus* species.** Biotechnol. Prog. **2004**, 20, 491-499
36. Trummer E, Fauland K, Seidinger S, Schriebl K, Lattenmayer C, Kunert R, Vorauer-Uhl K, Weik R, Borth N, Katinger H, Müller D **Process parameter shifting: Part I. Effect of DOT, pH, and temperature on the performance of Epo-Fc expressing CHO cells cultivated in controlled batch bioreactors.** Biotechnol. Bioeng. **2006**, 94, 1033-1044
37. Lamping S R, Zhang H, Allen B, Ayazi Shamlou P **Design of a prototype miniature bioreactor for high throughput automated bioprocessing.** Chem. Eng. Sci. **2003**, 58, 747 – 758
38. Arain S, John G T, Krause C, Gerlach J, Wolfbeis O S, Klimant I **Characterization of microtiterplates with integrated optical sensors for oxygen and pH, and their applications to enzyme activity screening, respirometry, and toxicological assays.** Sens. Actuators B **2006**, 113(2), 639-648
39. Deshpande R R, Wittmann C, Heinzle E **Microplates with integrated oxygen sensing for medium optimization in animal cell culture.** Cytotechnology **2004**, 46(1), 1-8
40. Arain S, Weiss S, Heinzle E, John G T, Krause C, Klimant I **Gas sensing in microplates with optodes: Influence of oxygen exchange between sample, air, and plate material.** Biotechnol. Bioeng. **2005**, 90(3), 271-280
41. Deshpande R R, Heinzle E **On-line oxygen uptake rate and culture viability measurement of animal cell culture using microplates with integrated oxygen sensors.** Biotechnol. Letters **2004**, 26(9), 763-767

42. John G T, Klimant I, Wittmann C, Heinzle E **Integrated optical sensing of dissolved oxygen in microtiter plates: a novel tool for microbial cultivation.** *Biotechnol. Bioeng.* **2003**, 81, 829-836
43. John G T, Goelling D, Klimant I, Schneider H, Heinzle E **pH - Sensing 96-well microtitre plates for the characterization of acid production by dairy starter cultures.** *J Dairy Research* **2003**, 70(3), 327-333
44. Zhang Z, Szita N, Boccazzi P, Sinskey A J, Jensen K F **A well-mixed, polymer-based microbioreactor with integrated optical measurements.** *Biosens. Bioelectron.* **2006**, 93, 286-296
45. Ferguson J A, Healey B G, Bronk K S, Barnard S M, Walt D R **Simultaneous monitoring of pH, CO₂ and O₂ using an optical imaging fiber.** *Anal. Chim. Acta* **1997**, 340, 123-131
46. Lin J **Recent development and applications of optical and fiber-optic pH sensors.** *TrAC- Trends in Analytical Chemistry* **2000**, 19(9), 541-552
47. Wolfbeis O S **Fiber optic chemical sensors and biosensors.** Vol. I, CRC Press, Boca Raton, **1991**
48. Nivens A D, Schiza M V, Angel S M **Multilayer sol-gel membranes for optical sensing applications: single layer pH and dual layer CO₂ and NH₃ sensors.** *Talanta* **2002**, 58, 543-550
49. Malins C, MacCraith B D **Dye-doped organically modified silica glass for fluorescence based carbon dioxide gas detection.** *Analyst* **1998**, 123, 2373-2376
50. Mills A, Chang Q **Fluorescence plastic thin-film sensor for carbon dioxide.** *Analyst* **1993**, 118, 839-843
51. Gouterman M, Callis J, Dalton L, Khalil G, Mebarski Y, Cooper K R, Greiner M **Dual luminophor pressure sensitive paint: III. Application to automotive model testing.** *Meas. Sci. Technol.* **2004**, 15, 1986-1993
52. Liebsch G, Klimant I, Wolfbeis O S **Luminescence lifetime temperature sensing based on sol-gels and poly(acrylonitrile)s dyed with ruthenium metal-ligand complexes.** *Adv. Mater.* **1999**, 11, 1296-1299
53. Apostolidis A, Klimant I, Andrzejewski D, Wolfbeis O S **A Combinatorial approach for development of materials for optical sensing of gases.** *J. Comb. Chem.* **2004**, 6, 325-331
54. McDonagh C, Kolle C, McEvoy A, Dowling D, Cafolla A, Cullen S, MacCraith B D **Phase fluorometric dissolved oxygen sensor.** *Sens. Actuators* **2001**, 74, 124-130

55. Klimant I, Kuehl M, Glud R, Holst G **Optical measurement of oxygen and temperature in microscale: strategies and biological applications.** Sens. Actuators **1997**, 38, 29-37
56. Furuto T, Lee S K, Amao Y, Asai K, Okura I **Oxygen sensing system using triple-triplet reflectance of zinc porphyrin immobilized in polymer membrane studies by laser flash photolysis.** J. Photochem. Photobiol. **2000**, 132, 81-86
57. Vasylevska A S, Karasyov A A, Borisov S M, Krause C **Novel coumarin-based fluorescent pH indicators, probes and membranes covering a broad pH range.** Anal. Bioanal. Chem. **2007**, 387(6), 2131-2141
58. Carter J C, Alvis R M, Brown S B, Langry K C, Wilson T S, McBride M T, Myrick M L, Cox W R, Grove M E, Colston B W **Fabricating optical fiber imaging sensors using inkjet printing technology: A pH sensor proof-of-concept.** Biosens. Bioelectronics **2006**, 21(7), 1359-1364
59. Goldstein S R, Peterson J P, Fitzgerald R V **A miniature fiber optic pH sensor for physiological use.** J. Biomech. Eng. **1980**, 102(2), 141-146
60. Jordan D M, Walt D R, Milanovich F P **Physiological pH fiber optic chemical sensor based on energy transfer.** Anal. Chem. **1987**, 59, 437-439
61. Liu Z, Liu J, Chen T **Phenol red immobilized PVA membrane for an optical pH sensor with two determination ranges and long-term stability.** Sens. Actuators B **2005**, 107, 311-316
62. Sotomayor P T, Raimundo I M, de Oliveira Neto G, de Oliveira W A **Evaluation of fiber optical chemical sensors for low analysis systems.** Sens. Actuators B **1998**, 51, 382-390
63. Lobnik A, Majcen N, Niederreiter K, Uray G **Optical pH sensor based on the absorption of antenna generated europium luminescence by bromothymol blue in a sol-gel membrane.** Sens. Actuators B **2001**, 74, 200-206
64. Allain L R, Sorasaene K, Xue Z **Doped thin-film sensors via a sol-gel process for high-acidity determination.** Anal. Chem. **1997**, 69, 3076-3080
65. Saari L A, Seitz W R **pH sensor based on the immobilized fluoresceinamine.** Anal. Chem. **1982**, 54, 821-823
66. Wolfbeis O S, Furlinger E, Kroneis H, Marsoner H **Fluorimetric analysis. 1. A study on fluorescent indicators for measuring near neutral ("physiological") pH values.** Fresenius Anal. Chem. **1983**, 314, 119-124
67. Whitaker J E, Haugland R P, Prendergast F G **Spectral and photophysical studies of benzo(c)xanthene dyes: dual emission pH sensors.** Anal. Biochem. **1991**, 194, 330-344

68. Offenbacher H, Wolfbeis O S, Förlinger E **Fluorescence optical sensors for continuous determination of near-neutral pH values.** *Sens. Actuators B* **1986**, 9, 73-84
69. Zhujun Z, Seitz W R A **A fluorescence sensor for quantifying pH in the range from 6.5 to 8.5.** *Anal. Chim. Acta* **1984**, 160, 47-55
70. Xu Z, Rollins A, Alcalá R, Marchant R E **A novel fibre-optic pH sensor incorporating carboxy SNAFL-2 and fluorescent wavelength-ratiometric detection.** *J. Biomed. Mater. Res.* **1998**, 39, 9-15
71. Wolfbeis O S, Offenbacher H **Fluorescence sensor for monitoring ionic strength and physiological pH values.** *Sens. Actuators* **1986**, 9(1), 85-91
72. Vishnoi G, Goel T C, Pillai P K C **pH optrode for the complete working range.** *Proc. SPIE* **1999**, 3538, 319-325
73. Moreno-Bondi M C, Jimenez M, Perez-Conde C, Camara C **Analytical performance of an optical pH sensor for acid-base titrations.** *Anal. Chim. Acta* **1990**, 230, 35-40
74. Papkovsky D B, Ponomarev G V, Wolfbeis O S **Protonation of porphyrins in liquid PVC membranes: effect of anionic additives and application to pH sensing.** *J. Photochem. Photobiol. A* **1997**, 104, 151-158
75. Nivens D A, Zhang Y, Angel S M **A fiber-optic pH sensor prepared using a base-catalyzed organo-silica sol-gel.** *Anal. Chim. Acta* **1998**, 376, 235-245
76. Jin W J, Costa-Fernández J M, Sanz-Medel A **Room temperature phosphorescence pH optosensor based on energy transfer.** *Anal. Chim. Acta* **2001**, 431, 1-9
77. Cajlakovic M, Lobnik A, Werner T **Stability of new optical pH sensing material based on cross-linked poly(vinyl alcohol) copolymer.** *Anal. Chim. Acta* **2002**, 455, 207-213
78. Kosch U, Klimant I, Werner T, Wolfbeis O S **Strategies to design pH optodes with luminescence decay times in the microsecond time regime.** *Anal. Chem.* **1998**, 70, 3892-3897
79. Peppas N A **Preparation methods & structures of hydrogels.** CRC Press: Boca Raton, **1986**
80. Werner T, Huber C, Heintz S, Kollmannsberger M, Daub J, Wolfbeis O S **Novel optical pH sensor based on a boradiazaindacene derivative.** *Fresenius' J. Anal. Chem.* **1997**, 359, 150-154
81. Draxler S, Lipitsch M E **Effect of polymer matrices in lifetime based sensing.** *Proc. SPIE* **1995**, 2388, 363-368

82. Parker J W, Laksin O, Yu C, Lau M L, Klima S, Fisher R, Scott I, Atwater B W **Fiber-optic sensor for pH and carbon dioxide using a self-referencing dye.** *Anal. Chem.* **1993**, 65, 2329-2334
83. Skoog D A, West D M, Holler F J **Fundamentals of analytical chemistry.** 5th ed., Saunders, Philadelphia **1998**, p. 344
84. Clark L C **Electrochemical device for chemical analysis.** US Pat. 2 913 386, **1959**
85. Freeman T M, Seitz W R **Oxygen probe based on tetrakis (alkylamino) ethylene chemiluminescence.** *Anal. Chem.* **1981**, 53, 98–102
86. Hendricks H D **Method of detecting oxygen in a gas.** US Pat. 3 709 663 **1973**
87. Vaughan A A, Baron M G, Narayanaswamy R **Optical ammonia sensing films based on an immobilized metalloporphyrin.** *Anal. Commun.* **1996**, 33, 393 - 396
88. Mohr G J, Wolfbeis O S **Optical sensing of anions via polarity-sensitive dyes: A bulk sensor membrane for nitrate.** *Anal. Chim. Acta* **1995**, 316, 239-246
89. McMurray H N, Douglas P, Busa C, Garley M S **Oxygen quenching of tris(2,2'-bipyridine) ruthenium(II) complexes in thin organic films.** *J. Photochem. Photobiol. A: Chem.* **1994**, 80, 283-288
90. He H, Fratz R J, Leiner M J P, Rehn M M, Tusa J K **Selection of silicone polymer matrix for optical gas sensing.** *Sens. Actuators B* **1995**, 29, 246-250
91. Xu W, Schmidt R, Whaley M, Demas J N, DeGraff B A **Oxygen sensor based on luminescence quenching: interactions of metal complexes with the polymer supports.** *Anal. Chem.* **1994**, 66, 4133-4141
92. Hartmann P, Trettnak W **Effects of polymer matrices on calibration functions of luminescent oxygen sensors based on porphyrin ketone complexes.** *Anal. Chem.* **1996**, 68, 2615-2620
93. Mills A **Controlling the sensitivity of optical oxygen sensors.** *Sens. Actuators B* **1998**, 51, 60-68
94. Mills A, Lepre A **Controlling the response characteristics of luminescent porphyrin plastic film sensors for oxygen.** *Anal. Chem.* **1997**, 69, 4653-4659
95. Amao Y, Miyashita T, Okura I **Platinum tetrakis(pentafluorophenyl)porphyrin immobilized in polytrifluoroethylmethacrylate film as a photostable optical oxygen detection material.** *J. Fluor. Chem.* **2001**, 107, 101-106
96. Yasuda H, Stannett V **Permeability coefficients.** *Polymer Handbook* 4th ed., Wiley, New York, **1999**

97. Chun-Man Chan, Mee-Yee Chan, Minquan Zhang, Waihung Lo and Kwok-Yin Wong **The performance of oxygen sensing films with ruthenium-adsorbed fumed silica dispersed in silicone rubber.** *Analyst* **1999**, 124, 691–694
98. McDonagh C, Bowe P, Mongey K, MacCraith B D **Characterisation of porosity and sensor response times of sol-gel-derived thin films for oxygen sensor applications.** *J. Non-Crystalline Solids* **2002**, 306, 138–148
99. Klimant I, Ruckruh F, Liebsch G, Stangelmayer A, Wolfbeis O S **Fast response oxygen micro-optodes based on novel soluble ormosil glasses.** *Mikrochim. Acta* **1999**, 131, 35-46
100. McDonagh C, McCraith B D, McEvoy A K **Tailoring of sol-gel films for optical sensing of oxygen in gas and aqueous phase.** *Anal. Chem.* **1998**, 70, 45-50
101. Mingoarranz F J, Moreno-Bondi M C, García-Fresnadillo D, de Dios C, Orellana G **Oxygen-sensitive layers for optical fibre devices.** *Microchim. Acta* **1995**, 121, 107 - 118
102. Klimant I, Wolfbeis O S **Oxygen-sensitive luminescent materials based on silicone-soluble ruthenium diimine complexes.** *Anal. Chem.* **1995**, 67, 3160 – 3166
103. Hartmann P, Leiner M J P, Lippitsch M E **Response characteristics of luminescent oxygen sensors.** *Sens. Actuators B* **1995**, 29, 251 - 257
104. Lee S K, Okura I **Photostable optical oxygen sensing material: platinum tetrakis(pentafluorophenyl)porphyrin immobilised in polystyrene.** *Anal. Commun.* **1997**, 34, 185 - 188
105. Papkovsky D B, Ponomarev GV, Trettnak W, O'Leary P **Phosphorescent complexes of porphyrin-ketones: optical properties and application to oxygen sensing.** *Anal. Chem.* **1995**, 67, 4112 - 4117
106. Kalyanasundaram K **Photochemistry of polypyridine and porphyrin complexes.** Academic Press, New York **1992**
107. Papkovsky D B, Ponomarev G V, Trettnak W, O'Leary P **Phosphorescent complexes of porphyrin ketones: optical properties and application to oxygen sensing** *Anal. Chem.* **1995**, 67, 4112-4117
108. Amao Y, Asai K, Okura I **Oxygen sensing based on lifetime of photoexcited triplet state of platinum porphyrin-polystyrene film using time-resolved spectroscopy.** *J. Porphyrins Phthalocyanines* **2000**, 4, 292–299
109. Wolfbeis O S, Oehme I, Papkovskaya N, Klimant I **Sol-gel based glucose biosensors employing optical oxygen transducers, and a method for compensating for variable oxygen background.** *Biosens. Bioelectron.* **2000**, 15(1-2), 69-76

110. Pasic A, Koehler H, Schaupp L, Pieber T R, Klimant I **Fiber-optic flow-through sensor for online monitoring of glucose.** Anal. Bioanal. Chem. **2006**, 386(5), 1293-1302
111. Li L, Walt D R **Dual -analyte fiber- optic sensor for the simultaneous and continuous measurement of glucose and oxygen.** Anal. Chem. **1995**, 67(20), 3746-3752
112. Tohda K, Gratzl M **Micro-miniature autonomous optical sensor array for monitoring ions and metabolites 2: color responses to pH, K⁺ and glucose.** Anal. Sciences **2006**, 22(7), 937-941
113. Zanzotto A, Szita N, Boccazzi P, Lessard P, Sinskey A J, Jensen K F **Membrane-aerated microbioreactor for high-throughput bioprocessing.** Biotech. Bioeng. **2004**, 87(2), 243-254
114. Harms P, Kostov Y, French J A, Soliman M, Anjanappa M, Ram A, Rao G **Design and performance of a 24-station high throughput microbioreactor.** Biotech. Bioeng. **2006**, 93(1), 6-13
115. Cooney C G, Towe B C **Miniaturized pH and pCO₂ intravascular catheter using optical monitoring and a dual concentric-flow microdialysis approach.** Sens. Actuators B **2000**, 62(3), 177-181
116. Wolfbeis O S, Weis L J, Leiner M J P, Ziegler W E **Fiber-optic fluorosensor for oxygen and carbon dioxide.** Anal. Chem. **1988**, 60(19), 2028-2030
117. Coyle L M, Gouterman M **Correcting lifetime measurements for temperature.** Sens. Actuators B **1999**, 61(1-3), 92-99
118. Borisov S M, Vasylevska A S, Krause C, Wolfbeis O S **Composite luminescent material for dual sensing of oxygen and temperature.** Adv. Funct. Mater. **2006**, 16(12), 1536-1542
119. Collison M E, Aebli G V, Petty J, Meyerhoff M E **Potentiometric combination ion carbon dioxide sensors for in vitro and in vivo blood measurements.** Anal. Chem. **1989**, 61(21), 2365-2372
120. Weigl B H, Holobar A, Trettnak W, Klimant T, Kraus H, O'Leary P, Wolfbeis O S **Optical triple sensor for measuring pH, oxygen and carbon dioxide.** J. Biotech. **1994**, 32, 127-138
121. Mou D G **Process dynamics, instrumentation and control.** Biotechnol. Adv. **1983**, 1(2), 229-245
122. Borisov S M, Wolfbeis O S **Temperature-sensitive europium (III) probes and their use for simultaneous luminescent sensing of temperature and oxygen.** Anal. Chem. **2006**, 78(14), 5094-5101

123. Zelelow B, Khalil G E, Phelan G, Carlson B, Gouterman M, Callis J B, Dalton L R **Dual luminophor pressure sensitive paint II. Lifetime based measurement of pressure and temperature.** Sens. Actuators B **2003**, 96(1-2), 304-314
124. Borisov S M, Neurauder G, Schroeder C, Klimant I, Wolfbeis O S **Modified dual lifetime referencing method for simultaneous optical determination and sensing of two analytes.** Appl. Spectrosc. **2006**, 60(10), 1167-1173
125. Wolfbeis O S, Weis L J, Leiner M J P, Zeigler W E **Fiber-optic fluorosensor for oxygen and carbon dioxide.** Anal. Chem. **1988**, 60, 2028-2030
126. Borisov S M, Krause C, Arain S, Wolfbeis O S **Composite materials for simultaneous and contactless luminescent sensing and imaging of oxygen and carbon dioxide.** Adv. Mater. **2006**, 18, 1511-1516
127. Vasylyevska G S, Borisov S M, Krause C, Wolfbeis O S **Indicator-loaded permeation-selective microbeads for use in fiber optic simultaneous sensing of pH and dissolved oxygen.** Chem. Mater. **2006**, 18(19), 4609-4616
128. Goepel W, Jones T A, Kleitz M, Lundstroem A, Seijama T (eds) **Sensors: A comprehensive review. Vol. 1: Chemical and biochemical sensors, part 1.** Verlag Chemie, Weinheim, **1991**
129. Goepel W, Jones T A, Kleitz M, Lundstroem A, Seiyama T (eds) **Sensors: A comprehensive review, Vol. I: Chemical and biochemical sensors part 2.** Verlag Chemie, Weinheim, **1991**
130. Ahmad F, Christenson A, Bainbridge M, Yusof A P M, Ab Ghani S **Minimizing tissue-material interaction in microsensor for subcutaneous glucose monitoring.** Biosens. Bioelectron. **2007**, 22(8), 1625-1632
131. Wang J, Zhang **Needle-type dual microsensor for the simultaneous monitoring of glucose and insulin.** Anal. Chem. **2001**, 73(4), 844-847
132. Wang J, Musameh M **Enzyme-dispersed carbon-nanotube electrodes: a needle microsensor for monitoring glucose.** Analyst **2003**, 128(11), 1382-1385
133. Wang W, Vadgama P **O₂ microsensors for minimally invasive tissue monitoring.** J. R. Soc. Interface **2004**, 1, 109-117
134. Irwin S, Wall V, Davenport J **Measurement of temperature and salinity effects on oxygen consumption of *Artemia franciscana* K., measured using fibre-optic oxygen microsensors.** Hydrobiologia **2007**, 575, 109-115
135. Esfandyarpour B, Mohajerzadeh S, Khodadadi A A, Robertson M D **Ultrahigh-sensitive tin-oxide microsensors for H₂S detection.** IEEE Sensors Journal **2004**, 4(4), 449-454

136. Tan W, Shi Z Y, Kopelman R **Development of submicron chemical fiber optic sensors.** *Anal. Chem.* **2001**, 64, 2985-2990
137. Song A, Parus S, Kopelman R **High-performance fiber-optic pH microsensors for practical physiological measurements using a dual-emission sensitive dye.** *Anal. Chem.* **1997**, 69, 863-867
138. Kosch U, Klimant I, Wolfbeis O S **Long-lifetime based pH micro-optodes without oxygen interference.** *Fresenius J. Anal. Chem.* **1999**, 364, 48-53
139. Rau J R, Chein S C, Sun H W **Characterization of a polypyrrole microsensor for nitrate and nitrite ions.** *Electrochim. Acta* **1994**, 39(18), 2773-2779
140. Bendikov T A, Kim J, Harmon T C **Development and environmental application of a nitrate selective microsensor based on doped polypyrrole films.** *Sens. Actuators* **2005**, 106(2), 512-517
141. Andersen K, Kjaer T, Revsbech N P **An oxygen insensitive microsensor for nitrous oxide.** *Sens. Actuators* **2001**, 81(1), 42-48
142. Klimant I, Meyer V, Kühl M **Fiber-optic oxygen microsensors, a new tool in aquatic biology.** *Limnol. Oceanogr.* **1995**, 40(6), 1159-1165
143. Villalba M, Ferrari D, Bozza A, DelSenno L, DiVirgilio F **Ionic regulation of endonuclease activity in PC12 cells.** *Biochem. J.* **1995**, 311, 1033-1038
144. Welch M, Margolin Y, Caplan S R, Eisenbach M **Rotational asymmetry of Escherichia coli flagellar motor in the presence of arsenate.** *Biochim. Biophys. Acta* **1995**, 1268, 81-87
145. Taira T, Paalasmaa P, Voipio J, Kaila K **Relative contributions of excitatory and inhibitory neuronal activity to alkaline transients evoked by stimulation of Schaffer collaterals in the rat hippocampal slice.** *J. Neurophysiol.* **1995**, 74, 643-649
146. Barton M E **Effect of pH on the growth cycle of HeLa cells in batch suspension culture without oxygen control.** *Biotechnol. Bioeng.* **1971**, 13(4), 471-492
147. Trummer E, Fauland K, Seidinger S, Schriebl K, Lattenmayer C, Kunert R, Vorauer-Uhl K, Weik R, Borth N, Katinger H, Mueller D **Process parameter shifting: part I. Effect of DOT, pH, and temperature on the performance of Epo-Fc expressing CHO cells cultivated in controlled batch bioreactors.** *Biotechnol. Bioeng.* **2006**, 94(6), 1033-1044
148. Schlichting E, Lyberg T **Monitoring of tissue oxygenation in shock: an experimental study in pigs.** *Crit. Care Med.* **1995**, 23, 1703-1710
149. Oeggerli A, Eyer K, Heinzle E **Online gas analysis in animal cell cultivation: I. control dissolved oxygen and pH.** *Biotechnol. Bioeng.* **1995**, 45(1), 42-53

150. Ji J, Rosenzweig Z **Fiber optic pH/Ca²⁺ fluorescence microsensor based on spectral processing of sensing signals.** Anal. Chim. Acta **1999**, 397, 93–102
151. Lakowicz J R **Time-domain lifetime measurements.** In **principles of fluorescence spectroscopy**. 2nd edition, Kluwer Academic/Plenum Publishers, New York, **1999**, 95-140
152. Klimant I **Verfahren und Vorrichtungen zur Referenzierung von Fluoreszenzintensitätssignalen.** Ger. Pat. Appl. **1997** DE 198 29 657
153. Klimant I, Huber C, Liebsch G, Neurauter G, Stangelmayer A, Wolfbeis O S **Dual lifetime referencing (DLR) – a new scheme for converting fluorescence intensity into a frequency-domain or time-domain information.** In **New Trends in Fluorescence Spectroscopy**, Springer Series on Fluorescence, **2001**, 257-274
154. Huber C, Klimant I, Krause C, Wolfbeis O S **Dual lifetime referencing as applied to a chloride optical sensor.** Anal. Chem. **2001**, 73, 2097-2103
155. Lakowicz J R, Castellano F N, Dattelbaum J D, Tolosa L, Rao G, Gryczynski I **Low frequency modulation sensors using nanosecond fluorophores.** Anal. Chem. **1998**, 70, 5115-5121
156. Szmajda H, Lakowicz J R **Optical measurements of pH using fluorescence lifetimes and phase-modulation fluorometry.** Anal. Chem. **1993**, 65, 1668-1674
157. Neurauter D **Frequency domain pCO₂ sensing.** PhD thesis, University of Regensburg, Regensburg, **2000**, p 106
158. Schroeder C R, Polerecky L, Klimant I **Time-resolved pH/pO₂ mapping with luminescent hybrid sensors.** Anal. Chem. **2007**, 79, 60-70

Chapter 2

Novel Coumarin-Based Fluorescent pH Indicators, Probes and Membranes Covering a Broad pH Range

A new family of coumarin-based pH indicators was synthesized. They are sensitive to pH in either weakly acidic or weakly basic solution. The indicators possess moderate to high brightness, excellent photostability and compatibility with light-emitting diodes (LEDs). The indicators were covalently immobilized on the surface of amino-modified polymer microbeads which in turn were incorporated into a hydrogel matrix. When using a mixture of two different microbeads, the membranes are capable of optical pH sensing over a very wide range comparable to the dynamic range of the glass electrode (pH 1 to 11). (Anal Bioanal Chem 2007, 387, 2131-2141)

2.1 Introduction

A lot of biological and geochemical processes occurring in freshwater, seawater and marine sediments involve strong pH changes¹⁻⁴. The output of many biotechnological processes (e.g. bacterial growth^{5,6} or sour fermentation of milk^{7,8}) depends on the pH value, which therefore needs to be monitored. Furthermore, it is often important to measure the pH in acidic media (e.g. for the study of acidic organelles in live cells^{9,10} or the analysis of acidic soils^{11,12}) or even at strongly acidic conditions which are present in the human stomach^{13,14}.

The glass electrode is the established tool for pH measurements. However, electrodes are limited to single-point measurements and are not suitable for obtaining information on pH distribution. Moreover, electrodes are bulky and invasive, and create the risk of electric shock during *in vivo* measurements. Fluorescent pH sensors are a suitable alternative. Such sensors can be easily produced in various shapes. The sensing films are suitable for imaging experiments. An ideal optical sensor is capable of sensing the concentration of an analyte

continuously and reversibly through changes of the optical properties of an indicator¹⁵. Leaching of the pH indicator from the sensor into the sample can be critical, because most indicators are hydrophilic and charged, and the matrix has to be permeable to ions like protons. Sensor properties can be substantially improved by using procedures for covalent coupling of indicators to appropriate polymer matrices¹⁶⁻¹⁸.

Most fluorescent optical sensors, however, suffer from several drawbacks compared to a glass pH electrode. Firstly, the signal is dependent on the ionic strength (= IS) of the sample solution. For some indicators even small changes in the IS can compromise the performance^{19,20}, therefore such sensors can only be used at constant IS. Secondly, a glass electrode is suitable for pH measurements over a very broad range. Optical sensors allow precise pH measurement only over a much narrower region, which is acceptable for most applications. However, sometimes it is necessary to determine the pH over a broader range^{21,22}. Some attempts have been made to broaden the dynamic range of optical pH sensors, for example by using a mixture of absorption-based pH indicators or a single indicator with multiple dissociation steps²³⁻²⁵. Most sensors based on individual pH indicators are suitable for measurements within 4-5 pH units only²⁶. A fluorescent pH indicator was reported for sensing pH in the broad dynamic range²⁷. This sensor, however, required UV excitation which is not suitable for most applications because of its incompatibility with fiber optics. Thus, designing a fluorescent sensor for measurements in the broad dynamic range is still of much importance.

Many examples for optical pH sensing in physiological samples were described^{28,29}. Carboxyfluorescein (CF) and its derivatives are the mostly used fluorescent pH indicators³⁰⁻³³ because of their high quantum yields in alkaline solution and compatibility with established immobilization protocols on polymer surfaces. CF, however, features only moderate photostability, so that continuous measurements over a long period of time result in signal drifts. This can become critical in the case of microsensors, where high light densities are required. Besides, CF is not suitable for pH measurements in strongly basic or acidic media. Only few fluorescent sensors for monitoring of pH in marine systems (pH ~ 7.2 – 8.2) are known^{1,34,35}, other optical pH sensors for this application mainly use absorption as the analytical information source^{36,37}. Fluorescent sensors are usually more sensitive and precise than those based on absorption. Seminaaphthofluorescein (SNAFL) and seminaaphthorhodafluors (SNARF) are fluorescent indicators which fulfill this requirement^{38,39}. The synthesis of these indicators is, however, complicated. Similar to optical pH sensing based on absorbance, measurement of slightly acidic pH values with fluorescent indicators is

often problematic because few fluorescent indicators meet the requirements of brightness and photostability.

Here we describe the syntheses and characterization of novel pH-sensitive iminocoumarin derivatives. We show that the fluorescent indicators covalently coupled to an amino-modified polymer surface can be used successfully in pH sensing for different pH ranges.

2.2 Experimental

2.2.1 Materials

Most reagents for the syntheses were obtained from Merck (www.merck.de) and were of analytical grade. Dicyclohexylcarbodiimide (DCC), N-hydroxysuccinimide (NHS), formaldehyde, acetonitrile, triethylamine, 2,4,6-trichlorotriazine and ethanol were purchased from Fluka (www.sigmaaldrich.com). Polyurethane hydrogel (type D4) was obtained from Cardiotech (www.cardiotech-inc.com). Amino-modified polyacrylamide (AA-Q-N2), aminocellulose (AMC) and amino-modified poly(hydroxyethyl methacrylate) (p-HEMA) in the form of microbeads (\varnothing of 1 – 3 μm) were obtained from OptoSense (www.optosense.de). A polyethylene terephthalate support (Mylar[®], 125 μm thickness) was obtained from Goodfellow (www.goodfellow.com). The phosphorescent reference particles (Ru-dpp in polyacrylonitrile derivative polymer nanospheres) were obtained from PreSens GmbH (www.presens.de).

2.2.2 Synthesis

Fig. 2.1 gives the chemical structures of the synthesized dyes. The synthesis of iminocoumarin (**I**) was reported elsewhere^{40,41}. In essence, it is obtained from 4-diethylaminosalicylaldehyde and cyanomethylbenzimidazole by heating for 3 h in methanolic solution. Piperidine was used as a basic catalyst. Its derivatives were obtained upon condensation of **I** with aromatic aldehydes using the following procedures.

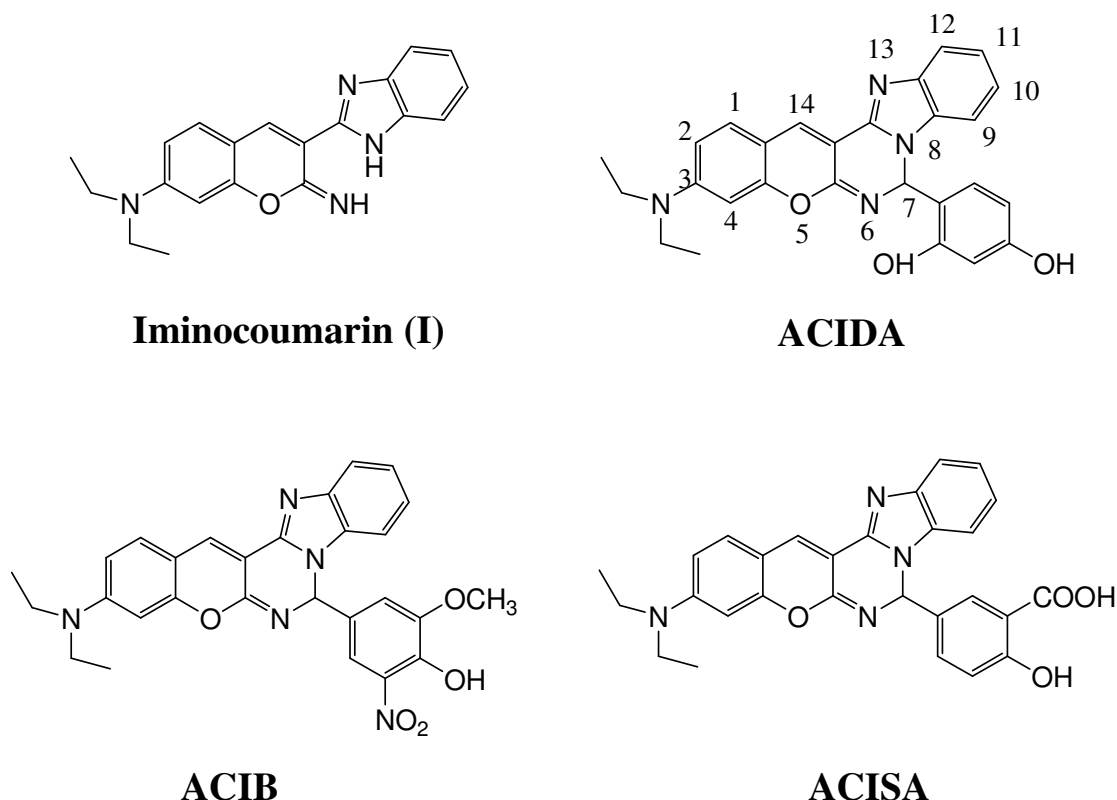


Figure 2.1 Chemical structures of the dyes used for the new pH sensors.

Synthesis of 4-(9-diethylamino-5H-7-oxa-4b,6,13-triaza-indeno [2,1-a] anthracen-5-yl)-2-methoxy-6-nitro-phenol (ACIB):

0.17 mL (1.7 mmol) of piperidine were added to a suspension of 0.6 g (1.7 mmol) of 7-diethylamino-3-(2-benzimidazolyl)-iminocoumarin (**I**) and 0.4 g (4.8 mmol) of dry ammonium acetate in 20 mL of dry methyl alcohol. 0.34 g (1.7 mmol) of 4-hydroxy-3-methoxy-5-nitrobenzaldehyde were added to the stirred suspension. The reaction mixture was refluxed for 2 h. After cooling, the yellow precipitate was separated by filtration and recrystallized from benzene. MS: m/z for $C_{28}H_{25}N_5O_5$, 511.54 calc., 512.3 found. Analysis (%) calc./found: C: 65.74/65.94, H: 4.93/5.11, N: 13.69/13.48. 1H NMR (300 MHz, DMSO- D_6): δ , ppm: 10.6 (s, 1H, OH), 8.13 (s, 1H, H(14)), 7.63 (d, 1H), 7.50 (d, 1H), 7.44 (d, 1H), 7.33 (s, 1H), 7.52 (d, 1H), 7.26 – 7.08 (m, 3H), 6.65 (q, 1H), 6.27 (d, 1H, H(7)), 3.82 (s, 3H, OCH₃), 3.45 (q, 4H, 2CH₂), 1.15 (t, 6H, 2CH₃).

Synthesis of 4-(9-diethylamino-5H-7-oxa-4b,6,13-triaza-indeno [2,1-a] anthracen-5-yl)-benzene-1,3-diol (ACIDA):

3 mL of piperidine were added to a solution of 0.55 g (1.65 mmol) of **I** in 30 mL of absolute methanol. After formation of a yellow precipitate, 0.21 g (1.65 mmol) of 2,4-

dihydroxybenzaldehyde were added. The reaction mixture was refluxed for 30 min. A red precipitate was formed after cooling. It was purified by repeated recrystallization from absolute methanol.

MS: m/z for $C_{27}H_{24}N_4O_3$, 452.7 calc., 453.4 found. Analysis (%) calc./found: C: 71.67/69.65, H: 5.35/5.58, N: 12.38/11.90. 1H NMR (300 MHz, DMSO- D_6): δ , ppm: 9.6 (s, 1H, OH), 9.35 (s, 1H, OH), 8.08 (s, 1H, H(14)), 7.58 (d, 1H), 7.46 (d, 1H), 7.17 (s, 1H), 7.22 – 6.94 (m, 4H), 6.61 (q, 1H), 6.43 (d, 1H), 6.22 (d, 1H, H(7)), 6.15 (q, 1H), 3.45 (q, 4H, 2CH₂), 1.06 (t, 6H, 2CH₃).

Synthesis of 5-(9-diethylamino-5H-7-oxa-4b,6,13-triaza-indeno [2,1-a] anthracen-5-yl)-benzene-1,3-diol (ACISA):

3 ml of piperidine were added to a suspension of 0.498 g (1.5 mmol) of **I** and 0.25 g (1.5 mmol) of salicylic aldehyde in absolute methanol. The mixture was stirred for 45 min. A yellow precipitate was formed after cooling and purified via recrystallization from methanol.

MS: m/z for $C_{28}H_{24}N_4O_4$, 480.5 calc., 481.3 found. Analysis (%) calc./found: C: 69.99/66.89, H: 5.03/6.43, N: 11.66/11.69. 1H NMR (300 MHz, DMSO- D_6): δ , ppm: 8.23 (s, 1H, OH), 8.13 (s, 1H, H(14)), 7.60 (d, 1H), 7.55 (d, 1H), 7.47 (d, 1H), 7.21 – 7.03 (m, 5H), 6.62 (q, 1H), 6.57 (d, 1H), 6.45 (d, 1H, H(7)), 3.45 (q, 4H, 2CH₂), 1.15 (t, 6H, 2CH₃).

2.2.3 Preparation of the pH-Sensitive Sensor Beads and Sensor Membranes

Table 2.1 summarizes the materials used for the various pH sensors. The sensor membranes (M) are made of sensor beads (B) in a hydrogel matrix. The membranes are obtained by spreading water/ethanol solutions of the sensor membrane material onto a solid transparent support (such as polyethylene terephthalate or glass) and allowing the solvent to evaporate to give sensor membranes M of a thickness of ~10 μ m.

Table 2.1 Probes and materials for the preparation of pH –sensitive membranes and pK_a values of the pH membranes.

Code	Indicator –loaded bead (B) or bead – loaded sensor membrane (M)	pK _a
B-1	ACIB on AA-Q-N2 microbeads	-
B-2	ACIB on AMC microbeads	-
B-3	Iminocoumarin on AMC microbeads	-
B-4	Iminocoumarin on p-HEMA microbeads	-
B-5	ACISA on AMC microbeads	-
B-6	ACISA on p-HEMA microbeads	-
M-1	ACIB on AA-Q-N2 microbeads suspended in an ~ 10 µm layer of hydrogel	3.65
M-2	ACIB on AMC microbeads suspended in an ~ 10 µm layer of hydrogel	3.36
M-3	Iminocoumarin on AMC microbeads suspended in an ~ 10 µm layer of hydrogel	7.30
M-4	Iminocoumarin on p-HEMA microbeads suspended in an ~ 10 µm layer of hydrogel	8.42
M-5	ACISA on AMC microbeads suspended in an ~ 10 µm layer of hydrogel	2.67
M-6	ACISA on p-HEMA microbeads suspended in an ~ 10 µm layer of hydrogel	3.80
M-7	B-2 and B-4 particles in an ~ 10 µm layer of hydrogel	

Immobilization of ACIB via a Mannich reaction:

The immobilization procedure for the indicators via the Mannich reaction was adapted from Hermanson⁴². 10 mg of **ACIB** were dissolved in 5 mL of ethanol/water solution (1:1, v/v) containing 50 µL of 36 % HCl. Then 200 µL of a 37% aqueous solution of formaldehyde were added. 300 mg of amino-modified polymer beads (AA-Q-N2 and AMC) were added to the solution and stirred at 60 °C for 12 h. The particles were separated from the solution by centrifugation and washed several times with water and ethanol until the washing ethanol became colourless. The particles were dried at ambient air to give pH-sensitive particles B-1 and B-2.

In order to obtain the membranes M-1 and M-2, 15 mg of the beads B-1 and B-2, respectively were added to 600 mg of a 5% (wt/wt) solution of hydrogel in ethanol/water (9:1,

v/v). The cocktail was spread as an approximately 120 μm thick film onto a polyester support of 125 μm thickness. After evaporation of the solvents, the yellow-colored films had a thickness of 10 μm (as calculated from the employed amounts).

Immobilization of **I**

The immobilization was performed in two steps (see Fig. 2.2). First, the triazine moiety was attached to the surface of the polymer beads (amino-modified p-HEMA or AMC). 10 mg of 2,4,6-trichlorotriazine were dissolved in 3 mL of acetonitrile, and 100 mg of the polymer were added. The suspension was stirred for 12 h at room temperature. After stirring, the polymer powder was filtered and dried under vacuum.

The second step involves attachment of the indicator to the triazine linker. The corresponding polymer beads obtained in the first step were added to a solution of the dye (2 mg of **I** and 20 μL of triethylamine in 2 mL of DMF for AMC, or 4 mg of **I** and 40 μL of triethylamine in 2 mL of DMF for amino-modified p-HEMA). The suspension was stirred for 1 h at 50 $^{\circ}\text{C}$. The particles were separated from the solution by centrifugation and washed several times with water and ethanol until the solvents remained colourless. The particles were dried at ambient air to give the sensor beads B-3 and B-4.

The preparation of the respective sensor membranes was similar to M-1. 15 mg of beads B-3 (B-4) were added to 600 mg of a 5% (wt/wt) solution of hydrogel in ethanol/water (9:1, v:v). The cocktail was spread as an approximately 120 μm thick film onto a 125 μm polyester support. After evaporation of the solvents, the yellow-colored films M-3 and M-4 had a thickness of 6 μm .

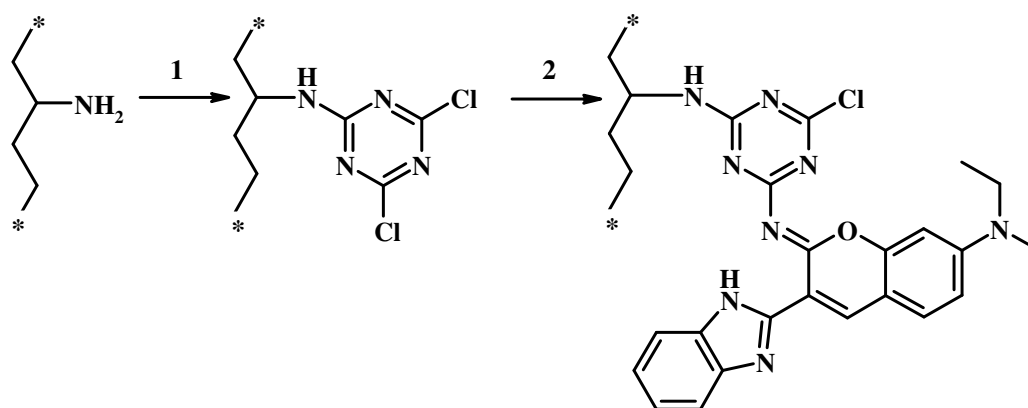


Figure 2.2 Immobilization of iminocoumarin on microbeads of AMC or amino-modified p-HEMA surface: (1) acetonitrile, 12 h at r.t.; (2) DMF and triethylamine, 1 h at 50 $^{\circ}\text{C}$.

Immobilization of ACISA:

ACISA was covalently attached to the surface of the beads using a standard peptide coupling procedure⁴³. First, 150 mg of amino-modified polymer beads (AMC, p-HEMA) were added to 3.0 g of a saturated aqueous solution of Na_2CO_3 and the suspension was stirred overnight. 3 mg of DCC, 3 mg of NHS, 3 mg of the dye and 10 μL of triethylamine were dissolved in 1 mL of DMF and the solution was also stirred overnight. Then, the suspension and the dye solution were mixed and stirred for 2 h. The particles were separated from the solution by centrifugation and washed several times with water and ethanol until the washing ethanol was colorless. The particles were dried at ambient air to give pH-sensitive beads B-5 and B-6.

2.2.4 Preparation of the Ratiometric Sensing Material

15 mg of the **ACISA**-based pH-sensitive beads B-5 and B-6, respectively were added to 600 mg of a 5% wt. solution of hydrogel D4 in ethanol/water (9:1, v/v). This sensor cocktail was stirred overnight, then knife-coated onto the polyester support and dried at ambient air to obtain the sensor films M-5 and M-6 with a thickness of about 10 μm .

2.2.5 Preparation of the Mixed-Indicator pH Sensitive Sensor Membrane

20 mg of the iminocoumarin/p-HEMA particles B-4 and 2 mg of ACIB/AMC microbeads B-2 were added to 600 mg of a 5% wt/wt solution of hydrogel D4 in ethanol/water (9:1, v/v). The cocktail was stirred overnight at room temperature and then knife-coated onto a polyester support to give the pH-sensitive sensor membrane M-7.

2.2.6 Instruments and Measurements

Fluorescence excitation and emission spectra as well as titration plots of the sensor foils were acquired with an Aminco-Bowman Series 2 luminescence spectrometer (www.thermo.com) equipped with a continuous wave 150 W xenon lamp as light source and with a home-made flow-through cell⁴⁴, (see Fig. 2.3). A piece of sensor foil was placed into the cell and the buffer solutions were allowed to pass through it at a rate of 1 $\text{mL}\cdot\text{min}^{-1}$. The sample solutions were transported by a Minipuls-3 peristaltic pump (www.gilson.com) via a silicone tube (\varnothing 1.0 mm). Absorption spectra were acquired on a Hitachi U-3000 UV-VIS spectrophotometer (www.hitachi-hitec.com).

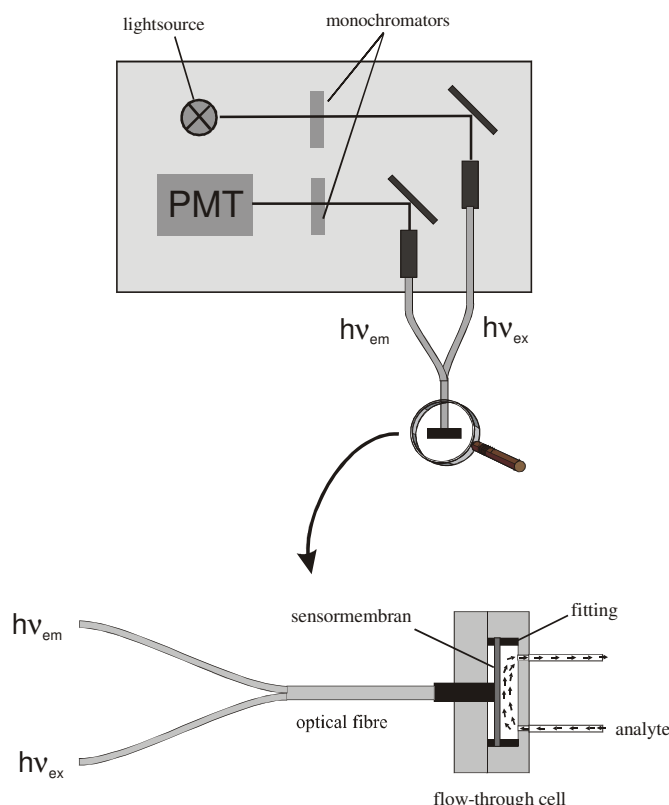


Figure 2.3 Schematic representation of the instrumental set-up.

Fluorescence quantum yields were evaluated using an aqueous solution of fluorescein as the standard (0.1 M NaOH, $QY = 0.9^{45}$).

The pK_a values of the indicators were determined by fluorimetric titration using the Boltzmann equation⁴⁶:

$$I = \frac{A_{\max} - A_{\min}}{1 + 10^{(pH - pK_a)/b}} + A_{\max}, \quad (2.1)$$

where I is fluorescence intensity, A_{\max} and A_{\min} are the intensities for the protonated and deprotonated forms of the indicator, respectively, and b is the numerical coefficient.

Photostability of the indicators (ethanol/aqueous buffer, 1/1 v/v, pH 2) was studied in comparison to carboxyfluorescein (ethanol/aqueous buffer, 1/1 v/v, pH 9) using a high pressure mercury lamp (Osram HBO 200 W, www.osram.com). The 436 nm emission line was isolated with a combination of a BG 25 band pass glass filter (Schott, www.schott.com) and GG 420 long pass glass filter (Schott).

For the preparation of the buffer solutions, doubly distilled water was used. The pH of the buffer solutions was adjusted using a Knick digital pH meter (www.knick.de) calibrated at

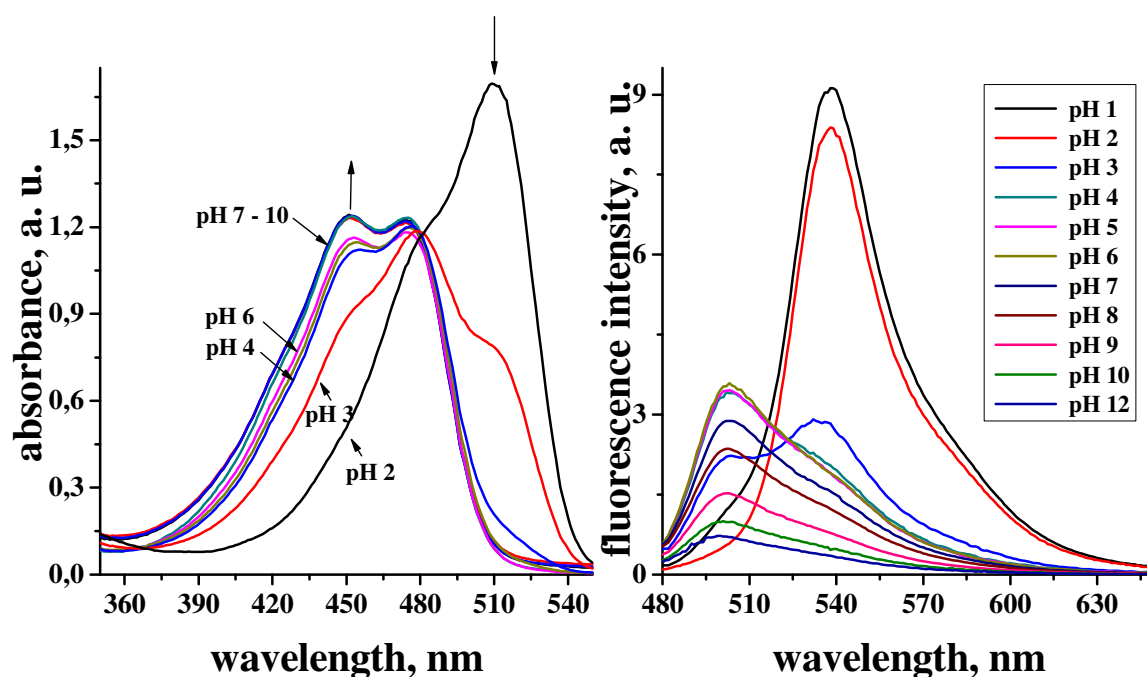
20 \pm 2 °C using standard buffers of pH 7.0 and 4.0 (www.merck.de). The pH was adjusted to the desired values using MOPS (for pH 6 to 10) and MES (for pH 2 to 5) buffer salts. The buffers were adjusted to constant ionic strength (I = 140 mM) using sodium chloride as the background electrolyte⁴⁷.

2.3 Results and Discussion

2.3.1 Spectral Properties of the pH Indicators in Solution

Absorption and emission spectra of the indicator ACIB at different pH values are shown in Fig. 2.4A. The spectral properties of the dye are strongly dependent on the pH value. Protolytic equilibria are illustrated in Fig. 2.4B. Three forms of the indicator can be distinguished.

A.



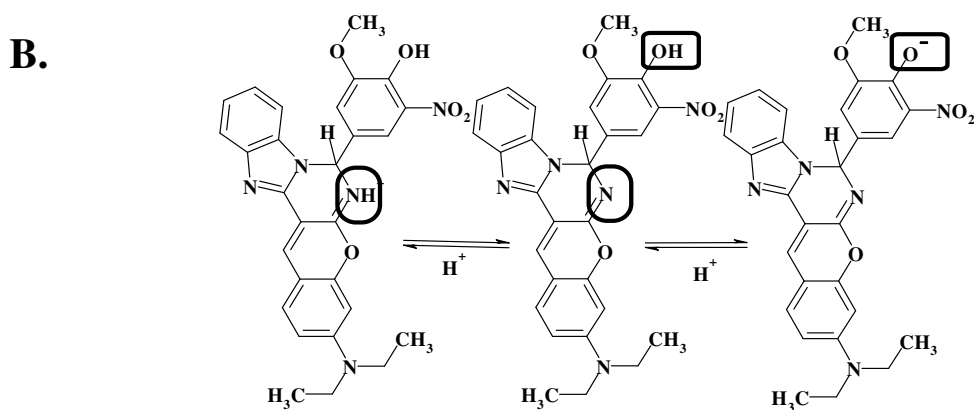


Figure 2.4 A. Absorption and emission spectra of ACIB at pH values from 2 to 10, using a solution of the indicator in an ethanol – water mixture (1:1, v/v), $\lambda_{\text{ex}} = 470 \text{ nm}$; **B.** Protolytic equilibria of ACIB in solution.

Only the acidic and the neutral forms display fluorescence. The imino group of the fluorescent acidic form of the dye ($\lambda_{\text{max}} = 510 \text{ nm}$) is deprotonated in slightly acidic media ($\text{pK}_{\text{a}} \sim 3$) which results in a hypsochromic shift of the absorption band ($\lambda_{\text{max}} = 450 \text{ nm}$). The second step involves dissociation of the peripheral hydroxy group of the benzoic ring. Here, no change in the absorption spectrum is observed, the fluorescence is, however, quenched (Fig. 2.5). This can be attributed to photoinduced electron transfer (PET)⁴⁸. The fluorimetric titration of ACIB at different excitation wavelengths confirms the above equilibria (Fig. 2.5). When excited at 470 nm, the fluorescence intensity undergoes a 25-fold decrease in two steps on changing pH from 2 to 12, showing pK_{a} values of 2.7 and 7.8. While the first step involves equilibrium between the two fluorescent forms, the second step results in complete quenching of fluorescence. However, when the dye is excited at 505 nm or 520 nm, where only the acidic form absorbs, no second step is observable. Because titration in two steps is undesirable, excitation at $\sim 505 \text{ nm}$, which can be performed by a cheap blue-green LED, is preferred.

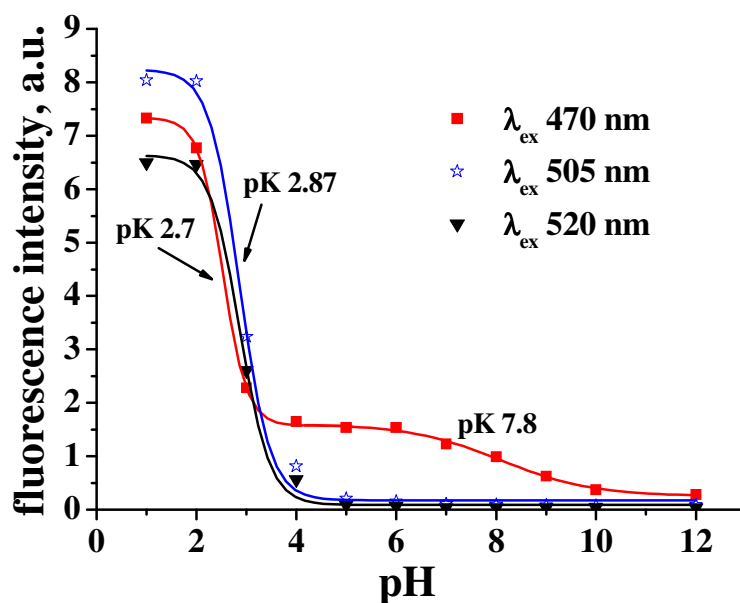


Figure 2.5 Titration plots of ACIB at different excitation wavelengths 470, 505 and 520 nm ($\lambda_{em} = 540$ nm). The ionic strength of the buffer solution was 140 mM.

The titration plots of ACIDA are similar to ACIB and show fluorescence changes in two steps from pH 2 to 11 at excitation at 490 nm ($pK_1 = 3.80$ and $pK_2 = 9.02$). Likewise, the titration shows only one pK_a value (3.84) when the dye is excited at 507 nm (Fig. 2.6B). The emission of the indicator in solution is shown in Fig. 2.7.

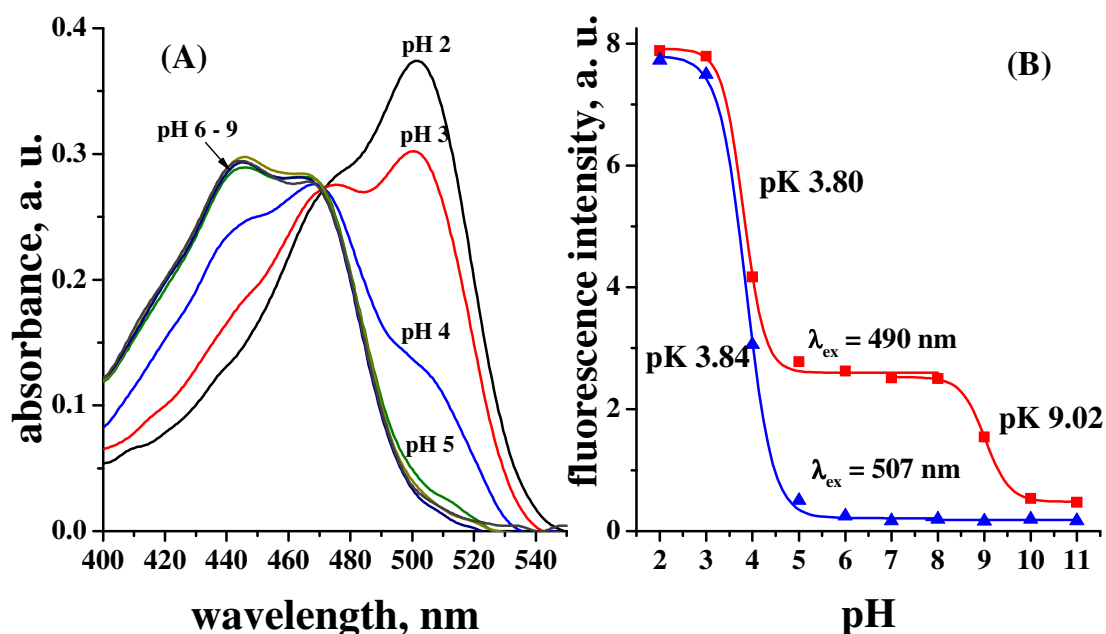


Figure 2.6 A, absorption spectra of ACIDA at pH from 2 to 9 in an ethanol – water mixture

(1:1, v/v)); **B**, titration plots of ACIB at different excitation wavelengths 490 and 507 nm ($\lambda_{em} = 540$ nm). The ionic strength of the buffer solution was 140 mM.

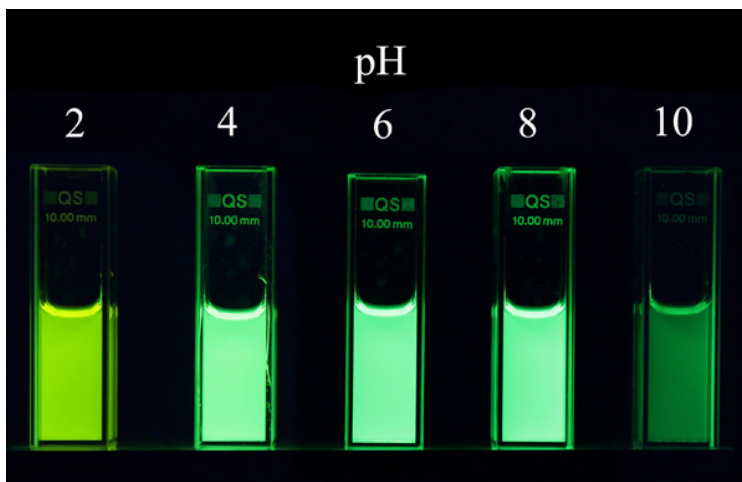


Figure 2.7 Photography of the emission of indicator ACIDA in ethanol-water mixture (1:1, v/v) from pH 2 to 10.

The absorption spectra of ACISA (Fig. 2.8A) are similar to the absorption spectra of ACIB Fig. 2.4A and ACIDA Fig. 2.6A. The isosbestic point is observed at 477 nm. Both the protonated and the deprotonated form are emissive (Fig. 2.9A). Unlike ACIB and ACIDA, no quenching is observed at basic conditions. The fluorescence intensity remains constant when increasing pH from 5 to 12 (Fig. 2.9A). It is likely that the dissociation of the COOH group of the phenyl ring prevents dissociation of the OH group, and thus the PET effect. ACISA, therefore, can be used as a ratiometric pH indicator. Fluorescence intensity is an ambitious parameter, because it is strongly influenced by the intensity of the excitation light, the dye concentration, turbidity of the probe, scattering etc. Ratiometric measurement overcomes these drawbacks. When excited at the isosbestic point, the ratio of the luminescence intensities at 502 and 537 nm (corresponding to the maxima of the basic and acidic forms) is dependent only on the pH (Fig. 2.9B). A linear dependence was observed in the pH range 2.5 – 4.5. At a pH higher than 6.0 the ratio remains constant.

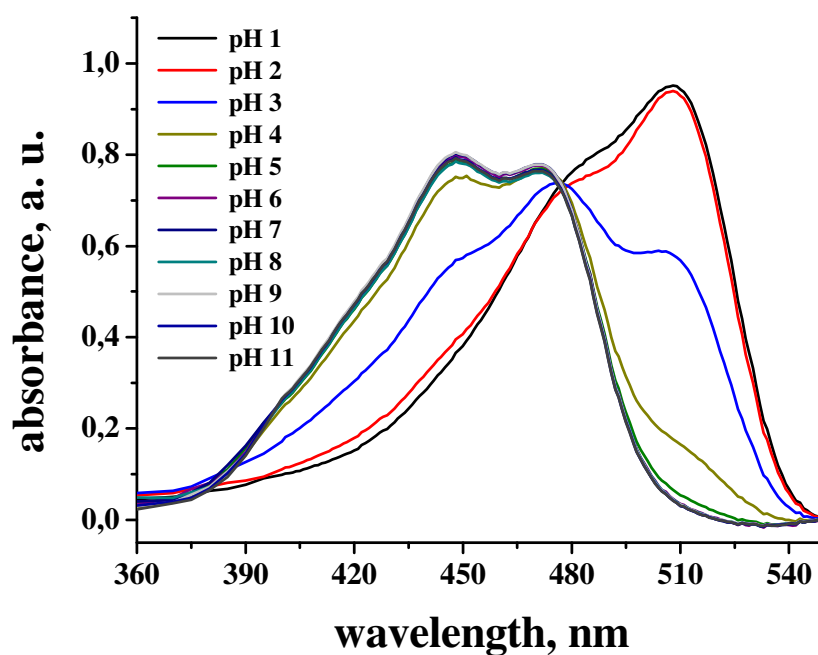


Figure 2.8 Absorption spectra of ACISA in ethanol – water solution (1:1, v/v) at pH values from 1 to 11.

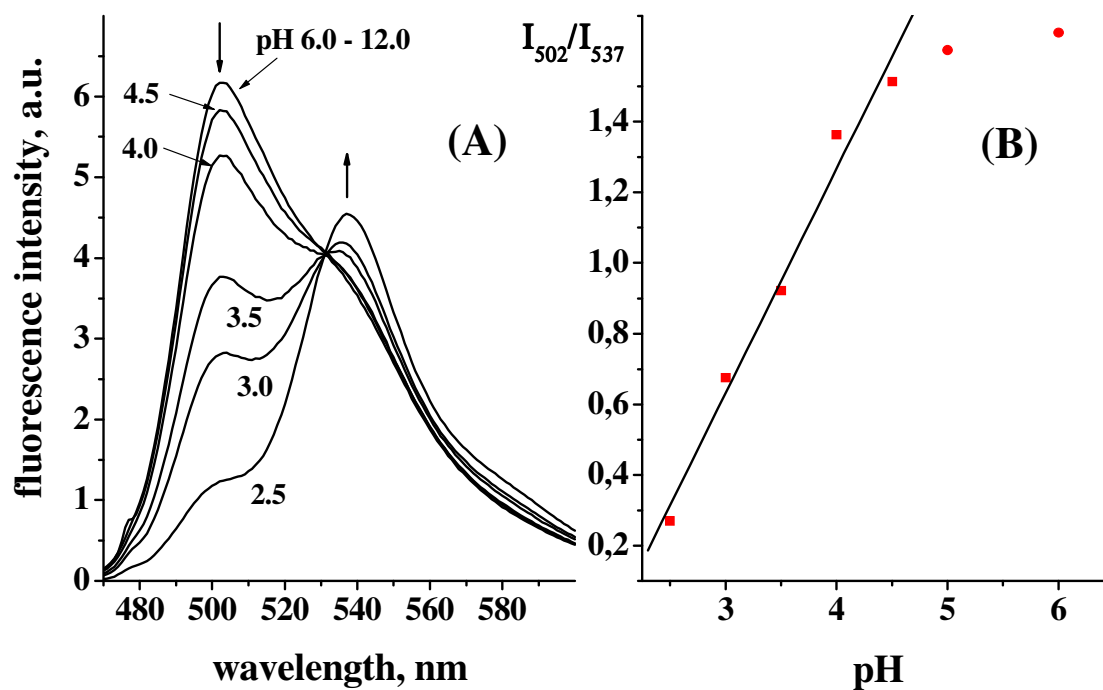


Figure 2.9 pH dependence of the fluorescence of the ACISA indicator: **A**, emission spectra in ethanol : aqueous buffer (1:1, v/v), IS 140 mM, $\lambda_{exc} = 477$ nm; **B**, dependence of the intensity ratio.

The spectral properties of the indicators are summarized in Table 2.2. As mentioned above, the protolytic equilibria for ACIB and ACIDA involve three forms of the indicators. The basic form is non-emissive due to the PET effect. Although the intermediate forms of ACIB and ACIDA are fluorescent, it is impossible to determine the fluorescence quantum yields precisely, because the equilibrium includes the two other forms. The obtained smaller quantum yields of the ACIB dye compared to ACIDA and ACISA are attributed to the quenching effect of the nitro group in the benzene ring.

Table 2.2 Spectral properties of the pH indicators in ethanol – aqueous buffer (1 : 1, v/v) solution.

Dyes	<i>Acidic form (pH 2)</i>				<i>Basic form (pH 11)</i>			
	$\lambda_{\max}^{\text{abs}}$	$\epsilon, \cdot\text{M}^{-1}\cdot\text{cm}^{-1}$	$\lambda_{\max}^{\text{em}}$	Φ_{em}	$\lambda_{\max}^{\text{abs}}$	$\epsilon, \cdot\text{M}^{-1}\cdot\text{cm}^{-1}$	$\lambda_{\max}^{\text{em}}$	Φ_{em}
I	480	62900	520	0.51	430	48400	480	0.88
ACIB	510	64100	540	0.18	452, 474	54000	505	< 0.01
ACIDA	500	58400	539	0.50	444, 465	41300	500	< 0.01
ACISA	507	55400	537	0.56	447, 471	46400	502	0.89

2.3.2 Photostability of the pH Indicators

Photostability is one of the critical criteria of luminescent indicators, particularly of fluorescent ones. Generally, measurement of the decay time of long-lived luminescent indicators (e.g. oxygen or temperature indicators) has become very popular and is now possible with unsophisticated and comparatively cheap equipment. Photodecomposition of such indicators always results in lower luminescence intensity, but not necessarily in a drift of the decay time. It is often only slightly or not at all affected by partial decomposition. The situation is, however, different in case of short-lived fluorescent indicators. Fluorescence intensity is influenced by many factors as discussed above. Therefore, different referencing techniques were developed. The fluorescence intensity can be referenced against the intensity^{49,50} or the decay time (in the Dual Lifetime Referencing method, see Chapter 3)⁵¹⁻⁵³ of another luminophore. It is evident that photodecomposition of the fluorescent indicators will severely affect the referenced data as well.

Photostability of the novel pH indicators was tested using carboxyfluorescein as a standard, which is by far the most popular fluorescent indicator (Fig. 2.10). After 60 min of

continuous illumination using a mercury lamp, the fluorescence intensity was reduced by 10 – 13 % for all of the presented indicators. Under the same conditions, a ~ 65 % decrease in fluorescence intensity was observed for carboxyfluorescein. Thus, the coumarin chromophores possess superior photostability.

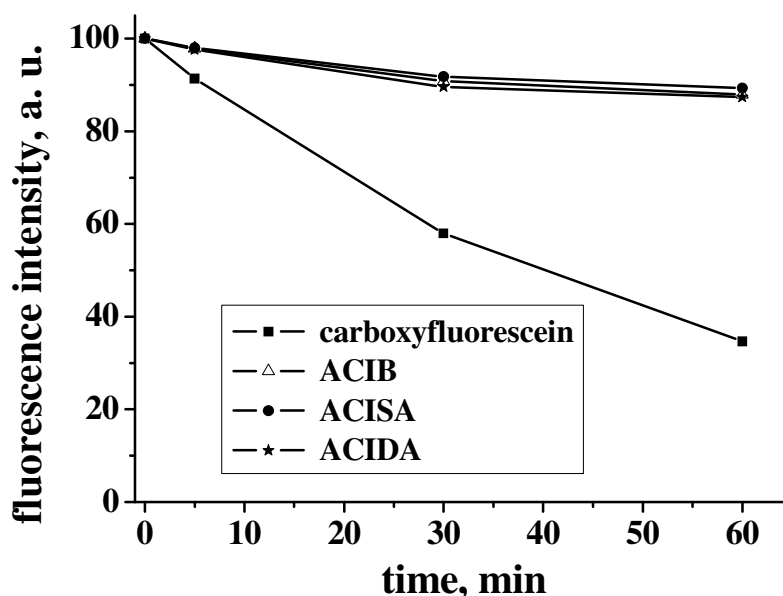


Figure 2.10 Photobleaching of the pH indicators. The solutions were irradiated by the 436 nm line of a mercury lamp, the fluorescence was measured at 530 nm ($\lambda_{\text{exc}} = 490$ nm).

2.3.3 pH-Sensitive Membranes

Excellent photostability, relatively high brightness and good compatibility with inexpensive light-emitting diodes (470 nm and 505 nm LEDs) make the indicators suitable for the preparation of membranes for pH-sensing in different ranges.

A polyurethane hydrogel was selected as the polymer matrix, because this biocompatible material has excellent ion permeability⁵⁴, good mechanical properties and high stability at various pH values and temperatures. Although the pH indicators can simply be dissolved in the matrix, this is undesirable because of potential leaching into the sample. Leaching can be prevented by using dyes containing highly lipophilic moieties^{55,56}, or by covalent immobilization of the indicators on the surface of a polymer/polymer microbeads^{33,57,58}. Such microbeads can then be easily dispersed in the matrix together with a reference luminophore.

Although the pK_{a} of the probe is mainly influenced by the properties of the indicator

itself, the material of the polymer particles can shift the pK_a significantly as well. Therefore, three different dye-polymer combinations were investigated. We used polymer microbeads of aminocellulose (AMC), an amino-modified polyacrylamide derivative (AA-Q-N2) and an amino-modified poly(hydroxyethyl) methacrylate (p-HEMA). They differ significantly in their properties, particularly with respect to polarity and charges at the surface. The titration curves for the probes obtained by covalent immobilization of ACIB via the Mannich reaction on the surface of AA-Q-N2 and AMC microbeads are shown in Fig. 2.11 (1 and 2). The pK_a values calculated using eq. 2.1 are 3.65 and 3.36, respectively. The titration curves show only one inflection point at pH 3.5 at an excitation wavelength of 500 nm, which is comparable with the characteristics of the dye in solution.

The pK_a values are slightly higher for the immobilized form of the dye compared to the values in aqueous solution ($pK_a = 2.8$). Usually, a small increase in pK_a is observed upon covalent⁵⁹ or electrostatic⁶⁰ immobilization of an indicator, which is attributed to the decrease in the polarity of the microenvironment. Due to their low pK_a values, both probes are suitable for pH monitoring during sour fermentation of milk or analyses of acidic soils.

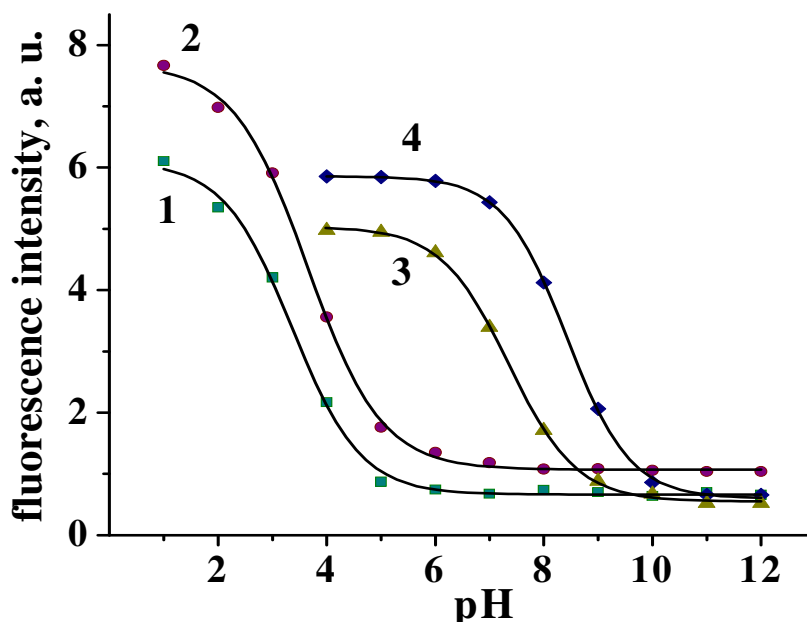


Figure 2.11 Titration curves for the pH-sensitive membranes: 1, ACIB/AMC (M-2) $\lambda_{ex} = 495$ nm, $\lambda_{em} = 520$ nm; 2, ACIB/ AA-Q-N2 (M-1) $\lambda_{ex} = 500$ nm, $\lambda_{em} = 530$ nm; 3 and 4, iminocoumarin/AMC (M-3) and iminocoumarin/p-HEMA (M-4), respectively $\lambda_{ex} = 488$, $\lambda_{em} = 520$ nm.

For many important applications such as measurements of pH in seawater or marine sediments (which are slightly basic) it is necessary that the pK_a values of a pH-sensitive probe are in the pH range from 7 to 9. The titration curves for iminocoumarin immobilized via a triazin linker onto the surface of AMC (pK_a of 7.30) and p-HEMA (pK_a of 8.42) are shown in Fig. 2.11. Again, immobilization of the indicator results in increase of the pK_a compared to the indicator in solution ($pK_a = 7.0$), the effect being more significant for the less polar p-HEMA.

While the polymer microbeads B-2 (ACIB/AMC) and B-4 (iminocoumarin/p-HEMA) are suitable for the determination of pH in acidic and basic media, respectively, mixing the beads results in an indicator system (M-7), which possesses sensitivity to pH over a broad range, similar to the dynamic range of the glass electrode (Fig. 2.12).

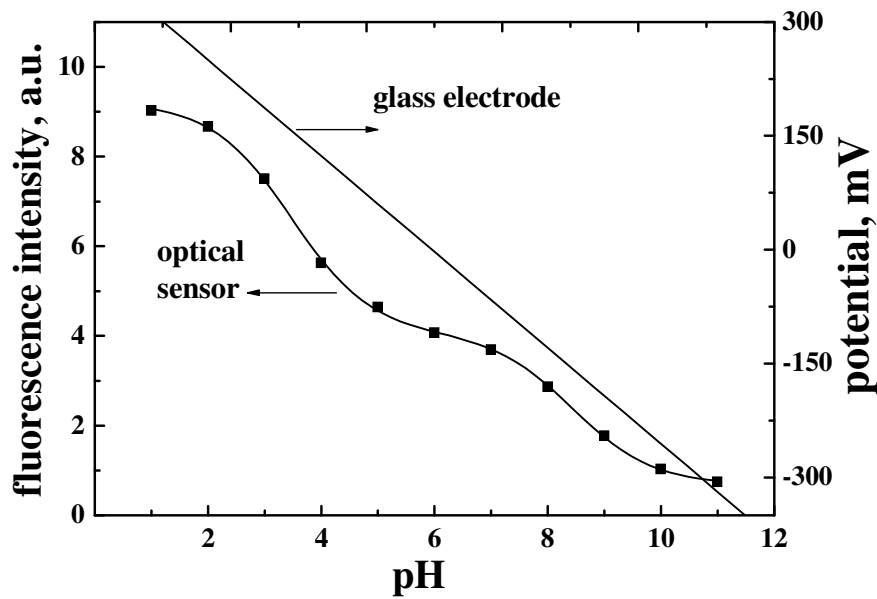


Figure 2.12 pH dependence of the fluorescence intensity of the mixed indicator sensor membrane M-7 and calibration plot of the glass electrode at 25 °C (linear). The curve represents a fit via eq. 2.3.

The titration curve presented in Fig. 2.12 is actually a combination of two sigmoidal response curves described by eq. 2.1. Because the overall intensity I is a sum of the intensities of the components I^1 and I^2 , the following equation is valid:

$$I = I^1 + I^2 = \frac{A_{\max}^1 - A_{\min}^1}{1 + 10^{(pH - pK_a^1)/b^1}} + A_{\max}^1 + \frac{A_{\max}^2 - A_{\min}^2}{1 + 10^{(pH - pK_a^2)/b^2}} + A_{\max}^2 \quad (2.2)$$

Assuming that $A_{\min}^1 = A_{\max}^2$ and coefficients b^1 and b^2 are similar the equation can be

transformed into the following form:

$$I = \frac{A_{\max}^1 - A_{\max}^2}{1 + 10^{(pH - pK_a^1)/b}} + A_{\max}^1 + \frac{A_{\max}^2 - A_{\min}^2}{1 + 10^{(pH - pK_a^2)/b}} + A_{\max}^2 \quad (2.3)$$

The above equation describes the experimental dependence very well (correlation coefficient r^2 is 0.9998). The following fit parameters are obtained by fitting (with Microcal™ Origin® 6.0): $A_{\max}^1 = 7.19$, $A_{\max}^2 = 2.03$, $A_{\min}^2 = -1.35$, $pK_a^1 = 3.47$, $pK_a^2 = 8.45$, $b = 1.63$. Although the pK_a values are very close to those obtained for the individual probes (3.36 and 8.42 for B-2 and B-4, respectively), the fit parameters A_{\max}^1 , A_{\max}^2 and A_{\min}^2 are smaller than expected. Nevertheless, excellent fitting is achieved.

The equilibrium response times (t_{95}) for the sensor based on the mixture of microbeads of types B-2 and B-4 as well as for those based on individual microbeads do not exceed 25 s when going from pH 12 to pH 2, and 60 s for the reverse direction. Such response times are typical for most optical pH sensors reported in literature^{33,17,61}.

It is necessary to stress that the presented sensor membrane (M-7) for a broad region of pH is only a model which is hardly suitable for practical purposes because of the drawbacks of fluorescence intensity measurements. One of the possible solutions for obtaining reproducible signals is a ratiometric system using an inert fluorescent dye with an absorbance similar to that of the pH indicators and a red-shifted emission (e.g. rhodamines or 4-dicyanomethylene-2-methyl-6-(p-(dimethylamino)styryl)-4H-pyran (DCM)). Alternatively, a DLR scheme can be applied.

The behavior of the ACISA indicator coupled to the polymer surface via amide linkage is similar to what was observed for the indicator solution (Fig. 2.9). Similarly, when the intensity ratio of the two forms of the indicator (I_{501}/I_{534} ; λ_{\max} are 501 and 534 nm for the basic and the acidic forms, respectively) is plotted vs. pH, a linear part is observed (Fig. 2.13). Again, the less polar p-HEMA favors higher pK_a values than aminocellulose (3.80 and 2.67 for M-6 and M-5, respectively).

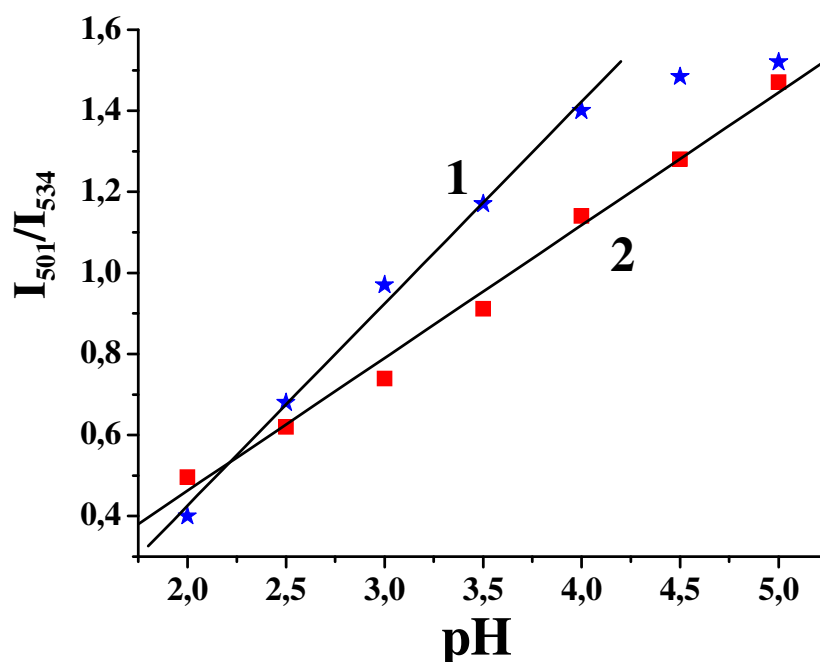


Figure 2.13 Response of ACISA to pH; 1, ACISA/AMC beads M-5 and 2, ACISA/p-HEMA beads M-6 ($\lambda_{\text{exc}} = 477 \text{ nm}$).

As was shown, the ACISA-based pH-sensitive microbeads do not need any additional referencing to obtain unbiased pH values.

2.4 Conclusion

Several iminocoumarin derivatives were synthesized, which represent a new type of fluorescent pH indicators. The indicators possess moderate to high brightness, excellent photostability and are compatible with commercially available LEDs. In each case, two forms of the indicators are fluorescent, which was used for the design of a ratiometric sensor in the case of the ACISA dye. In case of ACIB and ACIDA, a PET effect is observed at higher pH which results in quenching of fluorescence. The titration curves are highly dependent on the excitation wavelength and show two inflection points when excited at $\sim 470 \text{ nm}$, but only one inflection point when excited by a 505-nm LED.

We have shown that all of the presented indicators can be immobilized onto the surface of polymer microbeads using different procedures yielding pH-sensitive microparticles. ACIB, ACIDA or iminocoumarin-containing fluorescent microbeads can be dispersed in

polyurethane hydrogel together with reference luminescence particles to obtain a DLR sensor. Due to the possibility of ratiometric self-referencing the ACISA-based microbeads do not require a reference dye. The sensing membranes are suitable for measuring pH in different ranges, the properties being mainly influenced by the nature of the pH indicator used, but also by the material of the polymer. Generally, a shift to higher pK_a is observed for polymers of lower polarity. A sensor membrane was introduced, which is based on the mixture of two different pH-sensitive microbeads (iminocoumarin/p-HEMA and ACIB/AMC) and makes pH measurements in the broad range of pH from 1 to 11 possible. Therefore, the covered range is comparable to a glass electrode.

The materials are promising for pH-sensing in seawater and marine environments (iminocoumarin-based microparticles), as well as in acidic soils and upon sour fermentation of milk (ACIB, ASIDA and ACISA-based microbeads).

2.5 References

1. Schroeder C, Weidgans B M, Klimant I **pH Fluorosensors for use in marine systems.** *Analyst* **2005**, 130(6), 907-916
2. Neurauter G, Klimant I, Wolfbeis O S **Fiber-optic microsensor for high resolution pCO₂ sensing in marine environment.** *Fresenius J. Anal. Chem.* **2000**, 366, 481-487
3. Mekhail K, Khacho M, Gunaratnam L, Lee S **Oxygen sensing by H⁺. Implications for HIF and hypoxic cell memory.** *Cell Cycle* **2004**, 3, 1027-1029
4. Kojima S, Suzuki H **A micro sensing system for blood gas analysis.** *Chem. Sensors* **2003**, 19, 25-27
5. Juarez Tomas M S, Wiese B, Nader-Macias M E **Effects of culture conditions on the growth and auto-aggregation ability of vaginal Lactobacillus johnsonii CRL 1294.** *J. Appl. Microbiol.* **2005**, 99, 1383–1391
6. Drosinos E H, Mataragas M, Nasis P, Galiotou M, Metaxopoulos J **Growth and bacteriocin production kinetics of Leuconostoc mesenteroides E131.** *J. Appl. Microbiol.* **2005**, 99, 1314–1323
7. Marshall A J, Blyth J, Davidson C A B, Lowe C R **pH-Sensitive Holographic Sensors** *Anal. Chem.* **2003**, 75, 4423-4431

- 8 Simova E, Simov Z, Beshkova D, Frengova G, Dimitrov Z, Spasov Z **Amino acid profiles of lactic acid bacteria, isolated from Kefir grains and kefir starter made from them.** International J. Food Microbiol. **2006**, 107, 112 – 123
9. Diwu Z, Chen C S, Zhang C, Klaubert D H, Haugland R P **A novel acidotropic pH indicator and its potential application in labeling acidic organelles of live cells.** Chem. Biol. **1999**, 6, 411-418
10. Hara-Chikuma M, Wang Y, Guggino S E, Guggino W B, Verkman A S **Impaired acidification in early endosomes of CIC-5 deficient proximal tubule.** Biochem. Biophys. Research Commun. **2005**, 329, 941–946
11. Simek M, Jisova L, Hopkins D W **What is the so-called optimum pH for denitrification in soil?** Soil Biol. Biochem. **2001**, 34, 1227–1234
12. Muhrizal S, Shamshuddin J, Fauziah I, Husni M A H **Changes in iron-poor acid sulfate soil upon submergence.** Geoderma **2006**, 131, 110– 122
13. Topaloglu U, Muftuoglu T, Akturk Z, Ekinci I H, Peker O, Unalmis S **Omeprazole is More Effective than Famotidine for Preventing Acute Gastritis in Rats.** Surg. Today **2004**, 34, 690–694
- 14 Wiczling P, Markuszewski M J, Kaliszan M, Galer K, Kaliszan R **Combined pH/organic solvent gradient HPLC in analysis of forensic material.** J. Pharm. Biomed. Anal. **2005**, 37, 871-875
15. Wolfbeis OS **Fiber-Optic Chemical Sensors and Biosensors.** Anal Chem **2006**, 78, 3859-3873 and references therein.
16. Cajlakovic M, Lobnik A, Werner T **Stability of new optical pH sensing material based on cross-linked poly(vinyl alcohol) copolymer.** Anal Chim Acta **2002**, 455, 207-213
17. Niu C G, Gui X Q, Zeng G M, Guan A L, Gao P F, Qin P Z **Fluorescence ratiometric pH sensor prepared from covalently immobilized porphyrin and benzothioxanthene.** Anal. Bioanal. Chem. **2005**, 383, 349–357
18. Bernhard D D, Mall S, Pantano P **Fabrication and characterization of microwell array chemical sensors.** Anal. Chem. **2001**, 73, 2484–2490
19. Leiner M J P, Wolfbeis O S (eds) **Fiber Optic Chemical Sensors and Biosensors.** CRC Press, Boca Raton, **1991**, 63
20. Leiner M J P, Hartmann P **Theory and practice in optical pH sensing.** Sens. Actuators B **1993**, 11, 281-289
21. Niu C-G, Gui X-Q, Zeng G-M, Yuan X-Z **A ratiometric fluorescence sensor with broad dynamic range based on two pH-sensitive fluorophores.** Analyst **2005**, 130(11),

1551-1556

22. Miliani C, Romani A, Favaro G **Acidichromic effects in 1,2-di- and 1,2,4-tri-hydroxyanthraquinones. A spectrophotometric and fluorimetric study.** J. Phys. Org. Chem. **2000**, 13, 141-150
23. Lin J, Liu D **An optical pH sensor with a linear response over a broad range.** Anal. Chim. Acta **2000**, 408, 49-55
24. Netto EJ, Peterson GJ, McShane M, Hampshire V **A fiber-optic broad-range pH sensor system for gastric measurements.** Sens. Actuators B **1995**, 29, 157-163
25. Faiz Bukhari Mohd Suah, Musa Ahmad, Mohd Nasir Taib **Optimisation of the range of an optical fibre pH sensor using feed-forward artificial neural network.** Sens. Actuators B **2003**, 90, 175-181
26. Lobnik A, Majcena N, Niederreiterb K, Uray G **Optical pH sensor based on the absorption of antenna generated europium luminescence by bromothymol blue in a sol-gel membrane.** Sens. Actuators B **2001**, 74, 200-206
27. Nishimura G, Shiraishi Y, Hirai Y **A fluorescent chemosensor for wide-range pH detection.** Chem. Commun. **2005**, 5313-5315
28. Sartoris F J, Bock C, Serendero I, Lannig G, Poertner H O **Temperature-dependent changes in energy metabolism, intracellular pH and blood oxygen tension in the Atlantic cod.** J. Fish Biology **2003**, 62(6), 1239-1253
29. Arain S, John G T, Krause C, Gerlach J, Wolfbeis O S, Klimant I **Characterization of microtiterplates with integrated optical sensors for oxygen and pH, and their applications to enzyme activity screening, respirometry, and toxicological assays.** Sens. Actuators B **2006**, 113(2), 639-648
30. Smith J P, Drewes L R **Modulation of Monocarboxylic Acid Transporter-1 Kinetic Function by the cAMP Signaling Pathway in Rat Brain Endothelial Cells.** J. Biol. Chem. **2006**, 281(4), 2053-2060
31. An Z, Moehwald H, Li J **pH Controlled Permeability of Lipid/Protein Biomimetic Microcapsules.** Biomacromolecules **2006**, 7(2), 580-585
32. Herrmann J M, Kantarci A, Long H, Bernardo J, Hasturk H, Wray L V, Simons E R, Van Dyke T E **Simultaneous measurements of cytoplasmic Ca²⁺ responses and intracellular pH in neutrophils of localized aggressive periodontitis (LAP) patients.** J. of Leukocyte Biology **2005**, 78(3), 612-619

33. Vasylevska G S, Borisov S M, Krause C, Wolfbeis O S **Indicator-Loaded Permeation-Selective Microbeads for Use in Fiber Optic Simultaneous Sensing of pH and Dissolved Oxygen**. Chem. Materials 2006, 18, 4609-4616
34. Mordon S, Devoisselle M, Soulie J **Fluorescence spectroscopy of pH in vivo using a dual-emission fluorophore (C-SNAFL-1)**. J. Photochem. Photobiol. B **1995**, 1, 19-23
35. Leiner M J P **Optical sensors for in vitro blood gas analysis**. Sens. Actuators B **1995**, 1-3, 169-173
36. Bellerby R G J, Olsen A, Johannessen T, Croot P A **A high precision spectrophotometric method for on-line shipboard seawater pH measurements: the automated marine pH sensor (AMpS)**. Talanta **2002**, 1, 61-69
37. Martz T R, Carr J J, French C R, DeGrandpre M D A **A submersible autonomous sensor for spectrophotometric pH measurements of natural waters**. Anal. Chem. **2003**, 8, 1844-1850
38. Whitaker J E, Haugland R P, Prendergast F G **Spectral and photophysical studies of benzo[c]xanthene dyes: dual emission pH sensors**. Anal. Biochem. **1991**, 2, 330-344
39. Parker J W, Laksin O, Yu C, Lau M L, Klima S, Fisher R, Scott I, Atwater B W **Fiber-optic sensors for pH and carbon dioxide using a self-referencing dye**. Anal. Chem. **1993**, 17, 2329-2334
40. Karasev A A, Lukatskaya L L, Rubtsov M I, Zhykol E K, Yarmolenko S N, Ponomarev O A **Synthesis, protolytic equilibrium and stability of 2-amino-3-(2-benzimidazolyl)-1-benzopyrylium salts in aqueous alcoholic medium**. Russ. J. Gen. Chem. **1995**, 65, 1416-1425
41. Rajagopal R, Shenoy V U, Padmanabhan S, Sequeira S, Seshadri S **Synthesis of fluorescent 2,3-fused coumarin derivatives**. Dyes Pigm. **1990**, 13(3), 167-175
42. Swindlehurst, Ben R.; Narayanaswamy, Ramaier. (eds) **Optical sensing of pH in low ionic strength waters**. Manchester, UK. 1(Optical Sensors), **2004**, 281-308
43. Hermanson G T **Bioconjugate Techniques**. Academic Press, New York, **1996**, 785 pp
44. Huber C, Werner T, Krause C, Leiner M J P, Wolfbeis O S **Overcoming the pH dependency of optical sensors: a pH-independent chloride sensor based on co-extraction**. Anal. Chim. Acta **1999**, 398, 137-143
45. Demas J N, Crosby G A **Measurement of photoluminescence quantum yields**. Review. J. Phys. Chem. **1971**, 76(8), 991-1024

46. Krause C, Werner T, Huber C, Wolfbeis O S, Leiner M J P **pH-Insensitive Ion Selective Optode: A Coextraction-Based Sensor for Potassium Ions.** *Anal. Chem.* **1999**, 71, 1544-1548
47. Perrin D D, Dempsey B *Laboratory Manuals*, Chapman & Hall, London, **1974**
48. Syzova Z A, Doroshenko A O, Lukatskaya L L, Rubtsov M I, Karasyov A A **Bichromophoric fluorescent dyes with rigid molecular structure: fluorescence ability regulation by the photoinduced intramolecular electron transfer.** *J. Photochem. Photobiol. A* **2004**, 165, 59–68
49. Park E J, Brasuel M, Behrend C, Philbert M A, Kopelman R **Ratiometric optical PEBBLE nanosensors for real-time magnesium ion concentrations inside viable cells.** *Anal. Chem.* **2003**, 75, 3784-3791
50. Park E J, Reid K R, Tang W, Kennedy R T, Kopelman R **Ratiometric fiber optic sensors for the detection of inter- and intra-cellular dissolved oxygen.** *J. Mater. Chem.* **2005**, 15, 2913-2919
51. Klimant I, Huber C, Liebsch G, Neurauter G, Stangelmayer A, Wolfbeis O S (eds) **Dual Lifetime Referencing (DLR) – a New Scheme for Converting Fluorescence Intensity into a Frequency-Domain or Time-Domain Information.** Springer, Berlin, **2001**
52. Lakowicz J R, Castellano F N, Dattelbaum J D, Tolosa L, Rao G, Gryczynski I **Low-Frequency Modulation Sensors Using Nanosecond Fluorophores.** *Anal. Chem.* **1998**, 70, 5115-5121
53. von Bultzingsloewen C, McEvoy A K, McDonagh C, MacCraith B D, Klimant I, Krause C, Wolfbeis O S **Sol-gel based optical carbon dioxide sensor employing dual luminophore referencing for application in food packaging technology.** *Analyst* **2002**, 127, 1478-1483
54. Peppas N A **Preparation, Methods & Structures of Hydrogels.** CRC Press, Boca Raton, **1986**
55. Drummen G P C, van Liebergen L C M, Op den Kamp J A F, Post J A **C11-BODIPY581/591, an oxidation-sensitive fluorescent lipid peroxidation probe: (micro)spectroscopic characterization and validation of methodology.** *Free Radical Biology Medicine* **2002**, 33, 473–490
56. Weidgans B M, Krause C, Klimant I, Wolfbeis O S **Fluorescent pH sensors with negligible sensitivity to ionic strength.** *Analyst* **2004**, 129, 645-650
57. Shortreed M, Kopelman R, Kuhn M, Hoyland B **Fluorescent Fiber-Optic Calcium Sensor for Physiological Measurements.** *Anal. Chem.* **1996**, 68, 1414-1418

58. Tan W, Shi ZY, Kopelman R **Development of submicron chemical fiber optic sensors.** Anal. Chem. **1992**, 64, 2985-2990
59. Kostov Y, Tzonkov S, Yotovan L, Krysteva M **Membranes for optical pH sensors.** Anal. Chem. Acta **1993**, 280, 15-19
60. Jones T P, Porter M D **Optical pH sensor based on the chemical modification of a porous polymer film.** Anal. Chem. **1988**, 60, 404-406
61. Sanchez-Barragan I, Costa-Fernandez JM, Sanz-Medel A **Tailoring the pH response range of fluorescent-based pH sensing phases by sol-gel surfactants co-immobilization.** Sens. Actuators B **2005**, 107, 69-76

Chapter 3

Dual Lifetime Referenced Sensor Membranes for Fiber Optic Determination of pH Using Microbeads and Nanoparticles

This chapter describes the application of new pH-sensitive membranes based on fluorescence lifetime measurement via the DLR method. A membrane has been developed that contains a pH indicator with a short decay time and an inert reference dye with a long decay time. Both dyes are embedded in microbeads which are contained in a hydrogel matrix. The luminescence of both dyes is excited by sinusoidally modulated light. The corresponding, pH-dependent emission intensity is also sinusoidal, and the resulting phase shift depends on the intensity ratio of the two luminophores. The fluorescence intensity of the pH indicator is the only variable parameter; therefore the phase shift is directly related to the analyte concentration.

3.1 Introduction

Fluorescence sensing is a rapidly expanding area and is widely used in biotechnology. Most sensing applications rely on measuring changes in fluorescence emission intensity. However, measuring the absolute intensity of fluorescence has proven to be a difficult task - it depends on too many factors, like intensity of the excitation light, concentration of the fluorescent dye, length of the optical path, primary and secondary inner filter effects, and quenching¹. One possible solution is the use of lifetime measurements; however, most available dyes have lifetimes in the nanosecond to picoseconds range. Measurements on this time scale require complex and sophisticated equipment². Furthermore, not every fluorescent dye that responds to an analyte changing its intensity exhibits a significant lifetime change. Another possible approach is to use ratiometric probes; however there are only a few, mostly for pH³⁻⁶, calcium⁷, and chloride⁸. Mixing two fluorophores having distinctly different spectra (excitation or emission) is also possible. The fluorophores should respond in opposite

directions to the analyte concentration⁹ or one of them should serve as an analyte-insensitive reference¹⁰. However, a specific problem is the requirement for a relatively narrow bandwidth of the excitation or the emission. If the demand is not met, the overlap of the spectra decreases the sensitivity of the measurement. A narrow bandwidth results in low light intensities, which imposes the use of highly sensitive photodetectors (photomultipliers or CCD-based detectors).

Another approach is to use modulated excitation light^{11,12} as in the Dual Lifetime Referencing (DLR) method^{13,14}. In this scheme, two fluorophores with significantly different lifetimes, and overlapping spectra are used. The ratio of the intensities of the two dyes is converted into a phase shift that depends on the differences in the decay times of the two luminophores, namely that of the fluorescent probe (indicator; $\tau_{\text{ind}} \sim$ several ns) and that of an added phosphorescent reference dye ($\tau_{\text{ref}} \sim$ several μs), respectively^{11,15}. Furthermore, this method does not require exclusion of ambient light which allows for measurement in real-time applications.

Suitable reference dyes for the DLR scheme are metal ligand complexes of ruthenium (II), osmium (III), rhenium (II), europium (III), terbium (III), platinum (II), and palladium (II). These metal complexes possess decay times in the microsecond or millisecond range and their luminescence is usually is not affected by the analyte. The problem of cross-sensitivity towards oxygen can be solved by incorporating the metal complex into nanobeads or polymers with very low oxygen permeability. In this work, the ruthenium(II)-tris-4,7-diphenyl-1,10-phenanthroline complex ($\text{Ru}(\text{dpp})_3^{2+}$) dissolved in polyacrylonitril (PAN) beads with a diameter of 100 nm was used to reference the intensity of a carboxyfluorescein-loaded PAN polymer acting as the pH-sensitive element. Optical pH sensors based on HPTS as the sensitive fluorophore and Ru^{2+} -PAN-beads as reference dye have been already described¹⁶ and are now commercially available, HPTS is known to display a strong cross-sensitivity towards ionic strength.

Another approach using the DLR method is the time domain. An imaging pH sensor based on fluorescein using the t-DLR scheme has been published¹⁷. However, the t-DLR system can only be used together with a complex and expensive set-up which allows time-gated measurements, whereas the set-up for the frequency domain DLR method is much cheaper. In this chapter, novel amino-modified polymers, based on polyacrylamide were loaded with pH-sensitive dyes and embedded into charge-free hydrogel together with phosphorescent reference particles. The resulting sensors were characterized by means of a

phase detection device (PDD 505) and showed a high photostability and only small to no cross-sensitivity towards ionic strength.

3.2 Material and Methods

3.2.1 Chemicals

The pH indicators 5(6)-carboxyfluorescein (CF), 5(6)-dichlorocarboxyfluorescein, and the chemicals N-(3-dimethylaminopropyl)-N'-ethylcarbodiimide hydrochloride (EDC), dimethylformamide, chloroform, triethylamine, acetonitrile, 2,4,6-trichlorotriazine and ethanol were purchased from Fluka (www.sigmaaldrich.com). The polyurethane hydrogel of type D4 was obtained from Cardiotech (www.cardiotech-inc.com), amino-modified poly(hydroxyethyl methacrylate) (p-HEMA) and the Ru(dpp)₃²⁺-PAN derivates beads (reference particles) from OptoSense (www.optosense.de). The inert and optically transparent poly(ethylene terephthalate) support foils (Mylar[®], thickness 125 µm) were obtained from Goodfellow (www.goodfellow.com). Ethanol, sodium hydroxide and hydrochloric acid were of analytical grade.

3.2.2 Apparatus

Emission spectra as well as response curves of the sensor foils were acquired with an Aminco-Bowman Series 2 luminescence spectrometer (www.thermo.com) equipped with a continuous wave 150 W xenon lamp as light source and with a home-made flow-through cell¹⁸. A piece of sensor foil was placed into the cell and the buffer solutions were allowed to pass through it at a rate of 1 ml min⁻¹. The sample solutions were transported by a Minipuls-3 peristaltic pump (www.gilson.com) via a silicone tube (Ø of 1.0 mm).

A spot of the sensor membrane **M_{DLR}** (**M_{CF}**, **M_{DCCF}** or **M_{IC}**: membranes for DLR measurements, containing a pH-sensitive indicator and an inert reference dye) with a diameter of 2.0 mm was glued onto the tip of a 2 mm PMMA bifurcated fiber (from GP Fiber Optics; www.gp-fiberoptics.de). A cross section of the resulting film is shown in Fig. 3.1 A. The other ends of the fiber were attached to a 505 nm LED and to a photodiode, respectively. The experimental setup is schematically shown in Fig. 3.1 B.

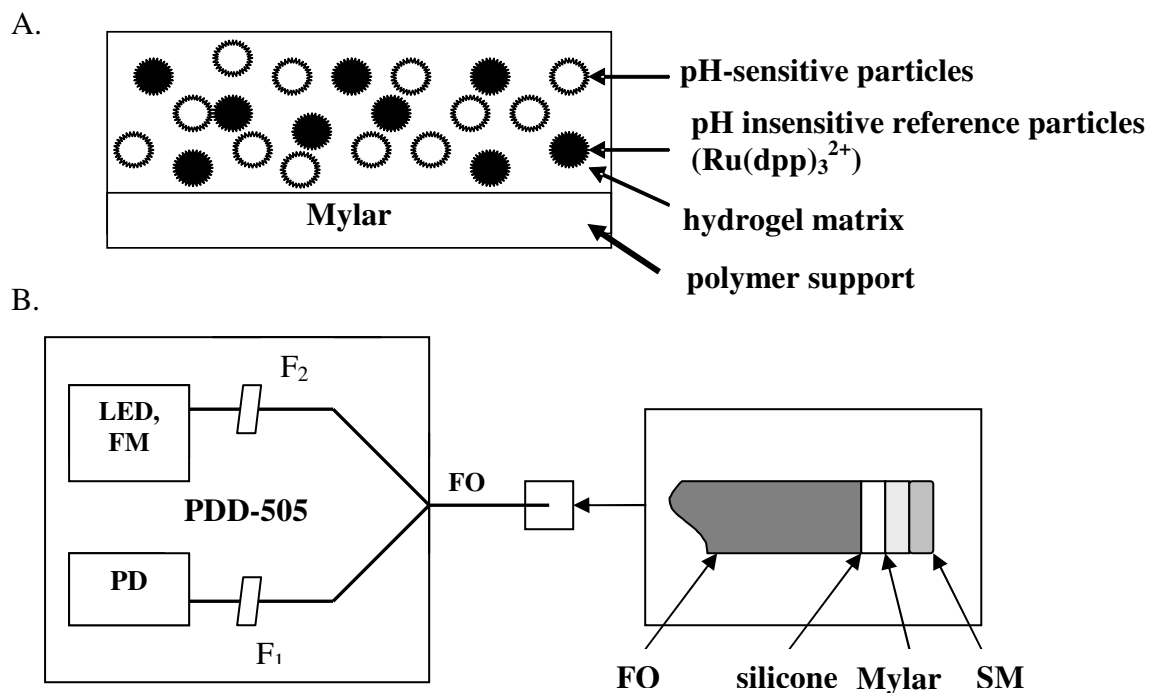


Figure 3.1 A. Scheme of a DLR sensor membrane for optical sensing of pH. B. Optical setup and components. LED: Light-emitting diode; FM: Frequency modulator; PD: Photodiode; F₁ and F₂: Optical filters; FO: Fiber-optic cable; SM: Sensor membrane **M_{DLR}** (glued to the tip of the fiber with silicone grease). The luminescence of the beads in the sensor membrane SM is excited through the fiber, and a fraction of their total emission is guided back through the fibers to a photodiode detector where phase shifts are determined.

Luminescence phase shifts of the fiber optic sensor (see Fig. 3.1 B) were measured with a phase detection device PDD-505 (from Presens GmbH; www.presens.de). Light of a 505 nm LED is filtered through a short-pass filter F₂ (BG 12; from Schott). The dual luminescence of material **M_{DLR}** was filtered through a 570-nm long-pass filter F₁ (OG 570, Schott). The fiber sensor was immersed into a 100-ml glass beaker containing 30 ml of a buffer solution of defined pH.

3.2.3 Buffer Preparation

Doubly distilled water was used for the preparation of the buffer solutions. Their pH was controlled with a digital pH meter (Knick, www.knick.de) calibrated at $20 \pm 2^\circ\text{C}$ with standard buffers of pH 7.0 and 4.0 (Merck; www.merck.de). The pH of solutions was adjusted to the desired value using MOPS buffers which were adjusted to a constant ionic strength (IS = 25 or 140 mM) using sodium chloride as the background electrolyte¹⁹.

3.2.4 Covalent Immobilization of the Indicators on Polymer Beads

Carboxyfluorescein (CF) was covalently attached to the surface of the polymer particles by standard procedure²⁰. Specifically, 300 mg of amino-modified p-HEMA were dispersed in 5 ml of water and 5 mg of CF were added to the suspension. After stirring for 10 min, 5 mg of EDC were added. The resulting suspension was stirred for another 2 h at room temperature. The particles were separated from the solution by centrifugation and washed several times with water, pH 4 buffer, pH 9 buffer, and ethanol until the washing solvent remained colorless. The resulting beads were dried at ambient air to give the pH-sensitive material CF/p-HEMA.

Dichlorocarboxyfluorescein (DCCF) was covalently attached to the surface of the beads using a standard peptide-coupling procedure²¹. 150 mg of amino-modified polymer beads (p-HEMA) were added to 3.0 g of saturated aqueous solution of Na₂CO₃ and the suspension was stirred overnight. 3 mg of DCC, 3 mg of NHS, 3 mg of the dye and 10 µl of triethylamine were dissolved in 1 ml of DMF and the solution was also stirred overnight. Then, the suspension and solution of the dye were mixed together and stirred for 2 h. The particles were separated from the solution by centrifugation and washed several times with water and ethanol until the washing ethanol was colorless. The particles were dried at ambient air to give the pH-sensitive beads DCCF/p-HEMA.

The preparation of pH-sensitive particles with iminocoumarin immobilized on the amino-modified polymer beads p-HEMA with 2,4,6-trichlorotriazine as linker was described in Chapter 2.2.3.

3.2.5 Membrane Preparation

For the preparation of the sensor membranes, 20 mg of beads of either CF/p-HEMA, DCCF/p-HEMA or ImC/p-HEMA, respectively, were added to 600 mg of a 5% wt/wt solution of hydrogel in an ethanol/water (9:1, v:v) mixture. The mixture was vigorously stirred overnight at room temperature. PAN-based reference particles were added to the hydrogel cocktail of the respective polymer. About 100 µl of each sensor cocktail were knife-coated onto dust-free 125 µm polyester support as shown in Fig. 3.2. 120 µm spacers were used to set the thickness of the layer. Table 3.1 gives information about the composition of the membranes.

Table 3.1 Membrane compositions; m is the mass of dyed polymer beads or reference particles [mg] incorporated in 300 mg of 5% wt. solution of hydrogel D4 in ethanol/water (9:1, v/v).

Membrane	pH-sensitive beads	DLR particles	$m(\text{dyed polymer}) / m(\text{ref. partic.})$
M₁	CF/p-HEMA	—	20
M₂	DCCF/p-HEMA	—	20
M₃	ImC/p-HEMA	—	20
M_{CF}	CF/p-HEMA	Ru(dpp) ₃ ²⁺ /PAN deriv.	25 / 2.5
M_{DCCF}	DCCF/p-HEMA	Ru(dpp) ₃ ²⁺ /PAN deriv.	15 / 10
M_{IC}	ImC/p-HEMA	Ru(dpp) ₃ ²⁺ /PAN deriv.	10 / 2.5

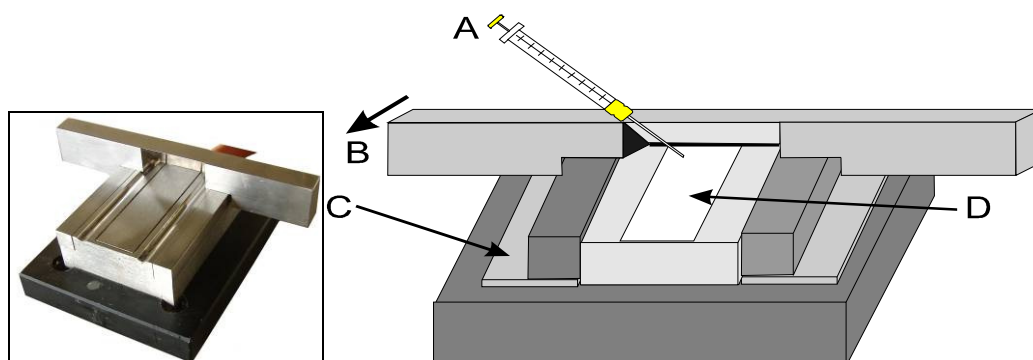


Figure 3.2 View of the knife-coating device: A- pipette containing the membrane cocktail; B- coating device; C- spacer and D- polyester support (Mylar).

3.2.6. Dual Lifetime Referencing Frequency-Domain (DLR) Method

The complete description of the DLR scheme for the pH-sensitive membrane is represented in Chapter 1.3.2. In the sensing scheme used here, two luminophores are incorporated into a hydrogel membrane. The pH-sensitive indicator has a short decay time (τ_{ind}); the pH-independent reference dye Ru(dpp)₃²⁺ a long decay time (τ_{ref}). Usually, the intensity and lifetime of long-decaying luminophores are quenched by oxygen. In this case, this effect was prevented by embedding the reference dye in a virtually gas-impermeable PAN matrix. The two luminophores have overlapping excitation and emission spectra so that they can be excited at the same wavelength and their fluorescence can be detected using the same photodetector.

3.3 Results and Discussion

3.3.1 Choice of Materials

For application of the DLR method in fluorescence sensing, the fluorescence indicator and the coimmobilized reference luminophore had to meet the following criteria: (a) The reference luminophore and indicator fluorophore have to have largely different decay times, (b) the decay time and quantum yield of the reference luminophore are not affected by the sample, (c) the indicator fluorophore changes its quantum yield in the presence of the analyte, (d) the reference and indicator have overlapping excitation spectra to allow the simultaneous excitation at a single wavelength of band, and (e) the luminescence of both the reference and the indicator can be detected at a common wavelength or band of wavelengths using a single photodetector.

The ruthenium complexes are particularly well established as reference luminophores due to their high quantum yields and decay times in the lower microsecond range^{21,22}. However, their luminescence is often quenched by molecular oxygen²³ and oxidative or reductive compounds²². Therefore, the dyes have to be encapsulated in a material which shields them from oxygen or other potential interferents so to warrant a constant background signal. Ru(dpp)₃²⁺ (Fig. 3.1 A) in polyacrylonitrile (PAN) beads was chosen as the optimal reference luminophore because of its high quantum yield (QY = 0.36²⁴), and its relatively long luminescence decay time of approximately 5 μ s. Incorporating Ru(dpp)₃²⁺ into PAN beads minimizes the problem of oxygen quenching because the polymer is virtually gas-impermeable²⁵.

The carboxyfluorescein derivatives are suitable indicators for fluorescence-based pH sensors. The fluorescein indicators used (carboxyfluorescein = CF, dichlorocarboxyfluorescein = DCCF) have: high absorption coefficients ($\epsilon > 80\,000\text{ L mol}^{-1}\text{ cm}^{-1}$), high fluorescence quantum yields (higher than 0.9²⁶), and absorption spectra which are well compatible with light emitting diodes (LED). Furthermore, the presence of functional groups makes their immobilization on the polymer surface easy.

Another applied pH indicator was iminocoumarin (IC). Iminocoumarin possesses suitable photophysical properties which include a high absorption coefficient of $62\,900\text{ L mol}^{-1}\text{ cm}^{-1}$, fluorescence QY of about 0.51 and compatibility with LEDs with emission maxima at 470 or 505 nm. Moreover, compared to fluorescein derivatives coumarins have

excellent photostability (see Chapter 2.3.2) which is a very important criterion for optical sensors.

The immobilization of pH indicators on the polymer is usually realized with one of the three widely used methods: Physical adsorption, entrapment and covalent binding. Here, covalent immobilization was chosen because it prevents leaching of indicators from the polymer matrix²⁷. A derivative of poly(hydroxyethyl methacrylate) (p-HEMA), which contains primary amino groups (due to the presence of 4 % of N-aminopropyl acrylamide) was used for immobilization of the pH indicators on the polymer surface. The material possesses excellent mechanical, chemical, and thermal stability, and does not dissolve in any solvents.

3.3.2 Sensor Characteristics

Before applying the DLR scheme, the membranes **M₁** to **M₃** (see Table 3.1), containing only the pH indicator without the reference dye, were tested in a flow-through cell with respect to the response of the fluorescence intensity to ionic strength (IS) at 25 mM and 140 mM. Fig. 3.3 shows the emission spectra of membranes **M₁** and **M₃** for various pH (IS = 140 mM). Maxima of the emission spectra for both pH-sensitive membranes were at 525 nm ($\lambda_{\text{ex}} = 490$ nm and 488 nm for **M₁** and **M₃** respectively). For **M₂** the maximum of emission spectra was bathochromically shifted ($\lambda_{\text{em}} = 537$ nm, $\lambda_{\text{ex}} = 505$ nm).

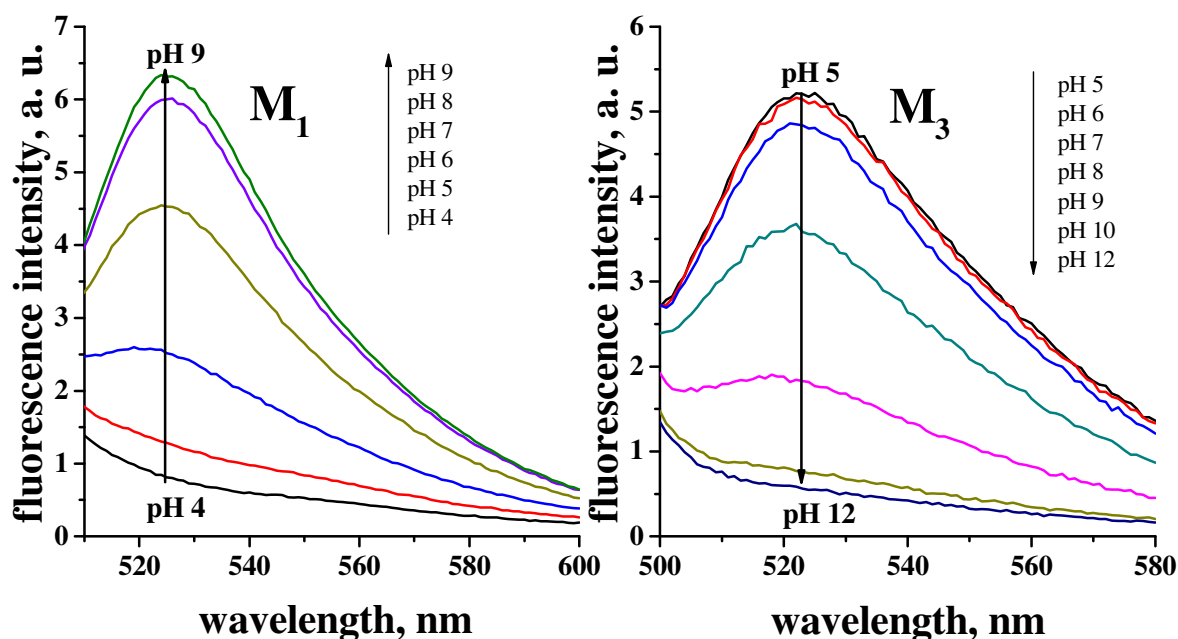


Figure 3.3 Emission spectra of membrane **M₁** ($\lambda_{\text{ex}} = 490$ nm) and **M₃** ($\lambda_{\text{ex}} = 488$ nm). The emission maxima are at 525 nm for both membranes.

Sensitivity to IS can be a serious problem in case of optical pH sensors, because it results in a shift of pK_a values and therefore in errors in pH determination^{28,29}. The effect of IS cannot be distinguished from signal changes caused by pH and therefore can compromise the sensor performance. Figure 3.4, 3.5 and 3.6 show titration plots of the pH-sensitive sensor membranes **M₁**, **M₂** and **M₃** at two different ionic strengths of 25 mM and 140 mM. The latter represents the upper limit of IS in most physiological solutions including blood. One can observe that the pK_a value for membrane **M₁** is slightly increased from 6.81 at 140 mM to 6.89 at 25 mM, whereas the pK_a of membrane **M₂** increases from 4.39 to 4.50. This larger influence of the ionic strength is also typical for other polymer particles with covalently immobilized carboxyfluorescein on the polymer surface³⁰.

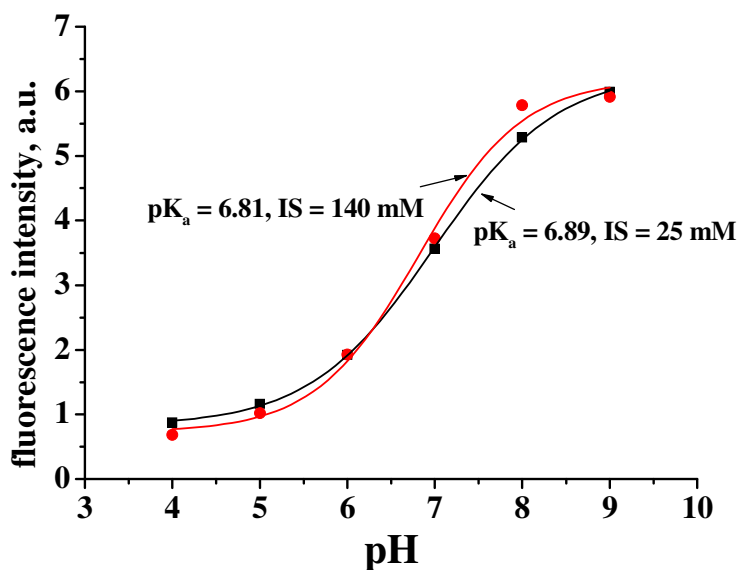


Figure 3.4 Titration plots of membrane M_1 at IS 25 mM and 140 mM adjusted with NaCl. The sensor membrane was excited at 490 nm and fluorescence intensity was detected at 530 nm.

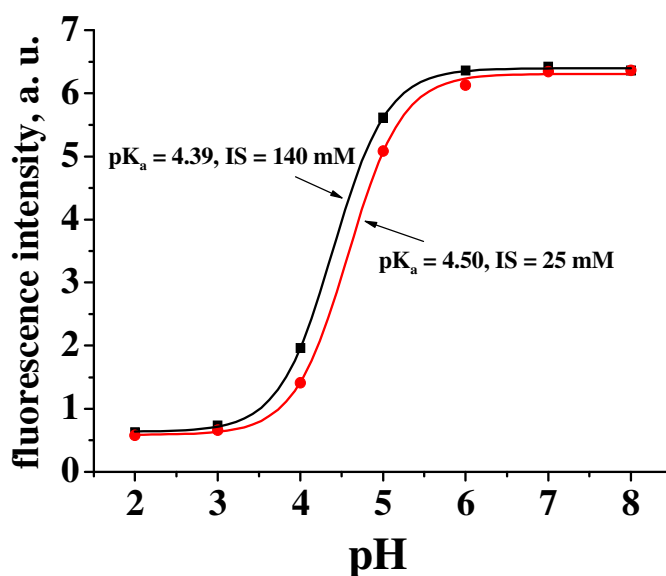


Figure 3.5 Titration plots of membrane M_2 at IS 25 mM and 140 mM adjusted with NaCl. The sensor membrane was excited at 505 nm and fluorescence intensity was detected at 537 nm.

Figure 3.6 shows the pH response of membrane M_3 at ionic strengths of 25 and 140 mM. The titration plots are identical which shows that this sensor membrane is independent of the ionic strength. The difference in pK_a values (8.46 at 25 mM, 8.42 at 140 mM) are within the

accuracy of measurement. Other coumarin-based sensor membranes show similar results, while pH indicators such as 8-hydroxypyrene-1,3,6-trisulfonic acid (HPTS)³¹ are known to have pronounced cross-sensitivity to IS. In contrast, the absence of charges in the coumarin molecule and different microenvironment inside the polymer result in negligible cross-sensitivity towards ionic strength³².

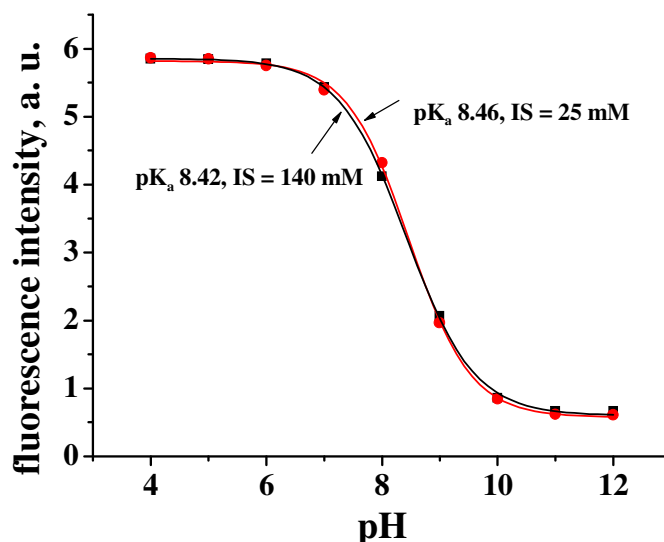


Figure 3.6 Titration plots of membrane M_3 at IS 25 mM and IS = 140 mM. The sensor membrane was excited at 488 nm and fluorescence intensity was detected at 525 nm.

3.3.3. DLR-Referenced pH Membranes

In contrast to the membranes M_{1-3} , the membranes M_{DLR} (M_{CF} , M_{DCCF} or M_{IC}) contain inert luminescent reference beads. The ruthenium(II) tris(4,7-diphenyl-1,10-phenanthroline) complex was used as a reference standard. Incorporated into nanospheres of a PAN derivative (average particle diameter 70 nm), it is efficiently shielded from external quenching by oxygen and other compounds³³⁻³⁵, due to the low gas permeability of PAN ($P = 1.5 \cdot 10^{-17} \text{ cm}^2 \cdot \text{s}^{-1} \cdot \text{Pa}$)³⁶. The reference standard is excitable in the range from 400 to 510 nm and shows a broad emission with a maximum of around 610 nm.

The sensor cocktail was prepared as described in Chapter 3.2.5. For each sensor membrane the optimal concentration of reference beads was determined as that showing the highest overall phase change at protonated and deprotonated form of the indicator.

In order to obtain the response curve of the sensors, M_{DLR} foils were placed in a flow through cell and the fluorescence intensity was measured with a fluorimeter. The analyte solution in the cell was changed from pH 9.0 to pH 4.0 for M_{CF} , from pH 10.0 to pH 5.0 for M_{IC} and from pH 7.0 to pH 2.0 for M_{DCCF} .

Figure 3.7A represents the response curve of sensor membrane M_{CF} at different pH values. The fluorescence of the pH indicator is strongly depended on the pH with its highest sensitivity in the physiological range, whereas the emission of the reference dye $Ru(dpp)_3^{2+}$ in PAN derivative particles at 600 nm remained constant (Fig. 3.7B). The titration curve of M_{IC} is analogous to M_{CF} , but the pK_a value for iminocoumarin in the DLR-sensor membrane M_{IC} is 8.0 compared to M_{CF} ($pK_a = 6.5$).

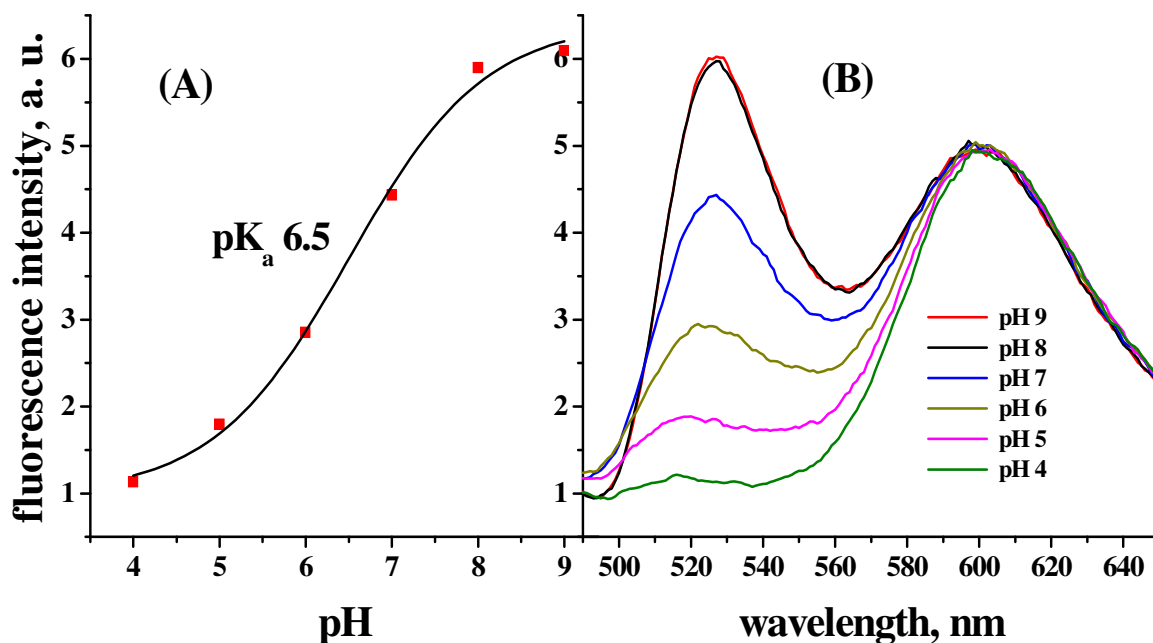


Figure 3.7 (A) Titration plot of the DLR sensor membrane M_{CF} ($\lambda_{ex} = 470$ nm, $\lambda_{em} = 525$ nm); (B) Emission of membrane M_{CF} at pH values from pH 9.0 to 4.0 ($\lambda_{ex} = 470$ nm).

For M_{DCCF} the fluorescence intensity of the pH indicator is increased from pH 2.0 to 7.0, whereas the emission of the reference dye is independent to pH changes (Fig. 3.8B). The pK_a value of M_{DCCF} obtained from the titration plot (Fig. 3.8A) is 4.15.

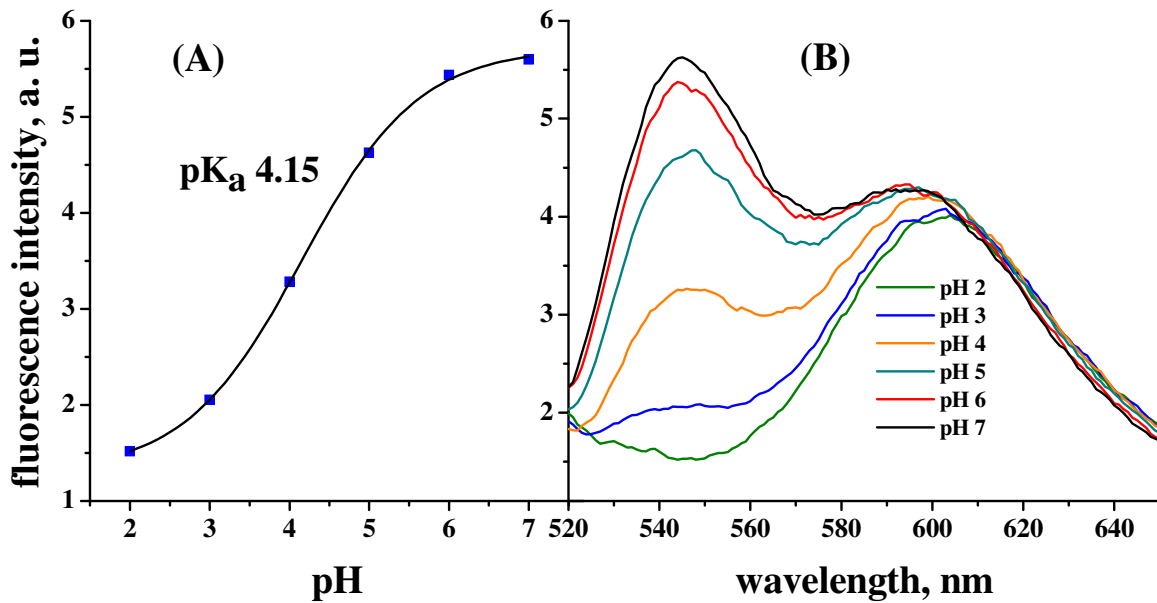


Figure 3.8 (A) Response curve of M_{DCCF} to pH ($\lambda_{ex} = 505$ nm, $\lambda_{em} = 545$ nm); (B) Emission spectra of the DLR-sensor membrane M_{DCCF} from pH 9.0 to 4.0 ($\lambda_{ex} = 505$ nm).

Analogously to the measurements of fluorescence intensity of the membranes without reference dye, the DLR-membranes were measured at different pH values. The titration plots, presented in Fig. 3.9 – 3.11, were recorded with the phase detection device PDD 505. The pH-sensitive membranes were fixed with silicone to the tip of a 2 mm fiber and dipped into MOPS solutions of various pH. The best dynamic of the sensor membranes was obtained using a blue-green LED ($\lambda_{max} = 505$ nm) for simultaneous excitation of both luminophores. The OG 570 long pass filter was used to pass the luminescence of both dyes.

Figure 3.9 shows the titration plots of membrane M_{CF} at different frequencies (f) of 30, 45 and 60 kHz of the sinusoidally modulated excitation light. The form of the sigmoid curves is depended on the measurement frequency, but the pK_a value for each plot remains constant. The highest change of the phase angle between pH 3.0 ($\Phi = 56.23^\circ$) and pH 9.0 ($\Phi = 32.57^\circ$) was obtained for the modulation frequency of 60 kHz. Therefore, this frequency was also selected for the calibration of the other two DLR-membranes M_{DCCF} and M_{IC} .

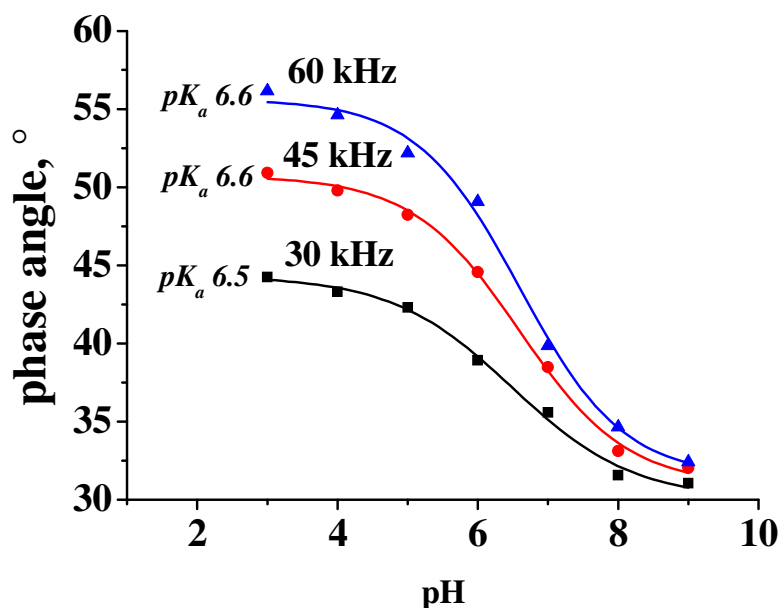


Figure 3.9 Titration curves of membrane M_{CF} for MOPS buffer of IS = 140 mM at 30, 45 and 60 kHz ($\lambda_{ex} = 505$ nm).

In case of membrane M_{DCCF} only a small difference of the phase angle was observed. For the protonated form of pH indicator the phase angle was 55.19° , for the deprotonated form it was 49.64° (Fig. 3.10). This small dynamic in phase angle is related to the excitation of the sensor membrane. Both protonated and deprotonated forms of DCCF are fluorescent, and excitation at 505 nm is not optimal for a selective separation of these forms from each other. Although the deprotonated form is excited to a higher extent than the protonated one, the amount of fluorescence from the protonated form is still too high to obtain a significant difference in phase shift for acidic and basic conditions.

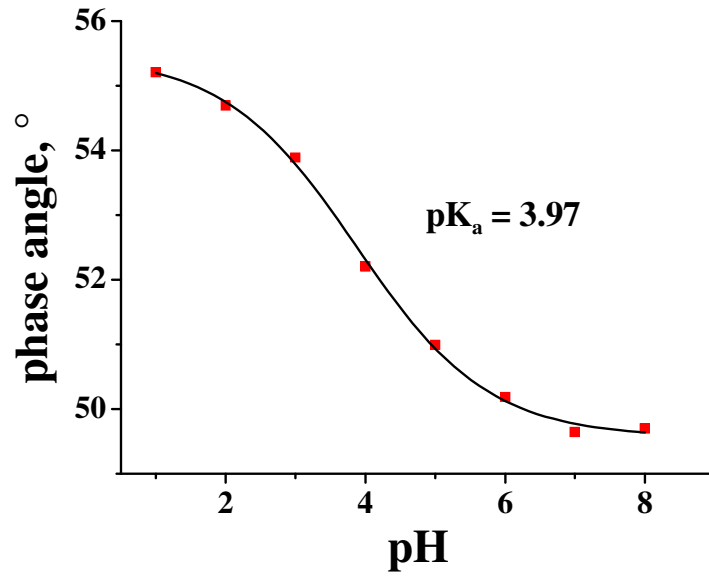


Figure 3.10 Titration plot of M_{DCCF} ($\lambda_{exc} = 505$ nm, $f = 60$ kHz, IS = 140 mM)

Figure 3.11 displays the titration curve of the DLR sensor M_{IC} . The sensor shows sufficient sensitivity to pH. The phase angle at pH 5.0 is 47.71° , at pH 10.0 it is 55.65° ($pK_a = 8.05$). The material is particularly promising for pH-sensing in slightly basic conditions because of its high brightness (see Table 2.2 in Chapter 2.3.1) and excellent photostability.

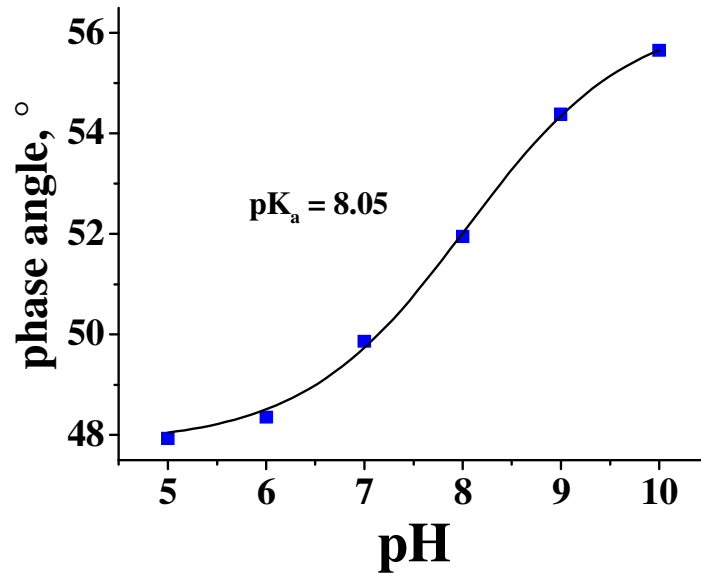


Figure 3.11 Titration plot of M_{IC} to pH ($\lambda_{exc} = 505$ nm, $f = 60$ kHz, IS = 140 mM).

The pK_a values for the M_{DLR} membranes and the pH-sensitive membrane without reference particles ($M_1 - M_3$) are summarized in Table 3.2. The DLR-based sensor membranes show lower pK_a values than the membranes without reference dye. The reference particles contain free carboxyl groups on their surface. When negatively charged particles are added to the positively charged particles containing the immobilized pH indicator, the total ionic strength in the system is increased, which evidently results in a lower pK_a .

Table 3.2 Comparison of apparent pK_a values of M_{DLR} and $M_{1,3}$ and corresponding pH error.

pH sensor membrane with DLR particles	pH sensor membrane without DLR particles	pK_a of M_{DLR} , IS = 140 mM	pK_a of membranes without refer. particles, IS = 140 mM	pK_a of membranes without refer. particles, IS = 25 mM
M_{CF}	M_1	6.50	6.81	6.89
M_{DCCF}	M_2	4.15	4.39	4.50
M_{IC}	M_3	8.00	8.42	8.46

3.4 Conclusion

Three different fiber optic pH sensors based on the DLR-scheme were fabricated. Polyacrylamide-based polymer beads were loaded with carboxyfluorescein, dichlorocarboxyfluorescein and iminocoumarin and embedded, along with Ru^{2+} -PAN-particles in a hydrogel matrix. A 505 nm LED was used as light source to excite both dyes. The fluorescein-based sensor membranes show only a small cross-sensitivity towards ionic strength, the coumarin derivative-based sensor membrane even none at all and furthermore display a high photostability. The variety of pH indicators in the DLR scheme results in pH sensors with pK_a values from 4 to 8. The materials are promising for pH-sensing in various fields: Measurement in seawater and marine environment (iminocoumarin based particles), in acidic soils and upon sour fermentation of milk (dichlorocarboxyfluorescein based particles) and in biotechnology (carboxyfluorescein-based particles) is possible applications.

3.5 References

1. Lakowicz J R **Principles of fluorescence spectroscopy**. 2nd ed, Plenum Press, New York **1999**
2. Laczko G, Gryczynsky I, Gryczynsky Z, Wiczak W, Malak H, Lakowicz J R **A 10 GHz frequency-domain fluorometer**. *Rev. Sci. Instr.* **1990**, 61, 2331–2337
3. Zignani M, Drummond D C, Meyer O, Hong K, Leroux J C **In vitro characterization of a novel polymeric-based pH-sensitive liposome system**. *Biochim. Biophys. Acta* **2000**, 1463, 383–394
4. Slavik J, Lanz E, Cimprich P **Measurement of individual intracellular pH and membrane potential values in living cells**. *Proc. SPIE Int. Soc. Opt. Eng.* **1999**, 3600, 76–83
5. Nedergaard M, Desai S, Pulsinelli W **Dicarboxydichlorofluorescein: A new fluorescent probe for measuring acidic intracellular pH**. *Anal. Biochem.* **1999**, 187, 109–114
6. Whitaker J E, Haugland R P, Prendergast F G **Spectral and photophysical studies of benzo[c]xanthene dyes: dual emission pH sensors**. *Anal. Biochem.* **1991**, 194, 330–344
7. June C H, Rabinovitch P S **Intracellular ionized calcium**. *Methods Cell. Biol.* **1994**, 41, 149–174
8. Jayaraman S, Biwersi J, Verkman A S **Synthesis and characterization of dual-wavelength Cl⁻-sensitive fluorescent indicators for ratio imaging**. *Am. J. Physiol.* **1999**, 276, C747-C757
9. Floto R A, Mahaut-Smith M P, Somasundaram B, Allen J M **IgG - induced Ca²⁺ oscillations in differentiated U937 cells; a study using laser scanning confocal microscopy and co-loaded Fluo-3 and Fura-Red fluorescent probes**. *Cell Calcium* **1995**, 18, 377–389
10. Huber C, Klimant I, Krause C, Wolfbeis O S **Dual lifetime referencing as applied to a chloride optical sensor**. *Anal. Chem.* **2001**, 73, 2097–2103
11. Lakowicz J R, Castellano F N, Dattelbaum J D, Tolosa L, Rao G, Gryczynski I **Low-frequency modulation sensors using nanosecond fluorophores**. *Anal. Chem.* **1998**, 70, 5115–5121
12. Abugo O O, Nair R, Lakowicz J R **Fluorescence properties of rhodamine 800 in whole blood and plasma**. *Anal. Biochem.* **2000**, 279, 142–150
13. Huber C, Klimant I, Krause C, Wolfbeis O S **Dual lifetime referencing as applied to a chloride optical sensor**. *Anal. Chem.* **2001**, 73, 2097–2103

14. Klimant I **Verfahren und Vorrichtung zur Referenzierung von Fluoreszenzintensitätssignalen.** DE 198 29 657 **1998**
15. Klimant I, Wolfbeis O S **Book of abstracts, 6th european conference on optical chemical sensors & biosensors (Europt(r)ode), 1998, 125**
16. Klimant I, Huber C, Liebsch G, Neurauder G, Stangelmayer A, Wolfbeis O S **Dual lifetime referencing (DLR) a new scheme for converting fluorescence lifetime into a frequency-domain or time-domain information.** In *New Trends in Fluorescence Spectroscopy*, chapter 13, Springer-Verlag, Berlin **2001**
17. Liebsch G, Klimant I, Krause C, Wolfbeis O S **Fluorescent imaging of pH with optical sensors using time domain dual lifetime referencing.** *Anal. Chem.* **2001**, 73(17), 4354-4363
18. Huber C, Werner T, Krause C, Leiner M J P, Wolfbeis O S **Overcoming the pH dependency of optical sensors: a pH-independent chloride sensor based on co-extraction.** *Anal. Chim. Acta* **1999**, 398, 137-143
19. Perrin D D, Dempsey B *Laboratory Manuals*, Chapman & Hall: London, **1974**, 62.
20. Hermanson G T **Bioconjugate Techniques**, Academic Press: New York, **1996**, 100
21. Juris A, Balzani V, Barigelletti F, Campagna S, Belser P, von Zelewsky A **Ruthenium(II) polypyridine complexes: photophysics, photochemistry, electrochemistry, and chemiluminescence.** *Coord. Chem. Rev.* **1988**, 84, 85-277
22. Lin C T, Boettcher W, Chou M, Creutz C, Sutin N **Mechanism of the quenching of the emission of substituted polypyridineruthenium(II) complexes by iron(III), chromium(III), and europium(III) ions.** *J. Am. Chem. Soc.* **1976**, 98, 6536-6544
23. Klimant I, Wolfbeis O S **Oxygen-sensitive luminescent materials based on silicone-soluble ruthenium diimine complexes.** *Anal. Chem.* **1995**, 67, 3160- 3166
24. Alford P C, Cook M J, Lewis A P, McAuliffe G S G, Skarda V, Thomson A J **Luminescent metal complexes. Part 5. Luminescence properties of ring-substituted 1,10-phenanthroline tris-complexes of ruthenium(II).** *J. Chem. Soc. Perkin Trans II* **1985**, 705-709
25. Liebsch G, Klimant I, Wolfbeis O S **Luminescence lifetime temperature sensing based on sol-gels and poly(acrylonitrile)s dyed with ruthenium metal-ligand complexes.** *Adv. Mater.* **1999**, 11, 1296-1299
26. Sun W C, Gee K R, Klaubert D H, Haugland R P **Synthesis of fluorinated fluoresceins.** *J. Org. Chem.* **1997**, 62(19), 6469-6475

27. Lobnik A, Oehme I, Murkovic I, Wolfbeis O S **pH optical sensors based on sol-gels. Chemical doping versus covalent immobilization.** Anal. Chim. Acta **1998**, 367(1-3), 159-165
28. Leiner M J P, Wolfbeis O S **Fiber optic chemical sensors and biosensors.** CRC Press, Boca Raton, **1991**, 63
29. Leiner M J P, Hartmann P **Theory and practice in optical pH sensing.** Sens. Actuators B **1993**, 11, 281-289
30. Weidgans B M **New fluorescent optical pH sensors with minimal effects of ionic strength.** Ph D thesis, University of Regensburg, Regensburg, **2004**, 138
31. Opitz N, Luebbers D W **New fluorescence photometrical techniques for simultaneous and continuous measurements of ionic strength and hydrogen ion activities.** Sens. Actuators B 1983, 4, 473-479
32. Wolfbeis O S, Offenbacher H **Fluorescence sensor for monitoring ionic strength and physiological pH values.** Sens. Actuators **1986**, 9, 85-91
33. Liebsch G, Klimant I, Wolfbeis O S **Luminescence lifetime temperature sensing based on sol-gels and poly(acrylonitrile)s dyed with ruthenium metal-ligand complexes.** Adv. Mater. **1999**, 11, 1296-1299
34. Borisov S M, Krause C, Arain S, Wolfbeis O S **Composite material for simultaneous and contactless luminescent sensing and imaging of oxygen and carbon dioxide.** Adv. Mater. 2006, 18, 1511-1516
35. Borisov S M, Vasylevska A S, Krause C, Wolfbeis O S **Composite fluorescent material for dual sensing of oxygen and temperature.** Adv. Funct. Mater **2006**, 16, 1536-1542
36. Brandrup J, Immergut E H, Grulke E A (eds) **Polymer Handbook.** John Wiley & Sons Inc, New York, **1999**

Chapter 4

Indicator-Loaded Permeation-Selective Microbeads for Use in Fiber-Optic Simultaneous Sensing of pH and Dissolved Oxygen

New materials are described that lead to sensors capable of simultaneous sensing of pH and oxygen via a single fiber-optic sensor. They make use of a pH probe based on carboxyfluorescein, and of a ruthenium(II) or palladium(II) complex acting as a probe for dissolved oxygen. The selectivity of the probes was considerably improved by incorporating them into two kinds of microparticles, each of specific permeation selectivity. The pH probe was immobilized on particles made from proton-permeable, amino-modified poly(hydroxyethyl methacrylate), while the oxygen probe was physically immobilized in beads made from an organically modified sol-gel. Both kinds of beads were dispersed into a hydrogel matrix and placed at the distal end of an optical fiber waveguide. A phase-modulated blue-green LED served as the light source for exciting luminescence, which average decay times or phase shifts serve as the analytical information. Data are evaluated by a modified dual luminophore referencing (m-DLR) method, which relates the phase shift measured at two different frequencies to pH and oxygen partial pressure. The dually sensing material performs best if the sensing matrix is very homogeneous and if the microbeads have a diameter of less than 3 μm . (Chem Mater 2006, 18, 4609-4616)

4.1 Introduction

Oxygen and pH are key parameters in many areas of technology and research, and are needed, for example, to control the quality of drinking water^{1,2}, the freshness of food³⁻⁷, or the optimum reaction conditions for monitoring cell activity in bioreactors⁸⁻¹². Knowing pH and oxygen concentration is also essential in clinical analysis of samples such as blood and other physiological liquids¹³⁻¹⁶, in seawater analysis^{17,18}, and in marine research¹⁹⁻²¹. So far, pH and oxygen have been determined simultaneously via two sensors operated in parallel, which is often difficult due to space limitations and in terms of available sample volumes. Hence, a

sensor enabling simultaneous monitoring of both parameters would represent a powerful tool in various areas of research and in (bio)technology.

Most optical chemical sensors for non-colored and non-fluorescent species (including pH and oxygen) are based on the optical interrogation of a material that undergoes a change in its optical properties on exposure to the analyte of interest. Such a change is referred to as the response of the material and ideally is specific for the species to be sensed. In most cases, the sensor material is composed of an indicator dye contained in an optically transparent polymer. The polymer not only acts as a solvent for the (often fluorescent) indicator dye, but also allows for fine-tuning of the response curve of the indicator (and thus of the sensing range). The polymer can also provide certain permeation selectivity, thus eliminating cross-sensitivity to other species. All known optical chemical sensors for gases, for example, are based on materials that are impermeable to charged species (ions) that may act as quenchers of fluorescence, or in other form.

Optical sensors nowadays can be miniaturized down to sub- μm dimensions and combined with fiber-optic technology to provide non-invasive^{22,23} or remote measurement of (bio)chemical parameters. Fibers allow the optical information to be carried from the sample to the instrument. Optical sensing has a second feature that is not provided by electrochemical sensors: Sensing can be performed in a contactless mode, for example through the glass (or plastic) wall of a bioreactor. This is of particular advantage if sterility is an issue.

A substantial fraction of (fiber-) optical sensors is based on the use of fluorescence as the optical information. This is due to the unsurpassed intrinsic sensitivity of fluorescence (that may reach the single molecule level), and because certain effects, which can be used as analytical information (such as static/dynamic quenching, or fluorescence resonance energy transfer) do occur in luminescence only. While the measurement of fluorescence intensity is simple in terms of instrumentation, its accuracy is often compromised by drifts in the opto-electronic set-up (light sources and light detectors), and by variations of the properties of the sensor layer (e.g. the dye concentration or the thickness of the sensor layer). Therefore, referencing methods were developed for the precise measurement of fluorescence intensity²⁴. One such method is based on the measurement of decay time which can be applied to indicator probes that undergo dynamic quenching (such as by oxygen), or resonance energy transfer (which usually changes the decay time as well).

The dual lifetime referencing (DLR) method is relatively new and enables self-referenced measurements both in the time domain and the frequency domain^{25,26}. In contrast

to the common ratiometric (i.e. 2-wavelength) method, this scheme uses luminophores with substantially different decay times. Usually, an analyte-insensitive phosphorescent reference dye (with a decay time in the μs -range) is combined with an analyte-sensitive fluorophore (having a decay time in the ns-range)²⁷. It is essential for the DLR scheme that the absorption and emission spectra of both indicators overlap to allow (a) simultaneous excitation of both probes with a single light source, and (b) simultaneous detection of luminescence. In frequency domain DLR, the combined luminescence intensity of both dyes is converted into a phase shift which is related to the analyte concentration.

We perceived that a material for simultaneous sensing of pH and oxygen may be obtained if the analyte-insensitive reference luminophore is converted into an oxygen-sensitive, luminescent indicator of similarly long decay time. In contrast to the conventional DLR method (in which the phase shift is only dependent on one parameter, e.g. pH), the overall phase shift in the resulting dual material now contains information on both parameters (pH and oxygen). If the phase shift is determined at two different modulation frequencies, two informations will be obtained that can be processed to give two specific analytical signals. The DLR method relies on the fact that at higher modulation frequencies (but still in the kHz range) the long-lived luminescence undergoes demodulation, i.e. a decrease in intensity²⁸, while the short-lived fluorescence (of the pH indicator) is not demodulated.

Since oxygen sensors based on the use of long-lived luminophores produce substantial quantities of singlet oxygen (which can deteriorate indicators), we further perceived that the use of microbeads (with a diameter of 1 – 3 μm) for each indicator species would warrant a spatial separation of the indicators large enough to prevent photo-induced decomposition. We present our results on a novel optical dual sensor that makes use of the permeation-selective microbeads placed in a hydrogel and sensitive to either pH or oxygen. It is shown that the material enables simultaneous and contactless measurement of pH and oxygen in physiological samples.

4.2 Experimental

4.2.1 Materials and Reagents

All chemicals and solvents were of analytical grade and were used without further purification. The preparation of ruthenium(II) tris-4,7-diphenyl-1,10-phenanthroline

dichloride, referred to as $\text{Ru}(\text{dpp})_3^{2+}$, has been described elsewhere²⁹ and is now commercially available. The pH indicator 5(6)-carboxyfluorescein (referred to as CF), and the chemicals N-(3-dimethylaminopropyl)-N'-ethylcarbodiimide hydrochloride (EDC), dimethylformamide, chloroform, triethylamine and ethanol were purchased from Fluka (www.sigmaaldrich.com). The palladium porphyrin complex (5,10,15,20-tetrakis-(2,3,4,5,6-pentafluorophenyl)-21,23H-porphyrin-Pd-(II)) was obtained from Porphyrin Systems (www.porphyrin-systems.de). Sodium 3-(trimethylsilyl)-1-propanesulfonate (Na-TMS; used as a lipophilic anion) was obtained from Aldrich (www.sigmaaldrich.com). The polyurethane hydrogel D4 was obtained from Cardiotech (www.cardiotech-inc.com), amino-modified polyacrylamide (AA-Q-N2) and amino-modified poly(hydroxyethyl methacrylate) (p-HEMA) from OptoSense (www.optosense.de). The copolymer poly(styrene-co-acrylonitrile) (referred to as PSAN) was obtained from Aldrich (www.aldrich.de). The inert and optically transparent poly(ethylene terephthalate) support foils (type Mylar[®], thickness 125 μm) were obtained from Goodfellow (www.goodfellow.com). Calibration gases (nitrogen and oxygen, each of 99.999 % purity) were purchased from Linde (www.linde-gase.de). The preparation of organically modified sol-gel beads ("ormosil") was reported elsewhere³⁰. The method used in the present work was similar to the method described by Klimant et al.³⁰ for material S1, the molar ratio of the monomers phenyltrimethoxysilane and tetramethoxysilane being 18:1.

4.2.2 pH Meter

The pH values of the solutions were checked using a digital pH meter (Knick, Germany, www.knick.de) calibrated at 20 ± 2 °C with standard buffers solutions of pH 7.0 and 4.0 (Merck, www.merck.de).

4.2.3 Buffer Preparation

Doubly distilled water was used for the preparation of the buffer solutions. MOPS buffers with a total concentration of 10 mM and with sodium chloride as background electrolyte to adjust ionic strength (IS = 25 or 140 mM) were used³¹. A stock solution of MOPS was prepared by dissolving 2.093 g of MOPS free acid (M = 209.3 g/mol) and 1.25 g of sodium chloride for ionic strength 25 mM or 7.965 g of NaCl for IS = 140 mM in 1 l of water.

4.2.4 Preparation of Sensor Beads and Sensor Membranes

Materials were prepared for (a) oxygen sensing, (b) pH sensing, and (c) simultaneous sensing of both parameters. Table 4.1 summarizes the materials used for the various sensors. We differentiate between sensor beads (SB) and sensor membranes (SM) which are SBs contained in a hydrogel matrix. The membranes were obtained by spreading water/ethanol solutions of the sensor membrane material onto a solid, transparent support (such as polyethyleneterephthalate or glass) and evaporating the solvent to give sensor membranes (SMs) or dual sensor membranes (DSs) with a thickness of $\sim 10\ \mu\text{m}$.

Table 4.1. Probes and materials used for the preparation of pH-sensitive and O_2 -sensitive membranes, and for the dually sensing material.

<i>Code</i>	<i>Indicator-loaded bead (SB) or bead-loaded sensor membrane (SM)</i>	<i>Analyte</i>
SB-1	PdTFPP in PSAN microbeads	O_2
SB-2	$\text{Ru(dpp)}_3(\text{TMS})_2$ in PtBuS microbeads	O_2
SB-3	$\text{Ru(dpp)}_3(\text{TMS})_2$ in ormosil microbeads	O_2
SB-4	CF on p-HEMA microbeads	pH
SB-5	CF on AA-Q-N2 microbeads	pH
SM-1	PdTFPP in PSAN microbeads contained in an $\sim 10\text{-}\mu\text{m}$ layer of hydrogel	O_2
SM-2	$\text{Ru(dpp)}_3(\text{TMS})_2$ in PtBuS microbeads contained in an $\sim 10\text{-}\mu\text{m}$ layer of hydrogel	O_2
SM-3	$\text{Ru(dpp)}_3(\text{TMS})_2$ in ormosil microbeads contained in an $\sim 10\text{-}\mu\text{m}$ layer of hydrogel	O_2
SM-4	CF on p-HEMA microbeads suspended in an $\sim 10\text{-}\mu\text{m}$ layer of hydrogel	pH
SM-5	CF on AA-Q-N2 microbeads suspended in an $\sim 10\text{-}\mu\text{m}$ layer of hydrogel	pH
DS-1	SB-1 and SB-4 in an $\sim 10\text{-}\mu\text{m}$ layer of hydrogel	O_2/pH
DS-2	SB-2 and SB-4 in an $\sim 10\text{-}\mu\text{m}$ layer of hydrogel	O_2/pH
DS-3	SB-3 and SB-4 in an $\sim 10\text{-}\mu\text{m}$ layer of hydrogel	O_2/pH

4.2.4.1 Preparation of the Oxygen-Sensitive Microbeads SB-1 and the Sensor Membrane SM-1

100 mg of copolymer polystyrene-acrylonitril were dissolved in 20 mg of DMF, and 5 mg of Pd porphyrin complex (PdTFPP) were added to the polymer solution to give polymer particles with incorporated PdTFPP dye. 100 ml of water were added dropwise (1 drop/3 sec) to the red-colored polymer solution during ultrasonication. A saturated solution of sodium chloride was then added. The suspension was washed with distilled water and ethanol by centrifugation. The suspension of the polymer beads in ethanol had 40 mg of dried polymer particles SB-1 in 1 g of ethanol/polymer beads solution.

In order to obtain membrane SM-1, 40 mg of hydrogel D4 were added to 1 g of a suspension of SB-1 in ethanol. The mixture was vigorously stirred overnight at room temperature. 100 μ l of the cocktail were knife-coated onto dust-free, 125 μ m polyester support as shown in Chapter 3.2.5. 120 μ m spacers were used to set the thickness of the layer. After evaporation of the solvent, the red-colored film had a thickness of 10 μ m (as calculated from the masses employed). The membranes were dried for 2 h before characterization. Spots of 25 mm diameter were cut with a hollow punch and mounted in a flow-through cell.

4.2.4.2 Preparation of the Oxygen-Sensitive Microbeads SB-2 and SB-3 and the Sensor Membranes SM-2 and SM-3

Ru(dpp)_3^{2+} dichloride was converted into its much more lipophilic TMS salt by addition of an equivalent quantity of Na-TMS to an aqueous solution of the dye, followed by extraction of the $\text{Ru(dpp)}_3(\text{TMS})_2$ ion pair into chloroform. Then, 200 mg of polymer microparticles (ormosil or PtBuS) were dispersed in 20 ml chloroform and 5 mg of the $\text{Ru(dpp)}_3(\text{TMS})_2$ salt were added to the solution. A suspension of the polymer beads in chloroform was spread on a glass surface and dried at ambient air. After removal of the solvent, the colored polymer film was mechanically ground, and the beads SB-2 and SB-3, respectively, were washed several times with ethanol, this followed by centrifugation. A suspension of the polymer beads in ethanol was spread on a glass surface and dried at ambient air to give oxygen-sensitive beads SB-2 (SB-3).

In order to obtain membrane SM-2 (SM-3), 20 mg of the beads of type SB-2 (SB-3) were added to 600 mg of a 5% wt solution of hydrogel in an ethanol/water (9:1, v:v) mixture. The cocktail was spread as an approximately 120 μ m thick film onto a 125 μ m polyester support.

After evaporation of the solvent, the orange-colored film had a thickness of 10 μm (as calculated from the masses employed).

4.2.4.3 Preparation of the pH-Sensitive Microbeads SB-4 and SB-5 and the Sensor Membranes SM-4 and SM-5

Carboxyfluorescein (CF) was covalently attached to the surface of the polymer particles using standard procedures³². Specifically, 300 mg of amino-modified p-HEMA were dispersed in 5 ml of water, and 5 mg of CF were added to the suspension. After stirring for 10 min, 5 mg of EDC were added. The resulting suspension was stirred for another 2 h at room temperature. The particles were separated from the solution by centrifugation and washed several times with water, pH 4 buffer, pH 9 buffer, and ethanol until the washing remained colorless. The resulting beads were dried at ambient air to give material SB-4. An analogous procedure was applied to immobilize CF on the polyacrylamide beads to give sensor beads SB-5.

The preparation of the respective sensor membranes was similar to that of SM-2 and SM-3: 20 mg of the beads SB-4 and SB-5, respectively, were added to 600 mg of a 5% wt solution of hydrogel in an ethanol/water (9:1, v:v) mixture. The cocktail was spread as an approximately 120 μm thick film onto a 125 μm polyester support. After evaporation of the solvent, the yellow films SM-4 and SM-5 had a thickness of 10 μm .

4.2.4.4 Preparation of Dually Sensing Materials DS-1, DS-2 and DS-3

To 15 mg of the pH-sensitive microbeads SB-4 and 50 mg of the oxygen-sensitive microbeads SB-1 in ethanol solution 500 mg of a 5% wt. solution of hydrogel D4 in ethanol/water (9:1, v:v) were added. The sensor cocktail was stirred overnight and then knife-coated onto the 125 μm polyester support as an approximately 120 μm thick film. The sensor membrane was dried at ambient air to obtain the sensor film DS-1.

To 20 mg of the pH-sensitive microbeads SB-4 and 10 mg of the oxygen-sensitive microbeads SB-2 (SB-3) 600 mg of a 5% wt. solution of the polyurethane hydrogel in ethanol/water (9:1, v:v) were added. The sensor cocktail was stirred overnight, knife-coated onto the polyester support, and dried at ambient air to obtain the yellow sensor film DS-2 (DS-3) in a thickness of about 10 μm . The schematic of the sensor membranes DS's is shown in Fig. 4.1.

4.2.5 Measurements

Fluorescence excitation and emission spectra as well as response curves of the sensor membranes were acquired with an Aminco-Bowman Series 2 luminescence spectrometer (SLM-Aminco; www.thermo.com) equipped with a home-made flow-through cell³³ (see Chapter 2.2.6 Fig. 2.3). A 25 mm diameter spot was punched out of sensor membrane DM-1 or DM-2 and mounted in the cell. Buffer solutions (of various pH and oxygen levels) were passed through the cell at a rate of 1 ml min⁻¹ with the help of a Minipuls-3 peristaltic pump (Gilson; www.gilson.com) via silicone tubing with an inner diameter of 1 mm. The excitation light passed through a monochromator and was focused to one branch of a bifurcated fiber bundle of glass fibers (\varnothing 6 mm). The fiber bundle was fixed to the back of the sensor membrane. The emitted light was guided by the other branch of the fiber bundle through a monochromator to the photomultiplier tube inside the spectrometer.

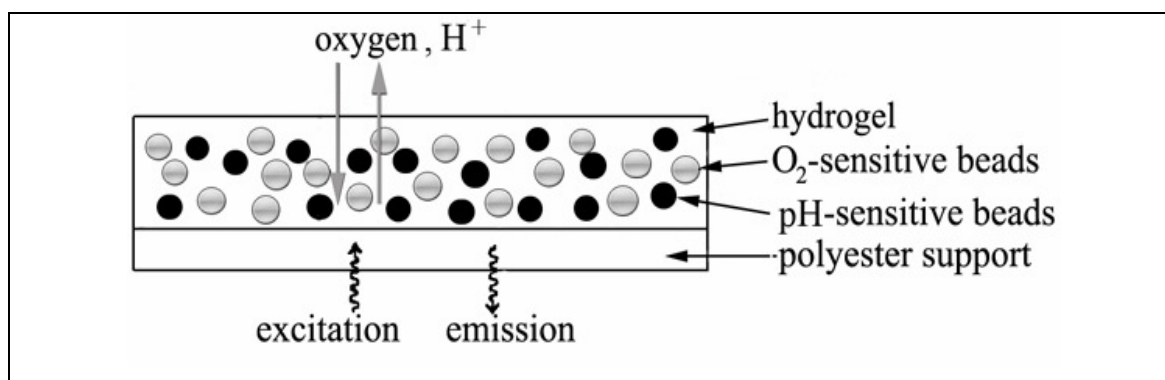


Figure 4.1 Schematic of the sensor membrane DS used for simultaneous sensing of oxygen and pH.

For the phase shift measurements of oxygen sensitive materials (SMs 1-3), the sensor's luminescence was excited with the light of a blue LED (λ_{max} 470 nm, Yoldal product no. YM-B5S15; www.yoldal.com), or a green LED (λ_{max} 525 nm, Yoldal YM-G5N30). After passing interference filters of type FITCA and FITCE (Schott; www.schott.com) it was sinusoidally modulated at different frequencies using a two-phase lock-in amplifier (SR830, Stanford Research Inc.; www.thinksrs.com). A bifurcated fiber bundle was used to guide the excitation light to the sensor foil and to guide back the luminescence after passing the Chroma 580 or the Chroma 680 interference filters (AHF Analysentechnik, www.ahf.de). The luminescence was detected with a photomultiplier tube (H5701-02, Hamamatsu,

www.sales.hamamatsu.com). Temperature was controlled by a Lauda RC6 cryostat (Lauda, www.lauda.de).

Homogeneity tests were performed on a FLUOstar microplate reader (BMG Labtech, www.bmg-labtechnologies.com). A spot of the sensor foil was placed into a Greiner 6-well microplate (Greiner Bio-one GmbH, www.gbo.com) and luminescence intensity at 25 °C and air saturation was measured. For the determination of the decay time the intensity was measured after a certain delay (0 μ s, 20 μ s, 40 μ s, etc) and the lifetime was calculated using a monoexponential decay model.

Luminescence phase shifts of the fiber-optic sensor (see Fig. 4.1) were measured with a phase detection device PDD-505 (from PreSens GmbH; www.presens.de). For the set-up please see Chapter 3.2.2 in Fig. 3.1 B. The sensor was immersed into a 100 ml glass beaker containing 30 ml of a buffer solution of defined pH. Nitrogen/oxygen gas mixtures, which composition and flow rate were controlled by a gas mixing device (GVS; from MKS; www.mksinst.com), were bubbled through the buffer solution to adjust the desired concentrations of dissolved oxygen. Temperature was kept constant at 20 °C by a RC 6 cryostat (Lauda; www.lauda.de). Photographic images of the sensor foil were acquired with a fluorescence microscope (Leica DMRE; Leica, www.leica.com, software from ACD-Systems).

4.3 Results and Discussion

4.3.1 Choice of Materials

Any material for simultaneous sensing of pH and oxygen via the modified DLR technique is expected to meet the following requirements: (a) the oxygen indicator (which also serves as a reference luminophore) and the fluorescent pH indicator need to have largely different decay times; (b) both indicators have to respond to the two analytes; (c) the excitation spectra of both indicators have to overlap in order to allow the simultaneous excitation of both indicators at a single wavelength; (d) the luminescence of both dyes has to be detectable at a single wavelength; (e) the ratio of the two components in a sensor cocktail must remain constant; and (f), the luminophores have to be compatible with an LED which is the most preferred light source in practice due to its low price.

We chose carboxyfluorescein (CF) as the pH indicator, ruthenium(II)-tris-4,7-diphenyl-

1,10-phenanthroline [Ru(dpp)_3^{2+}] and (5,10,15,20-tetrakis-(2,3,4,5,6-pentafluorophenyl)-21,23H-porphyrin-Pd(II)) [PdTFPP] as the oxygen indicators because they meet the above criteria. CF, whose chemical structure is given in Fig. 4.2, is highly fluorescent and one of the most common fluorescent acid–base indicators³⁴. The photochemical properties of CF in water solution at pH 9 are shown in Fig. 4.3 ($\lambda_{\text{abs}} = 490 \text{ nm}$, $\lambda_{\text{em}} = 514 \text{ nm}$). It covers the physiological pH range, with a pK_a of 6.5³⁵. Its carboxy group can be used for covalent immobilization of the dye on the surface of amino-modified polymer particles in order to avoid leaching of the indicator, which can be a serious problem³⁶.

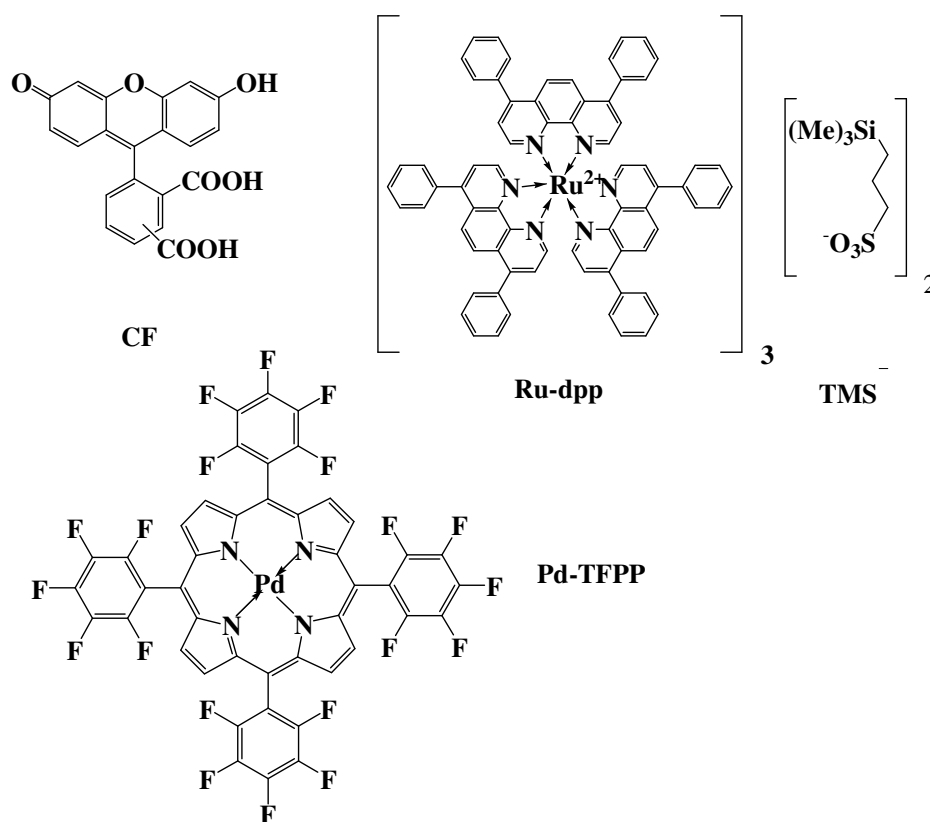


Figure 4.2 Chemical structures of the indicators carboxyfluorescein (CF), PdTFPP and Ru(dpp)_3^{2+} along with its counter ion 3-trimethylsilylpropane sulfonate (TMS^-).

CF was covalently immobilized on the surface of two kinds of polymer particles using standard procedures based on the peptide coupling reagent EDC³². The first polymer was a polyacrylamide derivative (AA-Q-N2) containing 4 % of aminopropyl acrylamide which provides free amino groups for attachment of carboxyfluorescein. The second is a derivative of poly(hydroxyethyl methacrylate)(p-HEMA), that also contains primary amino groups due to the presence of 4 % of N-aminopropyl acrylamide. Both materials possess excellent mechanical, chemical, and thermal stability, and do not dissolve in any solvents, but differ

significantly in their hydrophobic properties. Aminocellulose was another choice but was not employed because it serves as a nutrient for certain bacteria.

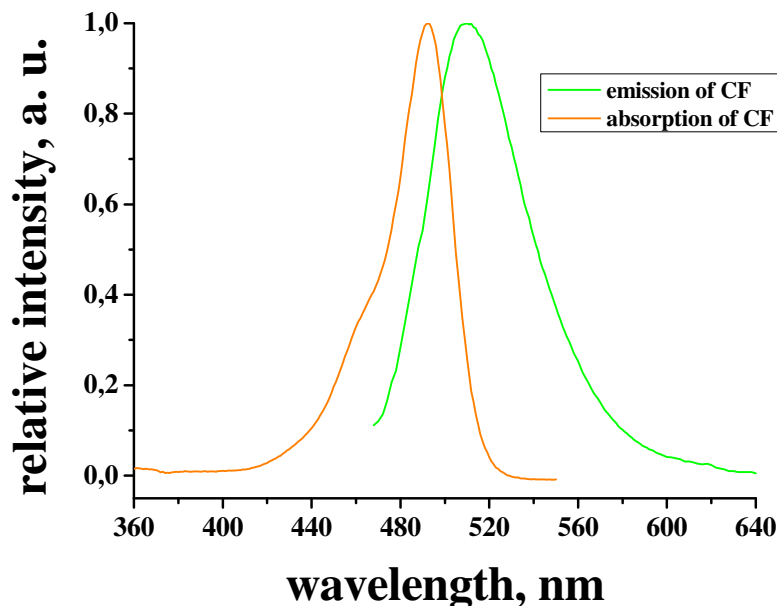


Figure 4.3 Emission and absorption spectra of carboxyfluorescein in aqueous solution at pH 9.

The oxygen sensor materials make use of the ruthenium(II) complex $\text{Ru}(\text{dpp})_3^{2+}$ and the palladium complex PdTFPP (Fig. 4.2). These indicators benefit from fairly strong absorption in the visible region ($\text{Ru}(\text{dpp})_3^{2+}$: $\lambda_{\text{max}} = 463 \text{ nm}$ (see Fig. 4.4 A), $\epsilon = 2.84 \cdot 10^4 \text{ M}^{-1} \cdot \text{cm}^{-1}$; PdTFPP: $\lambda_{\text{max}}^1 = 406 \text{ nm}$, $\lambda_{\text{max}}^2 = 515 \text{ nm}$ and $\lambda_{\text{max}}^3 = 550 \text{ nm}$ (see Fig. 4.4 B), $\epsilon_1 = 19.2 \cdot 10^4 \text{ M}^{-1} \cdot \text{cm}^{-1}$, $\epsilon_2 = 1.82 \cdot 10^4 \text{ M}^{-1} \cdot \text{cm}^{-1}$, $\epsilon_3 = 1.55 \cdot 10^4 \text{ M}^{-1} \cdot \text{cm}^{-1}$). Both oxygen indicators have a good luminescence quantum yield (QY) of 0.36³⁷ and 0.21³⁸ for the Ru and Pd complexes, respectively, which results in an excellent brightness (defined as $\epsilon \cdot \text{QY}$) of $10\,200 \text{ M}^{-1} \cdot \text{cm}^{-1}$ and $40\,320 \text{ M}^{-1} \cdot \text{cm}^{-1}$ for PdTFPP when excited at 406 nm and 515 nm, respectively and $3\,830 \text{ M}^{-1} \cdot \text{cm}^{-1}$ when excited at 550 nm. The value of brightness for $\text{Ru}(\text{dpp})_3^{2+}$ is $10\,224 \text{ M}^{-1} \cdot \text{cm}^{-1}$ when excited at 463 nm. They also exhibit good photostability³⁹. $\text{Ru}(\text{dpp})_3^{2+}$ has a decay time in the order of 3 – 5 μs and serves as an excellent oxygen probe when contained in a highly oxygen-permeable polymer⁴⁰⁻⁴². We had discovered³⁰ highly oxygen-permeable ormosils soluble in chloroform that can be prepared in the form of microbeads with a diameter of 1 – 3 μm ^{43,44}. Sol-gels used for preparation of sensitive particles in DS have been used successfully in sensors before⁴⁵ but are used here preferably for preparation of the oxygen microbeads in order to impart selectivity, stability, and adequate amphiphicity to

retain the oxygen indicator.

The indicator Ru(dpp)_3^{2+} was incorporated into the polymer beads by swelling them in chloroform. The decay time of PdTFPP is about 1 ms, the indicator shows a too high sensitivity to oxygen for use in a DLR sensor (see chapter 4.3.4). Therefore it was incorporated in a polymer with only limited permeation to oxygen (PSAN) to make possible the application of this indicator in water solutions.

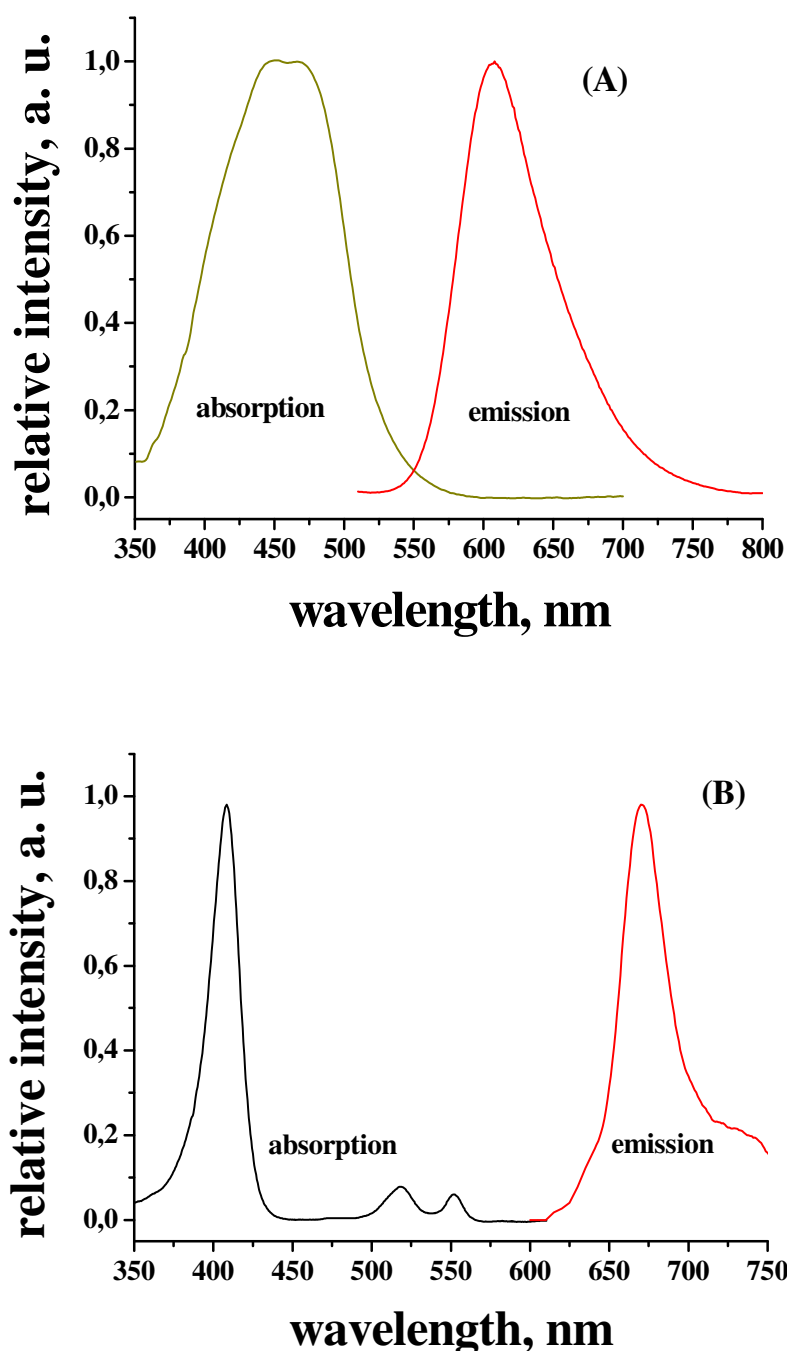


Figure 4.4 Absorption and emission spectra of Ru(dpp)_3^{2+} (A) and PdTFPP (B), in

deoxygenated chloroform solutions.

The sensor for simultaneous sensing of pH and oxygen contains both kinds of beads embedded in a single polymer matrix. Hydrogels (which are permeable to both protons and oxygen) have excellent mechanical properties and excellent stability at various pH values and temperatures⁴⁶. We used a polyurethane-based hydrogel because it displays excellent water uptake, and is biocompatible. The sensor membranes made from SB-4 (based on p-HEMA), according to visual inspection, possessed higher brightness than those made with beads SB-5. Thus, we prefer material SM-4 in the dual sensor.

4.3.2 Response of the pH Sensor Materials SM-4 and SM-5

In most biotechnological applications it is necessary that the pK_a values of a pH-sensitive probe are around 7. The apparent pK_a value of an indicator in a polymer not only depends on its intrinsic (thermodynamic) pK_a value, but also on the kind of polymer used. Two different dye-polymer combinations (materials SM-4 and SM-5) were investigated. Figure 4.5 shows response curves of the probes to pH. Sensor membranes SM-4 and SM-5 display good pH sensitivity over a range from pH 5 to 8.

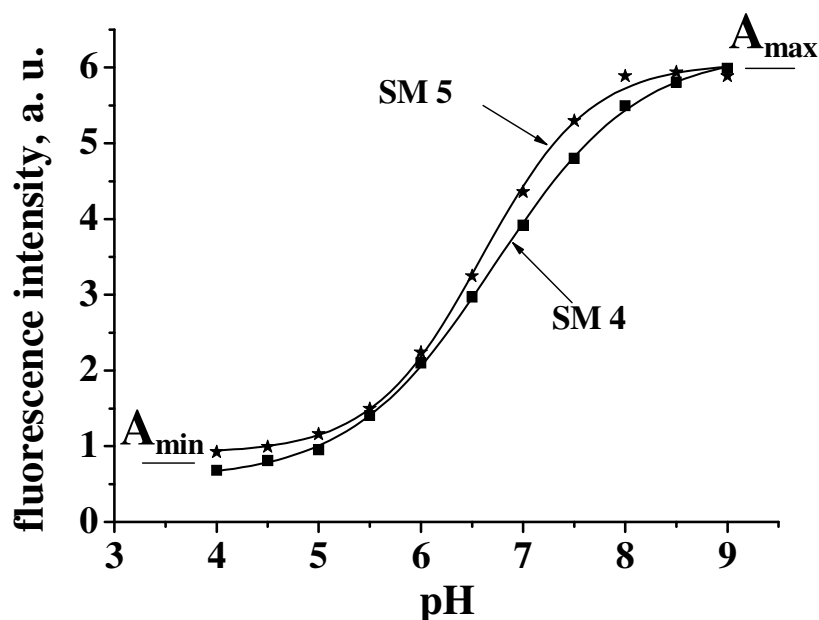


Figure 4.5 Titration plots of materials SM-4 and SM-5 ($\lambda_{ex} = 490$ nm, IS = 140 mM).

The curves can be described quite well (with a correlation coefficient of 0.999) by the following equation, adapted earlier⁴⁷ for optical pH sensors:

$$I = \frac{A_{\max} - A_{\min}}{1 + 10^{(pH - pK_a)/x}} + A_{\min}, \quad (4.1)$$

where I is fluorescence intensity, x is a numerical coefficient which describes the slope of the sigmoidal curve at its turning point (pK_a). A_{\max} and A_{\min} are numerical values of the fluorescence intensity of the pH indicator in fully protonated (A_{\min}) and fully deprotonated (A_{\max}) form, respectively. The equation gave pK_a values of 6.71 and 6.58, respectively, for materials SM-4 and SM-5.

Any polymer used as a matrix for immobilizing pH indicators has three kinds of effects on the properties of the pH indicator: a) on the pK_a value, b) on the spectra (shape and peaks), and c) on the shape of the response curves which for polymer-immobilized indicators are mostly different from those obtained for solutions. Indeed, the pK_a values are slightly higher for the immobilized form of the dye compared to the one in aqueous solution ($pK_a = 6.5$). A similar, but larger effect was found when fluorescein⁴⁸ was covalently attached to differently charged surfaces of certain polymers. Most likely, this is the result of the varying density of electrical charges on the surface. Usually, a rather small increase in pK_a occurs on covalent⁴⁹ or electrostatic⁵⁰ immobilization of an indicator even to non-ionic polymers, a fact that is attributed to the decrease in the polarity of the micro-environment.

The spectra of membrane SM-4 are different from those of CF in solution. While fluorescence intensity, as expected, drops strongly on going from pH 9 to pH 4, the fluorescence of CF in p-HEMA has its maximum at 526 nm and thus is strongly bathochromically shifted compared to CF in aqueous solution, which has a λ_{\max} of 515 nm at pH 9 (see Fig. 4.6). The effect is also assumed to be caused not only by a decrease in the polarity of the micro-environment, but also by different hydration of the immobilized indicator. A similar behavior was observed earlier for immobilized fluorescein^{51,52}.

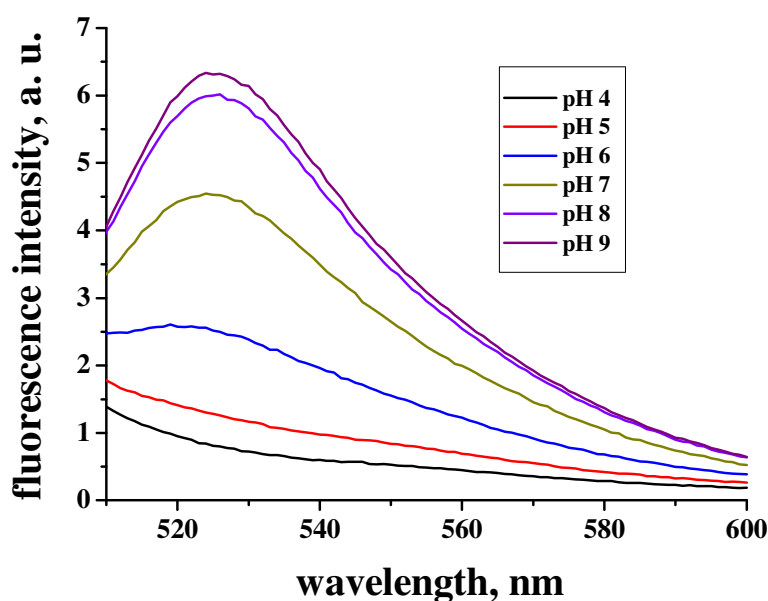


Figure 4.6 Emission spectra of the pH-sensitive probe SM-4 at different pH values (IS = 140 mM).

A disadvantage of optical pH sensors is the effect of ionic strength (IS) on the dissociation constant and, consequently, the pK_a of the dye^{53,54}. The effect of IS cannot be distinguished from signal changes caused by pH changes and therefore can compromise the sensor performance. Figure 4.7 shows titration curves for the pH sensor SM-4 at two ionic strengths (25 mM and 140 mM). The latter represents the upper limit of IS in most physiological solutions including blood. The pK_a decreases slightly (from 6.89 to 6.81 on going from 25 mM to 140 mM). Thus, the cross sensitivity of SM-4 to IS is surprisingly small compared to other polymer particles with covalently immobilized carboxyfluorescein on the polymer surface⁵⁵.

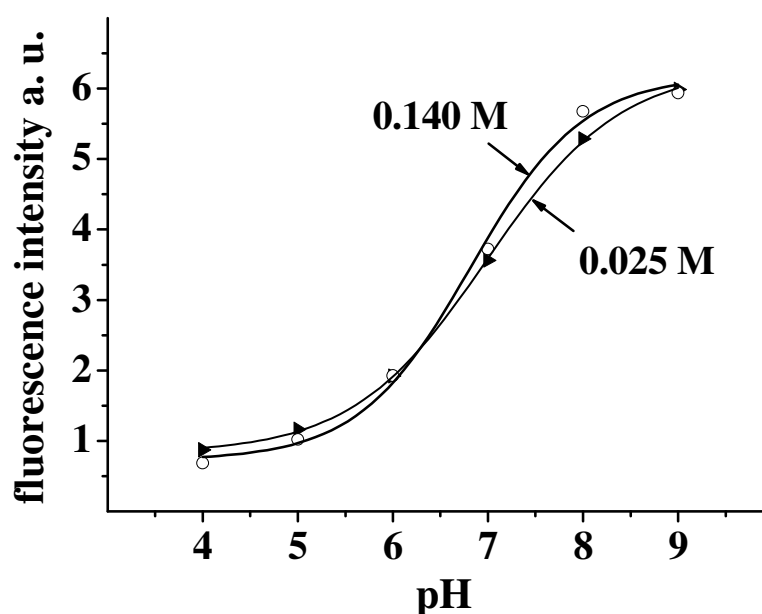


Figure 4.7 Titration curves for sensor membrane SM-4 at ionic strengths of 25 and 140 mM adjusted with NaCl ($\lambda_{\text{ex}} = 490 \text{ nm}$, $\lambda_{\text{em}} = 530 \text{ nm}$).

The response time of the pH-sensitive probe SM-4 was determined from a series of time traces using MOPS buffers with different pH values. The measurement interval was 10 s. The kinetic of membrane SM-4 is shown in Fig. 4.8.

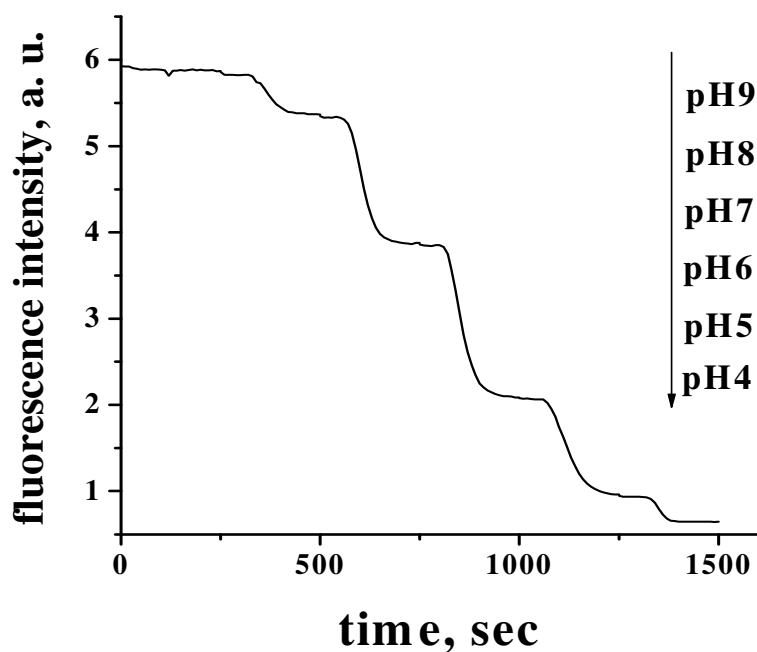


Figure 4.8 Time trace of the fluorescence intensity of membrane SM-4 for MOPS buffers of pH 9 to pH 4 (IS = 140 mM).

The response time t_{95} (i.e. the time for 95 % of the total change in fluorescence intensity to occur) was not exceeding 1 min on going from pH 4 to pH 9, and 1.5 min in the reverse direction. The values are in good agreement with those obtained for other optical pH-sensitive materials based on the sol–gel silica matrix⁵³.

4.3.3 Response of the Oxygen Sensor Membranes

The response to dissolved oxygen was studied for the oxygen sensor membranes. We prefer to use oxygen partial pressure above the buffer solution to calculate oxygen content in sample solution. It is proportional to the concentration of the dissolved gas according to Henry's law:

$$C = K_H \cdot P \quad (4.2)$$

where C is concentration of dissolved gas in aqueous solution, K_H Henry's constant, and P the partial pressure of the gas. The decay times of SM-1, SM-2 and SM-3 were calculated using the equation:

$$\tau = \frac{\tan \Phi}{2\pi f}, \quad (4.3)$$

where Φ is the measured phase shift and f is the modulation frequency of the excitation light.

4.3.3.1 Oxygen-Sensitive Probe SM-1

Stern-Volmer plots (τ_0/τ vs. oxygen partial pressure) for quenching of the oxygen indicator are presented in Fig. 4.9. A non-linear behavior is common to most luminescent oxygen sensors. It can be described by a "two-site model"^{56,57}, which assumes the dye to be located in two regions of different microenvironment. The quenching constants are, therefore, different for these regions. Since the decay times determined by the phase modulation technique represent average values, it is possible to use the "two-site model" Stern-Volmer equation in the lifetime form:

$$\frac{I}{I_0} = \frac{\tau}{\tau_0} = \frac{f_1}{1 + K_{SV}^1 \cdot pO_2} + \frac{f_2}{1 + K_{SV}^2 \cdot pO_2}, \quad (4.4)$$

where I and I_0 , are the quenched and unquenched luminescence intensities of the respective sensor membrane, K_{SV}^1 and K_{SV}^2 are the Stern-Volmer constants for the two different microenvironments, and f_1 and f_2 are the fractions of the total emission for each component,

respectively (with $f_1 + f_2$ being 1). pO_2 is the oxygen partial pressure that causes the luminescence to drop from I_0 to I .

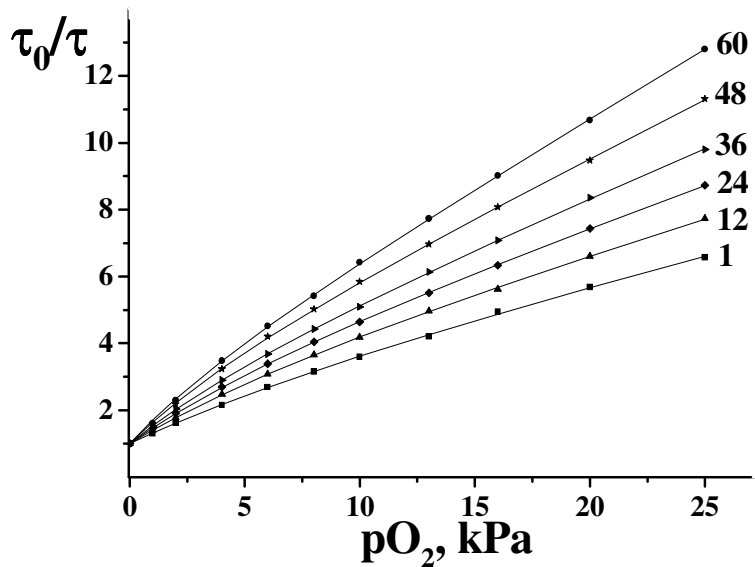


Figure 4.9 Stern-Volmer plots at temperatures between 1 and 60 °C. Lines reflect fitting via eq. 4.4.

As can be seen from Fig. 4.9, eq. 4.4 nicely matches the experimental findings ($r^2 > 0.9997$). The fits gave values of 0.89 ± 0.02 for f_1 and respectively 0.11 ± 0.02 for f_2 , this indicating that the dye is mainly localized at the first site.

The triplet state lifetime in the absence of oxygen is slightly temperature-dependent and drops from 0.83 ms at 1 °C to 0.77 ms at 60 °C as the result of thermal quenching. As can be seen from Fig. 4.9, phosphorescence quenching by oxygen is increasingly efficient at higher temperatures due to faster diffusion of the quencher within the film, which is the main reason for cross-sensitivity of the material to temperature⁵⁸.

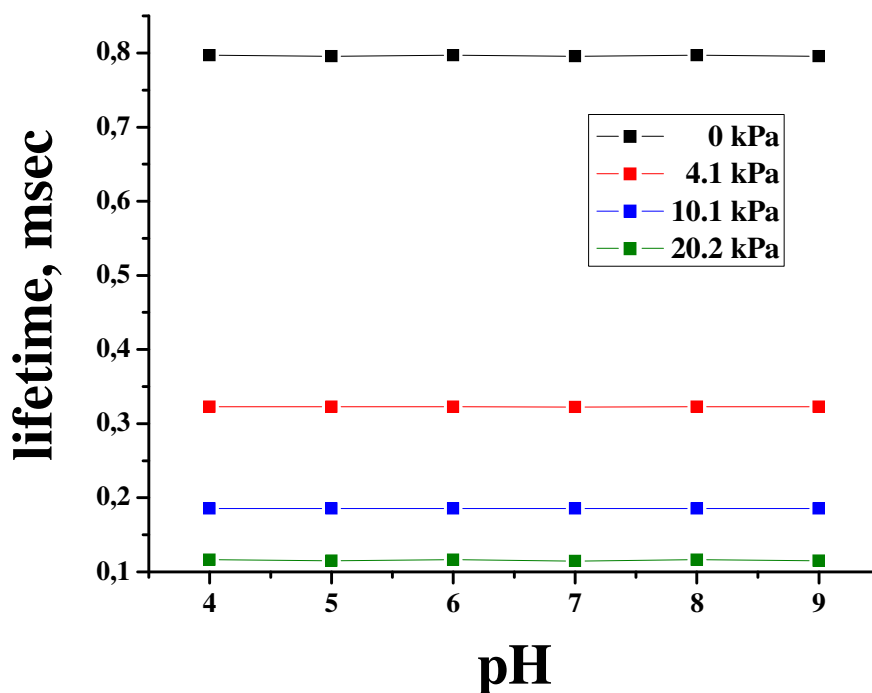


Figure 4.10 Lifetimes of SM-1 at different pH values and oxygen partial pressures in MOPS buffer solution ($\lambda_{\text{ex}} = 525 \text{ nm}$, $\lambda_{\text{em}} = 670 \text{ nm}$, 525 LED, excitations filter: FITCE; emissions filters: RG 645 and Flame Red).

The lifetimes of the sensor membrane SM-1 was studied at different pH values from 4 to 9 and different oxygen concentrations (0 to 21.3 kPa) in the buffer solutions. Figure 4.10 shows that no effect of the pH on the phosphorescence intensity of SM-1 is observed at either of the applied oxygen partial pressures.

4.3.3.2 Oxygen-Sensitive Probe SM-2

Stern-Volmer plots for sensor material SM-2 are given in Fig. 4.11. The response curves are nonlinear. As for the probe SM-1, the quenching intensity at oxygen partial pressures from 0 to 25 kPa was not dependent on the pH value.

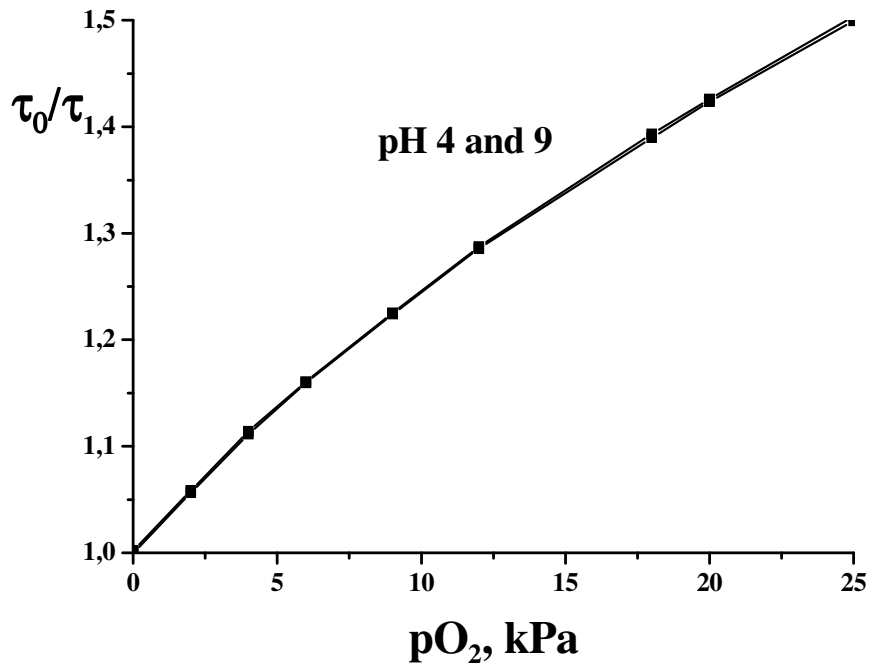


Figure 4.11 Stern-Volmer plots for membrane SM-2 at pH 4 and 9 (45 kHz, $\lambda_{ex} = 505$ nm, $T = 20^\circ\text{C}$).

The effect of temperature was studied for this oxygen-sensitive probe as well. Figure 4.12 shows the Stern-Volmer plots for SM-2 at 5 - 45°C which show non-linear behavior and can be well described by the two-site model (eq. 4.4). The calculated Stern-Volmer constants are summarized in Table 4.2.

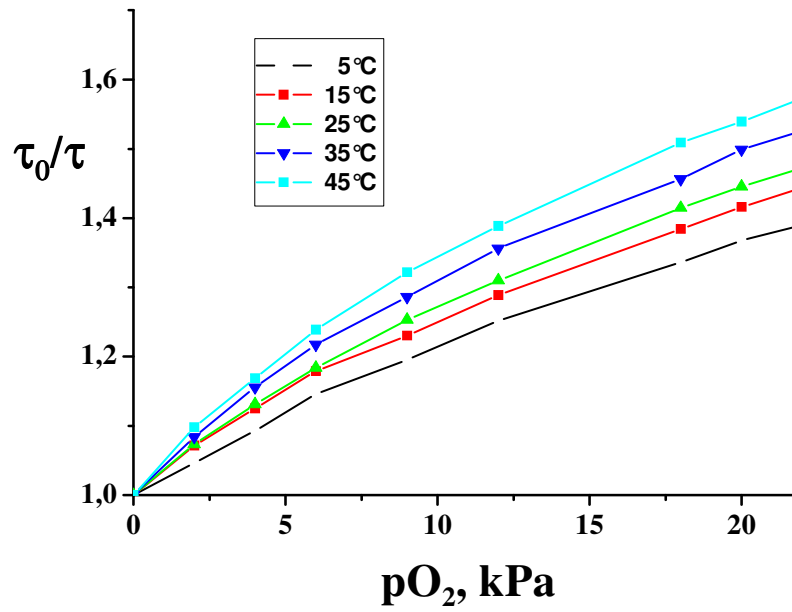


Figure 4.12 Stern-Volmer plots for SM-2 at temperatures between 5 and 45°C.

4.3.3.3 Oxygen-Sensitive Probe SM-3

Figure 4.13 shows the response curve for an oxygen sensor film made from SM-3 at pH 4 and pH 9. The plots are nonlinear and not dependent on the pH value. A deviation of the response curve from linear dependence is only observed for partial pressure more than 7 kPa.

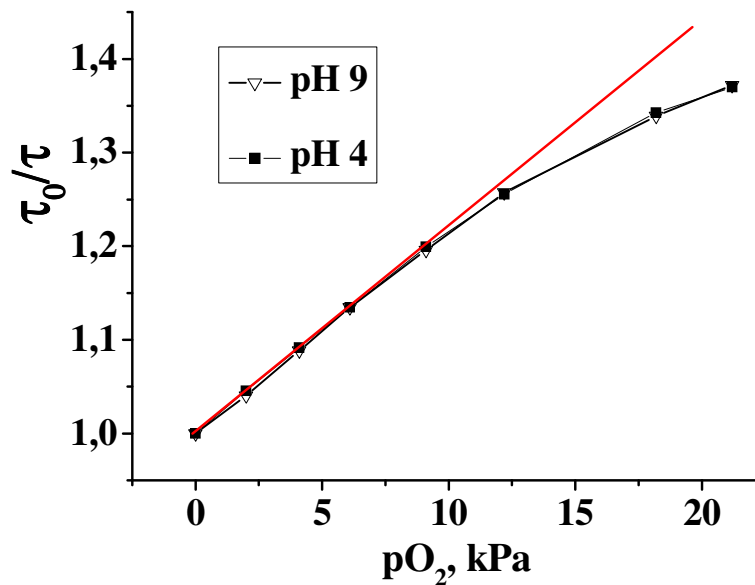


Figure 4.13 Stern-Volmer for the membrane SM-3 at pH 4 and 9 (30 kHz, $\lambda_{ex} = 505$ nm,

T = 20 °C), demonstrating the insensitivity to pH.

The decay time of the SM-3 sensor membrane calculated via eq. 4.3 is 5.2 μ s (at $f = 30$ kHz). The sensor material shows no cross-sensitivity towards the pH value.

The response to oxygen is very fast: A change from deoxygenated water to air-saturated water is indicated within only 6 s (t_{95}), for the reverse direction it was 7 s. Although even faster sensors have been reported^{30,59}, the response of our probe is faster than that of other sol-gel materials^{42,60}.

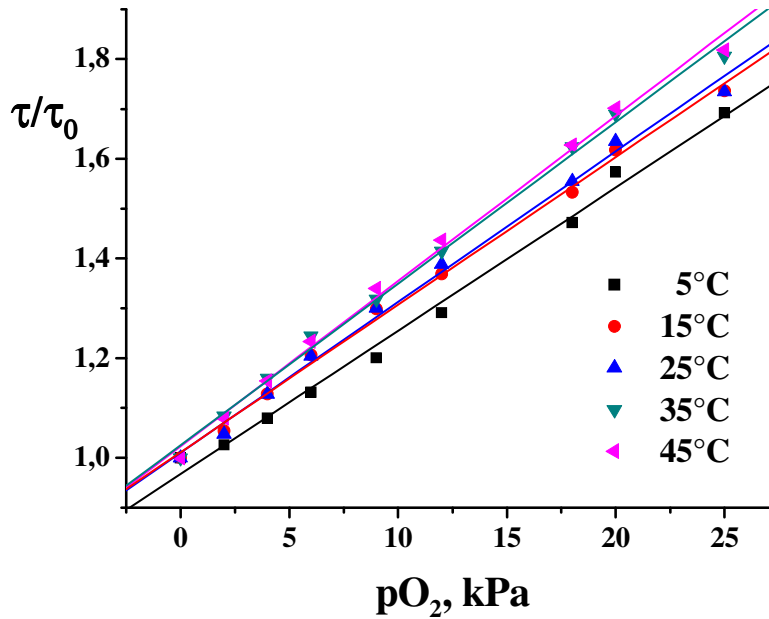


Figure 4.14 Stern-Volmer plots for SM-3 at temperatures between 5 and 45°C. Lines reflect fitting via eq. 4.5.

Figure 4.14 represents the Stern-Volmer plots for SM-3 at temperatures of 5, 15, 25, 35, and 45° C. The plots have nearly linear dependence and can be well described by the linear Stern-Volmer equation (with standard deviation $r^2 = 0.9989$):

$$\frac{I_0}{I} = \frac{\tau_0}{\tau} = 1 + K_{sv} pO_2 \quad (4.5)$$

where τ_0 and τ are the luminescence lifetimes in the absence and presence of oxygen, respectively, pO_2 is the oxygen partial pressure and K_{sv} the Stern–Volmer quenching coefficient. The plots supply information on the sensitivity of the SM-3 sensor probe to oxygen quenching.

The Stern-Volmer quenching constants which were determined at 25 °C are presented in Table 4.2 for the sensor membranes SM-1, SM-2 and SM-3.

Table 4.2 Quenching constants (kPa^{-1}) of sensor membranes SM-1, SM-2 and SM-3 as analyzed via eq. 4.4 (for SM-1 and SM-2) and eq. 4.5 (for SM-3) at 25°C.

Sensor membrane	K_{sv}^1	K_{sv}^2	Standard deviation
SM-1	0.54	0.04	0.9997
SM-2	0.088	0.0047	0.9999
SM-3	0.030	-	0.9989

4.3.4 Response of the Dual Sensor in the Intensity Mode

In the pH/oxygen dual sensor, the fluorescence of the pH indicator is referenced against the phosphorescence of the oxygen indicator. A too low sensitivity will result in higher error in oxygen partial pressure, but also in calculated pH values. On the other hand, if the sensitivity to oxygen is too high, the overall phase shifts in the dual sensor will be too low at oxygen saturation, resulting in low precision of pH-sensing under this condition.

Three kinds of dual sensor material are presented: PdTFPP in PSAN polymer particles with CF on pHEMA, both incorporated in hydrogel D4 (DS-1), $\text{Ru(dpp)}_3^{2+}/\text{PtBuS}$ microbeads and CF/pHEMA particles in hydrogel (DS-2) and $\text{Ru(dpp)}_3^{2+}/\text{ormosil}$ with CF/pHEMA microbeads in hydrogel D4 (DS-3). For each dually-sensing material the absorption spectra of the pH indicator and the oxygen indicator strongly overlap, which enables excitation of both indicators within a wavelength range from 470 to 510 nm or with a 470 nm (blue) LED or a 505 nm (blue-green) LED.

The emission spectra of the indicators for the dual sensors DS-1, DS-2 and DS-3 are shown in Fig. 4.15, 4.17 and 4.18. The fluorescence intensity of the pH indicator CF is weak at pH 4 and strong at pH 9. The emission of the oxygen-sensitive probe is not affected by pH. If the oxygen partial pressure is increased, the emission intensity of oxygen indicator decreases, while the emission of the pH indicator remains relatively constant or decreases about 3 % (at constant pH).

For the sensor membrane DS-1 (Fig. 4.15) the sensitivity of the oxygen indicator is satisfactory for adequate monitoring of dissolved oxygen in aqueous solution. Unfortunately, an inner-filter effect occurs at the emission of the pH indicator in the dual sensor membrane DS-1. For CF, two emission maxima at 535 nm and 570 nm were observed at pH 9 (see Fig. 4.15) as compared to the pH-sensitive sensor membrane SM-4 without oxygen indicator

PdTFPP/PSAN, which reveals only one maximum at 526 nm (see Fig. 4.6). In DS-1, the emitted light of CF is reabsorbed by PdTFPP ($\lambda_{\text{ex}}^1 = 525$ nm and $\lambda_{\text{ex}}^2 = 550$ nm; see marked area in Fig. 4.16).

The second sensor membrane DS-2 has excellent response to pH in the physiological range, but the sensitivity of the oxygen indicator in PtBuS polymer particles was rather low (Fig. 4.17). Thus, this sensor cannot be used as a dual sensor for precise determination of oxygen concentration and pH in the sample solution.

Figure 4.18 shows emission spectra of both indicators in DS-3 to oxygen partial pressure and pH. Sufficient response to these two parameters is observed. The Ru(dpp)_3^{2+} /ormosil oxygen-sensitive microbeads, thus, show optimal sensitivity to oxygen. Generally, the emission intensities at 530 and 610 nm and the decay time of the long-lived luminophore should be measured to estimate the suitability of the material as dual sensor.

The properties and composition of sensor membranes DS-1, DS-2 and DS-3 are summarized in Table 4.3.

Table 4.3 Figures of the materials used for dual sensing of oxygen and pH.

Type of dual sensor	O_2 sensitive probe	pH sensitive probe	Excitation	Characteristics
DS-1	PdTFPP/PSAN	CF/pHEMA	505 nm	inner-filter effect
DS-2	Ru(dpp)_3^{2+} /PtBuS	CF/pHEMA	470, 505 nm	low sensitivity to oxygen indicator in dual sensor
DS-3	Ru(dpp)_3^{2+} /ormosil	CF/pHEMA	470, 505 nm	good response to oxygen and pH

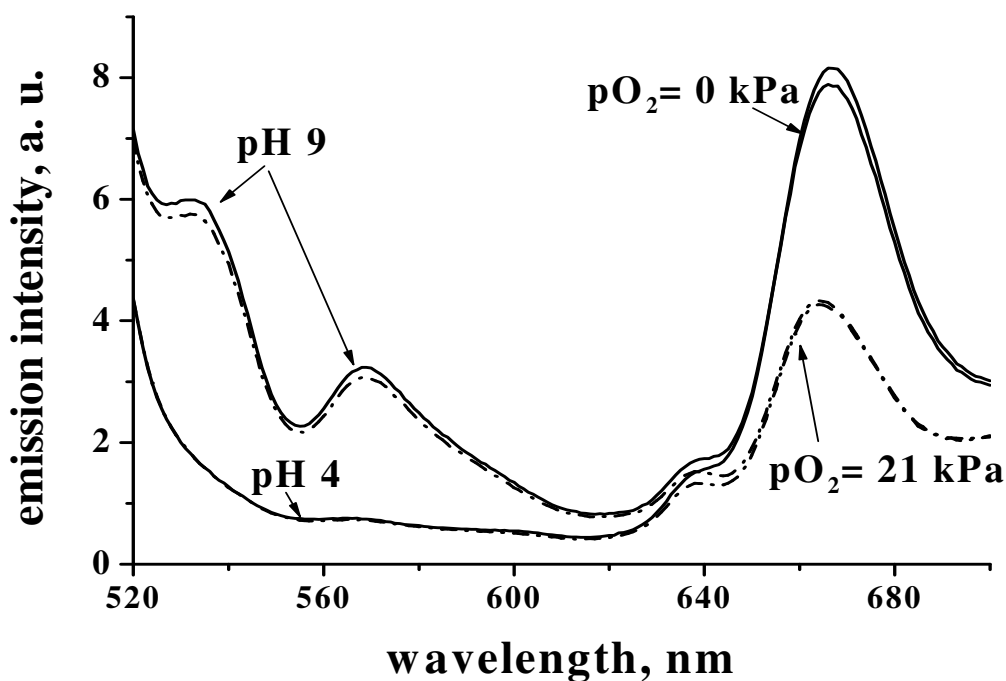


Figure 4.15 Emission spectra of the oxygen and pH indicators in dually sensor membrane DS-1 (CF/p-HEMA and PdTFPP/PSAN microbeads dispersed in hydrogel) at pH 4 and pH 9 and oxygen partial pressures of 0 kPa and 21 kPa (MOPS buffer, IS = 140 mM, $\lambda_{\text{ex}} = 490$ nm).

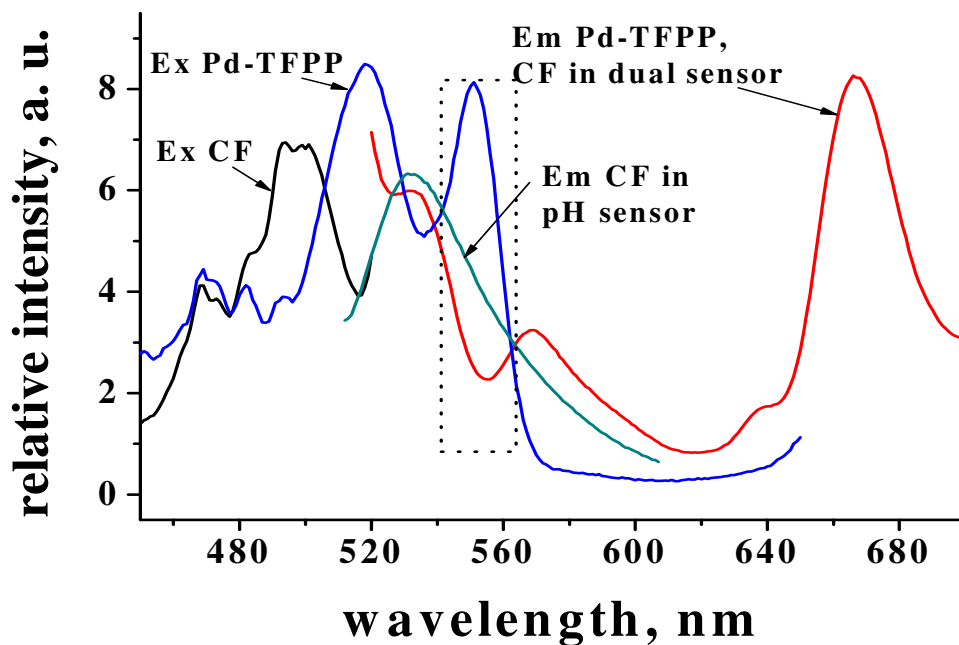


Figure 4.16 Excitation spectra of oxygen indicator and pH indicator, emission spectra of the dually sensing material DS-1 and pH-sensitive probe SM-4 in MOPS buffer solution (pH 9) at $p\text{O}_2 = 0$ kPa ($\lambda_{\text{ex}}/\lambda_{\text{em}} = 490/530$ nm for CF, $\lambda_{\text{ex}}/\lambda_{\text{em}} = 525/670$ nm for PdTFPP).

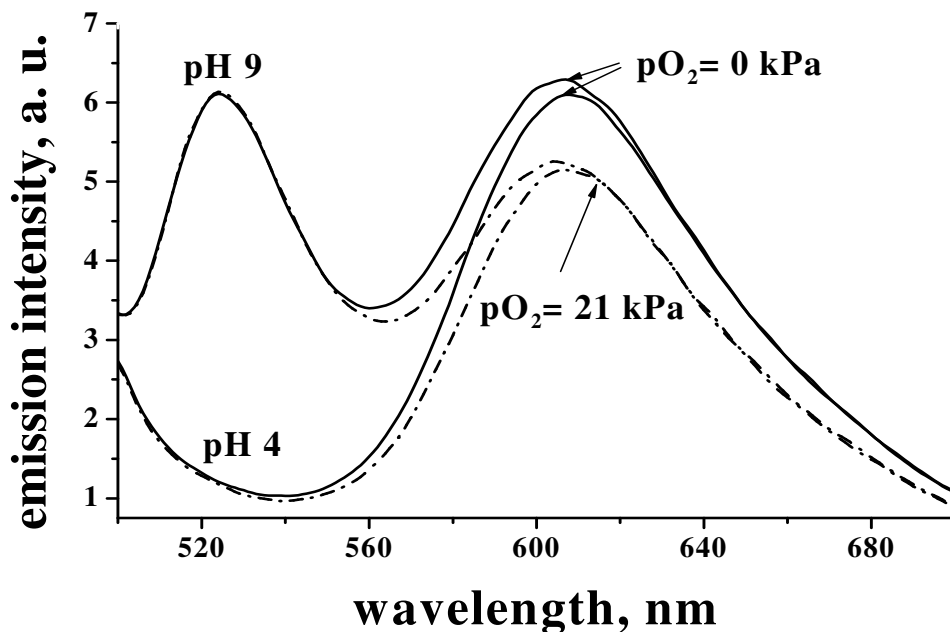


Figure 4.17 Emission spectra of oxygen and pH indicators in the dually sensor membrane DS-2 (CF/pHEMA as pH indicator and Ru(dpp)_3^{2+} /PtBuS as oxygen indicator, $\lambda_{\text{exc}} = 490 \text{ nm}$) at pH 4 and pH 9 and oxygen partial pressure $p\text{O}_2 = 0 \text{ kPa}$ and 21 kPa .

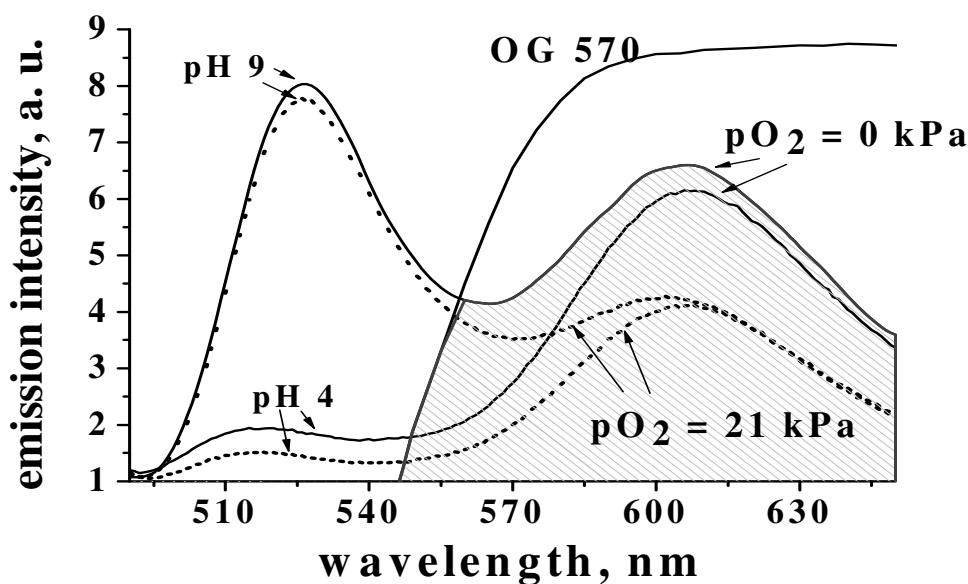


Figure 4.18 Emission spectra of the indicators in the dual sensor DS-3 (CF/p-HEMA and Ru(dpp)_3^{2+} /ormosil microbeads dispersed in hydrogel, $\lambda_{\text{exc}} = 470 \text{ nm}$) at pH 4 and 9 and oxygen partial pressures of 0 kPa and 21 kPa . Included are the spectral cutoffs of the absorbance filter used. The shaded area represents the signal detected by the photodetector.

4.3.5 Response of the Dual Sensor to pH in the Frequency Domain

In the conventional DLR sensor, the fluorescence of a pH indicator is related to the luminescence intensity of a completely inert, long-lived reference luminophore. The behavior of such a sensor can be described by a single calibration curve (phase shift Φ vs. pH), which is very similar to that presented in Fig. 4.19 (measured in the absence of oxygen). The long-lived inert reference luminophore of such sensors typically is contained in a gas-impermeable polymer (usually in the form of polyacrylonitrile microbeads¹⁸) and thus remains unaffected by oxygen. In the frequency-domain DLR method the emission of both indicators is measured simultaneously, which is achieved by using a 570 nm longpass filter (Fig. 4.18). The shaded area represents the part of the emission which passes the filter and is registered by the photodetector.

The situation becomes more complicated if the reference luminophore is substituted by an oxygen indicator. Now, the overall phase shift depends on the concentrations of both analytes (Fig. 4.19). We chose a modulation frequency of 30 kHz, which resulted in the work functions for pH shown in Fig. 4.19. They show that the response curves of the pH indicator have a similar shape at different oxygen concentration (pO_2 from 0 - 21.3 kPa).

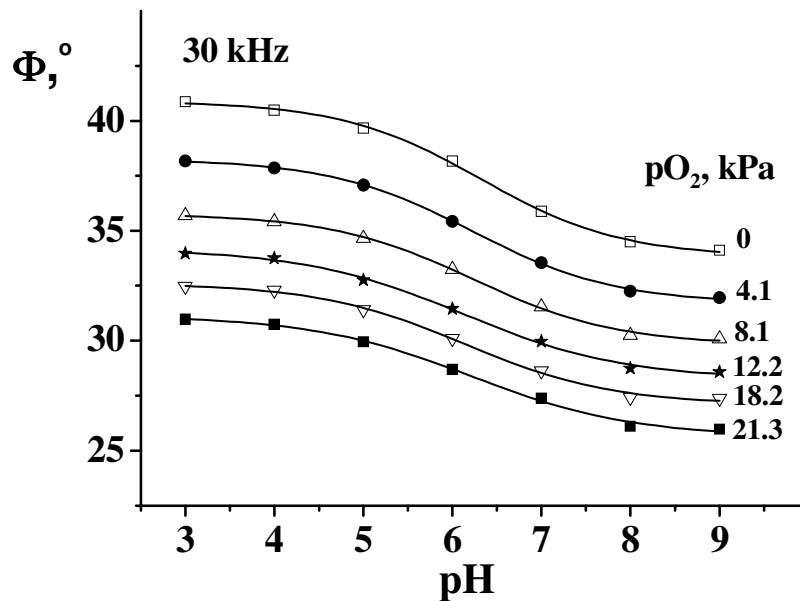


Figure 4.19 pH dependence of the phase shift at 30 kHz in the dual sensor at various oxygen partial pressures (in gas-equilibrated buffer solution). Lines represent fits via eq. 4.1.

For given oxygen level the plots are well described by eq. 4.1. Fitting gives a pK_a of 6.21, and x is 1.932, both parameters being independent of oxygen partial pressure. The fit parameters A_{min} and A_{max} reflect the contribution of the luminescence of the oxygen probe (which is quenched) to the overall phase shift.

The data could be well described by algorithms identified with the Table Curve 2D software. The resulting equations characterize the plots for the parameters A_{max} and A_{min} vs. the oxygen partial pressure (Fig. 4.20) by a mono-exponential decay model (standard deviation $r^2 = 0.99965$):

$$A = B \cdot e^{\left(-\frac{pO_2}{C}\right)} + D \quad (4.6)$$

where A is the phase shift at deprotonated (A_{max}) and protonated (A_{min}) form; and B , C and D are fit parameters.

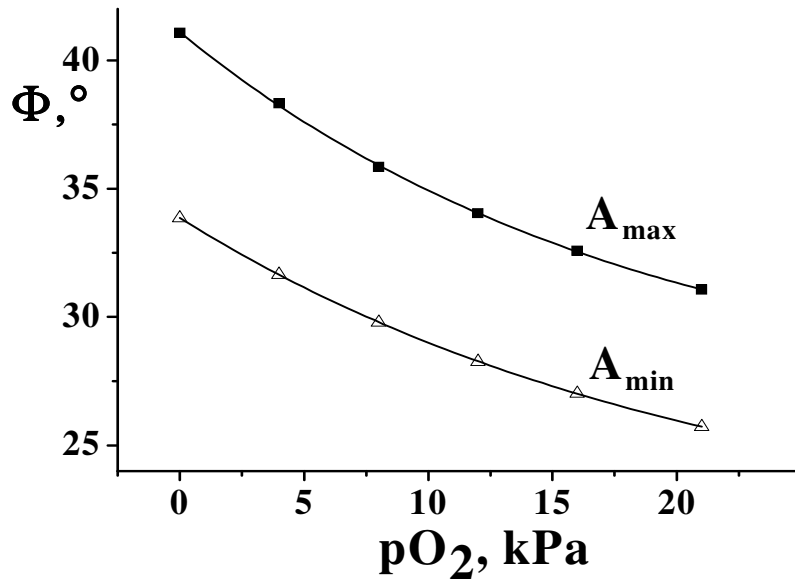


Figure 4.20 Dependence of the parameters A_{max} and A_{min} on the oxygen concentration at a modulation frequency of 30 kHz. Lines represent fits via eq. 4.6 (mono-exponential decay model).

The following fit parameters were thus obtained from eq. 4.6: $B_{max} = 14.817$, $C_{max} = 18.580$ and $D_{max} = 26.281$ for A_{max} , and $B_{min} = 12.984$, $C_{min} = 21.331$ and $D_{min} = 20.878$ for A_{min} . The fit parameters were introduced to eq. 4.1. After mathematical conversion, the following equation is obtained for pH calculation:

$$pH = 6.208 + \ln \left(\frac{(B_{min} \cdot \exp(-pO_2 / C_{min}) + D_{min}) - \Phi_{30kHz}}{\Phi_{30kHz} - (B_{max} \cdot \exp(-pO_2 / C_{max}) + D_{max})} \right) \cdot 0.8387 \quad (4.7)$$

4.3.6 Response of the Dual Sensor to Oxygen in the Frequency Domain

One way to describe the response of the sensor to oxygen is to use the formula for compensation of the background fluorescence⁶¹. The equation was used for screening the fluorescence of pH indicator in the dually sensor. The phase shifts are measured at 30 kHz (f_1) and 60 kHz (f_2). The fluorescence of the pH indicator does not affect the decay time of the long-lived luminophore calculated according to eq. 4.8 at two different frequencies:

$$\tau = \frac{1}{2\pi} \left(\frac{f_1^2 - f_2^2 \pm \sqrt{f_2^2 - f_1^2 - 4(\cot \Phi_2 \cdot f_2 \cdot f_1^2 - \cot \Phi_1 \cdot f_1 \cdot f_2^2)(\cot \Phi_2 \cdot f_2 - \cot \Phi_1 \cdot f_1)}}{2(\cot \Phi_2 \cdot f_2 \cdot f_1^2 - \cot \Phi_1 \cdot f_1 \cdot f_2^2)} \right), \quad (4.8)$$

where Φ_1 and Φ_2 are the phase shifts at modulation frequencies f_1 and f_2 .

The equation enables the calculation of the decay times of long-lived luminescent indicators in the presence of another fluorescent dye. Overall phase shifts measured at 30 and 60 kHz in the absence of oxygen (see Fig. 4.19) depend on the pH value since the luminescence of the pH indicator contributes to the overall phase shift. However, if eq. 4.8 is used, the decay time calculated for the oxygen indicator ($\tau_0 = 5.38 \pm 0.05 \mu\text{s}$) remains constant from pH 3 to pH 9.

The response function of the dual sensor towards oxygen is presented in Fig. 4.21. Again, eq. 4.6 was used for fitting (correlation coefficient $r^2 = 0.999$), and the following fit parameters were obtained: $B = 1.354 \cdot 10^{-6}$, $C = 11.956$ and $D = 4.031 \cdot 10^{-6}$. The oxygen concentration can be calculated via the following eq. 4.9:

$$pO_2 = -C \cdot \ln \left(\frac{\tau - D}{B} \right) \quad (4.9)$$

where τ is the decay time calculated via eq. 4.8.

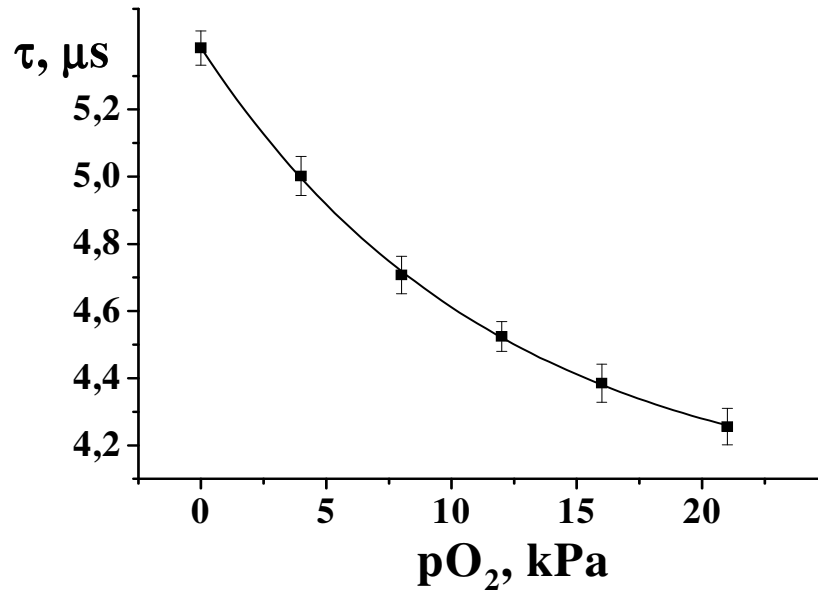


Figure 4.21 Response function of the dual sensor towards oxygen at pH 3 to 9. The data overlap completely. The square data points are the decay times as calculated via eq. 4.8. The line represents a fit via eq. 4.6.

4.3.7 Sensor Homogeneity

The homogeneity of the materials is very important for any sensor making use of the m-DLR technique along with bead indicators since good spatial resolution of calibration plots can be compromised by such inhomogeneities. Figure 4.22 shows a photographic image of a sensor membrane (DS-3) taken on a fluorescent microscope. In order to avoid aggregation of the particles, their concentration (at the same mass ratio of SB-3 to SB-4) in the hydrogel was reduced by a factor of 10. The size of both the pH-sensitive (green fluorescent) particles, and of the oxygen-sensitive (red fluorescent) particles is estimated to range between 1 and 3 μm .

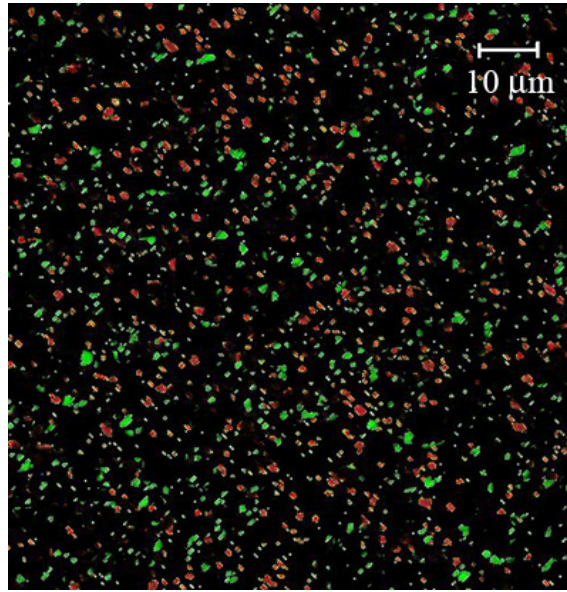


Figure 4.22 Photographic image of the sensor foil DS-3.

The size of the microparticles is indeed sufficient to obtain a highly homogeneous sensor layer for measurements using a 2 mm optical fiber, and also adequate for fiber tips as thin as 100 μm. This was proven by measurement of the phase shifts (at pH 8 and 0 kPa pO₂) of 7 randomly chosen spots of 2 mm diameter punched from a 20×30 mm piece of sensor foil. The standard deviation of the phase shift Φ at a modulation frequency of 60 kHz is higher ($\Phi = 41.17 \pm 0.19$) than at a frequency of 30 kHz ($\Phi = 33.56 \pm 0.07$), however it does not exceed 0.45%.

4.3.8 Validation

The response functions were validated with test solutions of pH 7.53, 6.50 and 4.46, respectively. They were equilibrated with oxygen to give a pO₂ of 5.10 and 15.20 kPa, respectively. Phase shifts were then determined at 30 and 60 kHz. The data obtained were used to calculate the oxygen concentration via eq. 4.9 and introduced into eq. 4.7 to obtain the pH value. Table 4.4 compares the calculated and real values of pH and pO₂. The deviations between real and calculated pO₂ do not exceed 15%, while the highest error in pH determination is 0.23 pH units. One can observe, however, that the calculated pO₂ is always slightly higher than the pO₂ applied. This systematic error is most likely due to the difference in the temperatures when calibrating (20 °C) and when validating (23 °C) the sensors, a fact that unfortunately was discovered after the completion of the experiments only. It is known^{62,63} that the sensitivity of this oxygen probe increases with temperature.

Table 4.4 Determination of the pH and pO₂ in kPa by the dual sensor in test solutions (at 20°C).

<u>Solution no.</u>	<u>analyte</u>	<u>adjusted values</u>	<u>calc. values</u>	<u>Error: ΔpO_2, ΔpH</u>
1	pO ₂	5.10	5.70	0.60
	pH	6.50	6.60	0.10
2	pO ₂	15.20	16.19	0.99
	pH	6.50	6.43	0.07
3	pO ₂	5.10	5.61	0.51
	pH	7.53	7.38	0.15
4	pO ₂	5.10	5.87	0.77
	pH	4.46	4.49	0.03
5	pO ₂	15.20	16.79	1.59
	pH	4.46	4.23	0.23
6	pO ₂	15.20	16.44	1.24
	pH	7.53	7.72	0.19

4.4 Conclusion

New sensor materials are introduced that enable simultaneous sensing of pH and dissolved oxygen. Three different dual sensor materials were investigated which consist of PdTFPP or Ru(dpp)₃²⁺ complexes as oxygen indicator and carboxyfluorescein as pH indicator. The fluorescent indicators are immobilized in different kinds of organic polymer microbeads, which in turn are contained in a hydrogel matrix. This approach displays significant advantages over sensor materials with homogeneously dissolved indicators in that (a) the selectivity and sensitivity of indicators can be controlled; (b) cross-sensitivities (e.g. due to quenching) can be reduced to a minimum; (c) the system is much more photostable because the singlet oxygen produced in the oxygen beads cannot decompose the pH indicator contained in the other beads. A disadvantage of the dually sensing material based on PdTFPP/PSAN and CF/pHEMA was an inner-filter effect, and of the sensor membrane with Ru(dpp)₃²⁺/PtBuS and CF/pHEMA microparticles the low sensitivity of the oxygen indicator. However, the dual sensor based on Ru(dpp)₃²⁺/ormosil and CF/pHEMA microparticles has no such effects and can be used for biological applications as a dual sensor for simultaneous

monitoring of oxygen and pH in aqueous sample solutions.

4.5 References

1. Canete F, Rios A, Luque de Castro M D, Valcarcel M **Determination of analytical parameters in drinking water by flow injection analysis. Part 1. Simultaneous determination of pH, alkalinity and total ionic concentration.** *Analyst* **1987**, 112, 263-266
2. Preininger C, Klimant I, Wolfbeis O S **Optical Fiber Sensor for Biological Oxygen Demand.** *Anal. Chem.* **1994**, 66, 1841-1846
3. John G T, Goelling D, Klimant I, Schneider H, Heinzle E **pH-sensing 96-well microtitre plates for the characterization of acid production by dairy starter cultures.** *J. Dairy Res.* **2003** , 70, 327-333
4. Marshall A J, Blyth J, Davidson C A B, Lowe C R **pH-sensitive holographic sensors.** *Anal. Chem.* **2003**, 75, 4423-4431
5. Young O A, Thomson R D, Merhtens V G, Loeffen M P F **Industrial application to cattle of a method for the early determination of meat ultimate pH.** *Meat Sci.* **2004**, 67, 107-112
6. O'Mahony F C, O'Riordan T C, Papkovskaya N, Kerry J P, Papkovsky D B **Non-destructive assessment of oxygen levels in industrial modified atmosphere packaged cheddar cheese.** *Food Control.* **2006**, 17, 286-292
7. Papkovsky D B, Papkovskaya N, Smyth A, Kerry J, Ogurtsov V I **Phosphorescent sensor approach for non-destructive measurement of oxygen in packaged foods: optimization of disposable oxygen sensors and their characterization over a wide temperature range.** *Anal. Lett.* **2000**, 33, 1755-1777
8. Suzuki M, Nakabayashi H, Honda M **Micro optical pH and oxygen sensor array for cell chips.** *Chem. Sensors* **2004**, 20, 562-563
9. Deshpande R R, Koch-Kirsch Y, Maas R, Krause C, Heinzle E **Microplates with integrated oxygen sensors for kinetic cell respiration measurement and cytotoxicity testing in primary and secondary cell lines.** *Assay Drug. Dev. Technol.* **2005**, 3, 299-307
10. O'Mahony F C, O'Donovan C, Hynes J, Moore T, Davenport J, Papkovsky D B **Optical oxygen microrespirometry as a platform for environmental toxicology and animal model studies.** *Environ. Sci. Technol.* **2005**, 39, 5010-5014

11. Alderman J, Hynes J, Floyd S M, Kruger J, O'Connor R, Papkovsky D B **A low-volume platform for cell-respirometric screening based on quenched-luminescence oxygen sensing.** *Biosens Bioelectron* **2004**, 19, 1529-1535
12. O'Donovan C, Hynes J, Yashunski D, Papkovsky D B **Phosphorescent oxygen-sensitive materials for biological applications.** *J. Mater. Chem.* **2005**, 15, 2946-2951
13. Kojima S, Suzuki H **A micro sensing system for blood gas analysis.** *Chem. Sensors* **2003**, 19, 25-27
14. Jeevarajan A S, Vani S, Tazlor T D, Anderson M M **Continuous pH monitoring in a perfused bioreactor system using an optical pH sensor.** *Biotechnol. Bioeng.* **2002**, 78, 467-473
15. Mekhail K, Khacho M, Gunaratnam L, Lee S **Oxygen sensing by H⁺. Implications for HIF and hypoxic cell memory.** *Cell Cycle* **2004**, 3, 1027-1029
16. Meruva R K, Meyerhoff M E **Catheter-type sensor for potentiometric monitoring of oxygen, pH and carbon dioxide.** *Biosens. Bioelectron.* **1998**, 13, 201-212
17. Bellerby R G, Olsen A, Johannessen T, Croot P A **high precision spectrophotometric method for on-line shipboard seawater pH measurements: the automated marine pH sensor (AMpS).** *Talanta* **2002**, 56, 61-69
18. Schroeder C, Weidgans B M, Klimant I **pH Fluorosensors for use in marine systems.** *Analyst* **2005**, 130, 907-916
19. Neurauter G, Klimant I, Wolfbeis O S **Fiber-optic microsensor for high resolution pCO₂ sensing in marine environment.** *Fresenius J. Anal. Chem.* **2000**, 366, 481-487
20. Gouin J F, Baros F, Birot D, Andre J C **A fiber-optic oxygen sensor for oceanography.** *Sens. Actuators, B* **1997**, 39, 401-406
21. Klimant I, Meyer V, Kühl M **Fiber-optic oxygen microsensors, a new tool in aquatic biology.** *J. Limnol. and Oceanogr.* **1995**, 40, 1159-1165
22. Song A, Parus S, Kopelman R **High-performance fiber-optic pH microsensors for practical physiological measurements using a dual-emission sensitive dye.** *Anal. Chem.* **1997**, 69, 863-867
23. Wolfbeis, O. S. **Materials for fluorescence-based optical chemical sensors.** *J. Mater. Chem.* **2005**, 15, 2657-2669
24. Park E J, Reid K R, Tang W, Kennedy R T, Kopelman, R. **Ratiometric fiber optic sensors for the detection of inter- and intra-cellular dissolved oxygen.** *J. Mater. Chem.* **2005**, 15, 2913-2919
25. Klimant I, Huber C, Liebsch G, Neurauter G, Stangelmayer A, Wolfbeis O S (edc)

Fluorescence spectroscopy: New Methods and Applications; Springer: Berlin, 2000

26. Lakowicz J R, Castellano F N, Dattelbaum J D, Tolosa L, Rao G, Gryczynski I **Low-Frequency Modulation Sensors Using Nanosecond Fluorophores**. *Anal. Chem.* **1998**, 70, 5115-5121
27. Liebsch G, Klimant I, Krause C, Wolfbeis O S **Fluorescent Imaging of pH with Optical Sensors Using Time Domain Dual Lifetime Referencing**. *Anal. Chem.* **2001**, 73, 4354-4363
28. Szmajcinski H, Lakowicz J R **Optical measurements of pH using fluorescence lifetimes and phase-modulation fluorometry**. *Anal. Chem.* **1993**, 65, 1668-1676
29. Klimant I, Wolfbeis O S **Oxygen-Sensitive Luminescent Materials Based on Silicone-Soluble Ruthenium Diimine Complexes**. *Anal. Chem.* **1995**, 67, 3160-3166
30. Klimant I, Ruckruh F, Liebsch G, Stangelmayer A, Wolfbeis O S **Fast response oxygen micro-optodes based on novel soluble ormosil glasses**. *Mikrochim. Acta* **1999**, 131, 35-46
31. Perrin D D, Dempsey B **Laboratory Manuals**; Chapman & Hall: London, **1974**, p 62
32. Hermanson G T **Bioconjugate Techniques**; Academic Press: New York, **1996**, p 100
33. Huber C, Werner T, Krause C, Leiner M J P, Wolfbeis O S **Overcoming the pH dependency of optical sensors: a pH-independent chloride sensor based on co-extraction**. *Anal. Chim. Acta* **1999**, 398, 137-143
34. Silcoff E R, Sheradsky T **Polymers containing backbone fluorescein, phenolphthalein and benzaurine. Synthesis and optical properties** *New J. Chem.* **1999**, 23, 1187-1192
35. Haugland R P **Handbook of fluorescent probes and research products**. Molecular Probes Inc, **2002**, Chapter 21 (www.probes.com)
36. Butler T M, MacCraith B D, McDonagh C J **Leaching in sol-gel-derived silica films for optical pH sensing**. *Non-Cryst Solids* **1998**, 224, 249-258
37. Alford P C, Cook M J, Lewis A P, McAuliffe G S G, Skarda V, Thomson A J **Luminescent metal complexes. Part 5. Luminescence properties of ring-substituted 1,10-phenanthroline tris-complexes of ruthenium(II)**. *J. Chem. Soc. Perkin Trans II* **1985**, 705-709
38. Spellane P J, Gouterman M, Antipas A, Kim S, Liu Y C **Porphyrins. 40. Electronic Spectra and Four-Orbital Energies of Free-Base, Zinc, Copper, and Palladium Tetrakis(perfluorophenyl)porphyrins** *Inorg. Chem.* **1980**, 19, 386-391
39. Xu H, Aylott J W, Kopelman R, Miller T J, Philbert M A **A real-time ratiometric method for the determination of molecular oxygen inside living cells using sol-gel-based**

- spherical optical nanosensors with applications to rat C6 glioma.** *Anal. Chem.* **2001**, 73, 4124-4133
40. Morin A, Xu W, Demas J, DeGraff B **Oxygen sensors based on quenching of tris-(4,7-diphenyl-1,10-phenanthroline)ruthenium(II) in fluorinated polymers.** *J. Fluorescence* **2000**, 10, 7-12
41. Mongey K F, Vos J G, MacCraith B D, McDonagh C M, Coates C, McGarvey J J **Photophysics of mixed-ligand polypyridyl ruthenium (II) complexes immobilized in silica sol-gel monoliths.** *J. Mater. Chem.* **1997**, 7, 1473-1479
42. McEvoy A, McDonagh C, MacGraith B **Optimization of sol-gel-derived silica films for optical oxygen sensing.** *J. Sol-Gel Sci. Technolog.* **1997**, 8, 1121-1125
43. Fröba M, Köhn R, Bouffaud G, Richard O, Van Tendeloo G **Fe₂O₃ Nanoparticles within Mesoporous MCM-48 Silica: In Situ Formation and Characterization.** *Chem. Mater.* **1999**, 11, 2858-2865
44. Wang H, Chen P, Zheng X **Hollow permeable polysiloxane capsules: a novel approach for fabrication, guest encapsulation and morphology studies.** *J. Mater. Chem.* **2004**, 14, 1648-1651
45. Wolfbeis O S, Reisfeld R, Oehme I **Sol-gels and chemical sensors.** *Structure and Bonding (Berlin)* **1996**, 85(Optical and Electronic Phenomena in Sol-Gel Glasses), 51-98.
46. Peppas N A **Preparation Methods & Structures of Hydrogels.** CRC Press: Boca Raton, 1986.
47. Weidgans B M, Krause C, Klimant I, Wolfbeis O S **Fluorescent pH sensors with negligible sensitivity to ionic strength.** *Analyst* **2004**, 129, 645-650
48. Agi Y, Walt D R **Fluorescence monitoring of the microenvironmental pH of highly charged polymers.** *J. Polym. Sci., A: Polym. Chem.* **1997**, 35, 2105-2110
49. Kostov Y, Tzonkov S, Yotov L, Krysteva M **Membranes for optical pH sensors.** *Anal. Chim. Acta* **1993**, 280, 15-19
50. Jones T P, Porter M D **Optical pH sensor based on the chemical modification of a porous polymer film.** *Anal. Chem.* **1988**, 60, 404-406
51. Fuh M-R S, Burgess L W, Hirschfeld T, Christian G D **Single fiber optic fluorescence pH probe.** *Analyst* **1987**, 112, 1159-1163
52. Sanchez-Barragan I, Costa-Fernandez J M, Sanz-Medel A **Tailoring the pH response range of fluorescent-based pH sensing phases by sol-gel surfactants co-immobilization.** *Sens. Actuators B* **2005**, 107, 69-76
53. Leiner M J P, Wolfbeis O S **Fiber Optic Chemical Sensors and Biosensors.** CRC Press,

Boca Raton, 1991, p 63

54. Leiner M J P, Hartmann P **Theory and practice in optical pH sensing.** Sens. Actuators B **1993**, 11, 281-289

55. Weidgans B M **New fluorescent optical pH sensors with minimal effects of ionic strength.** Ph D thesis, University of Regensburg, Regensburg, **2004**, p 138

56. Carraway E R, Demas J N, DeGraff B A, Bacon J R **Photophysics and photochemistry of oxygen sensors based on luminescent transition-metal complexes.** Anal. Chem. **1991**, 63, 337-342

57. Sacksteder L, Demas J N, DeGraff B A **Design of oxygen sensors based on quenching of luminescent metal complexes: Effect of ligand size on heterogeneity.** Anal. Chem. **1993**, 65, 3480-3483

58. Schanze K S, Carroll B F, Korotkevitch S, Morris M J **Temperature dependence of pressure sensitive paints.** Am. Inst. Aeron. Astron. J. **1997**, 35, 306

59. McNamara K P, Li X, Stull A D, Rosenzweig Z **Fiber-optic oxygen sensor based on the fluorescence quenching of tris(5-acrylamido-1,10-phenanthroline)ruthenium chloride.** Anal. Chim. Acta **1998**, 361, 73-83

60. Garcia-Fresnadillo D, Marazuela M D, Moreno-Bondi M K, Orellana G **Luminescent Nafion Membranes Dyed with Ruthenium(II) Complexes as Sensing Materials for Dissolved Oxygen.** Langmuir **1999**, 15, 6451-6459

61. Neurauter D **Frequency domain pCO₂ sensing.** PhD thesis, University of Regensburg, Regensburg, **2000**, p 106

62. Demas J N, DeGraff B A **Luminescence-based sensors: microheterogeneous and temperature effects.** Sens. Actuators B **1993**, 11, 35-41

63. Ogurtsov V I, Papkovsky D B **Modelling of phase-fluorometric oxygen sensors: Consideration of temperature effects and operational requirements.** Sens. Actuators B **2006**, 113, 917-929

Chapter 5

Fiber Optic Microsensor for Simultaneous Sensing of Oxygen and pH

Fiber optic microsensor with a tip diameter of ~140 μm have been developed that enable simultaneous measurement of dissolved oxygen (DO) and pH. The tip of the optical fiber was covered with a sensor composition based on luminescent microbeads that respond to the respective parameter by a change in the decay time and/or intensity of their luminescence. The use of microbeads enables the ratio of the signals to be easily varied and also reduces the adverse effect of singlet oxygen that is produced in the oxygen-sensitive beads. Luminescence measurements were performed in the frequency domain. The microsensor for DO/pH relies on a modified dual luminophore referencing (DLR) scheme in which measurements are performed at two different modulation frequencies and where only one excitation source (an LED) is used. The sensor material was read out with a commercially available reader. Since the sensing scheme is self-referenced in being based on the measurement of a phase shift, the microsensor does not suffer from drifts in the opto-electronic system and from variations in probe concentration, sensor layer thickness, sample turbidity and color, and sample refractive index, which are common drawbacks of intensity-based sensors. (Anal Chem 2007, submitted)

5.1 Introduction

Oxygen and pH are key parameters in environmental monitoring^{1,2}, marine research^{3,4}, in food industry⁵⁻⁷, biotechnology⁸⁻¹⁰, and in medicine¹¹. Simultaneous measurement of two of these parameters is often required in complex media and processes^{12,13}. Moreover, knowing temperature is particularly important in optical sensing of oxygen since quenching by oxygen always is highly temperature dependent^{14,15}. Recently, materials have been reported for simultaneous optical sensing of two parameters¹⁶⁻¹⁹. Optical sensing is particularly advantageous over other methods since it makes possible virtually non-invasive

measurements, e.g. through the glass window of a reaction vessel or bioreactor. In this case, a spot of sensing material is located on a wall inside the reaction vessel, while reading (by reflectance, fluorescence etc.) is performed from outside. There are, however, numerous situations where such a sensor spot cannot be easily located at the site to be monitored, for example when it comes to perform measurements inside the body.

Microsensors represent an elegant solution in this limitation. Because of its size (20 – 200 μm are typical), a microsensor can be placed inside the body using a protective housing such as a steel needle, and still will remain only minimally invasive²⁰. Fiber optic microsensors are easier to fabricate than micro-electrodes. While numerous kinds of fiber optic chemical sensor and biosensors have been described so far²¹, it must be noted that not a single fiber optic (or other) sensor has survived on the market for in-vivo monitoring of blood. One major reason (aside from problems associated with inflammation and sensor fouling) is the size of the sensor head, since at least three parameters are to be monitored in critical care medicine. If a single sensor tip can measure n parameters simultaneously, the size required for the sensor array is reduced by a factor of $1/n$, and the sample volume to a similar extent.

Microsensors capable of simultaneous measurement of several parameters also are the sensor of choice if high spatial resolution is required. Microsensors capable of measuring a single analyte such as oxygen²²⁻²⁴, pH²⁵⁻²⁷, carbon dioxide^{28,29}, or potassium ion³⁰ have been reported. To our knowledge, the only microsensor proposed so far that would enable simultaneous monitoring of two analytes was reported by Ji and Rosenzweig (a sensor for Ca^{2+} and pH)³¹. It makes use of a mixture of two indicators, both immobilized at the tip of an optical fiber and excited with a laser beam. It requires measurement of fluorescence intensity (rather than decay time) at three wavelengths using a CCD camera. The approach made by Walt and co-workers^{32,33} who positioned μm -sized sensing beads at the end of a fiber bundle array is highly promising in terms of multi-analyte sensing, but is intended for imaging purposes only and does not allow for dual sensing using a single fiber.

We report on microsensor that is capable of simultaneous and continuous sensing of pO_2 (DO) and pH. A frequency domain method is applied for interrogation in order to warrant excellent long-term stability. The approach is fully compatible with a commercially available compact fiber optic oxygen microsensor^{34,35}.

5.2 Experimental

5.2.1 Materials

The polyurethane hydrogel (type D4) was obtained from Cardiotech (www.cardiotech-inc.com). The pH-sensitive microbeads consisted of 8-hydroxy-pyrene-1,3,6-trisulfonate (HPTS; from Fluka, www.sigmaaldrich.com) that was covalently immobilized (via its trisulfochloride)³⁶ on an amino-modified poly(hydroxyethyl methacrylate) (p-HEMA) that was copolymerized with N-aminoethylacrylamide) and was obtained from Presens³⁷ (www.presens.de). The oxygen probe ruthenium(II)-tris-4,7-diphenyl-1,10-phenanthroline [Ru(dpp)₃(TMS)₂ salt] was synthesized as described before³⁸. The preparation of organically-modified sol-gel beads ("ormosil") polymer was reported elsewhere³⁵, as was the preparation of the oxygen-sensitive ormosil beads (Ru(dpp)₃²⁺ in ormosil)¹⁸. All chemicals and solvents were of analytical grade and used without further purification. Calibration gases (nitrogen and oxygen, each of 99.999 % purity) were purchased from Linde (www.linde-gase.de).

Doubly distilled water was used for the preparation of the buffer solutions. Their pH was controlled with a digital pH meter (Knick, www.knick.de) calibrated at 20 ± 1 °C with standard buffers of pH 7.0 and 4.0 (Merck; www.merck.de). The pH of solutions was adjusted (to within +/- 0.03 units) to the desired value using MOPS buffers. These were adjusted to constant ionic strength ($I = 140$ mM) using sodium chloride as the background electrolyte³⁹.

5.2.2 Preparation of the Microsensor

Sensor cocktail was prepared by dispersing 10 mg of the Ru(dpp)₃²⁺/ormosil microbeads and 14 mg of the HPTS/p-HEMA microbeads in 500 mg of a 5% wt. solution of the polyurethane hydrogel in an ethanol/water (9:1; v:v) mixture. This cocktail was stirred overnight. The tip of a 140-μm bifurcated optical glass fiber (from GP Fiber Optics; www.gp-fiberoptics.de) was coated with the sensor chemistry by immersing it into the cocktail and subsequently drying the material at ambient air for 24 h at room temperature. Figure 5.1 shows photographic images of the microsensor during excitation.

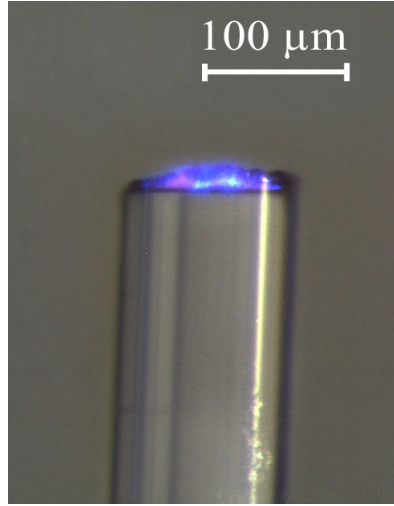


Figure 5.1 Photographic images during excitation with a 470-nm LED. The sensor tip (pH/O₂) displays the blue color of the 470-nm LED and some red and green luminescence that results from the dual sensor.

5.2.3 Components of the Optical System for Dual Sensing of O₂/pH

In case of SC-2, the measurements were performed using a single pH-1 Micro device (see Fig. 5.2). The light from a 470-nm LED was filtered through a short-pass filter (BG 12; Schott). Luminescence was detected by a photodiode (PD) after being filtered through a customized long-pass filter with a medium cut-off wavelength of 550 nm. The excitation light of a 470-nm LED was modulated at two modulation frequencies of 30 and 60 kHz, respectively. Decay times were calculated using the equation $\tau = \tan \phi / 2\pi f$, where ϕ is the measured phase shift and f the modulation frequency of the respective LEDs.

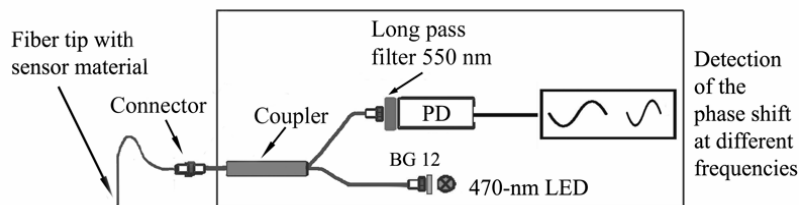


Figure 5.2 Components of the optical system used with the pH/O₂ dual microsensor using a phase-resolving reader (pH-1 Micro). PD: photodiode.

5.2.4 Response Curve

Microsensors (10 pcs.) were immersed into a 100-mL glass beaker containing 30 mL of buffer solution of defined pH. Nitrogen/oxygen gas mixtures, whose composition and flow rate was controlled by a gas mixing device (GVS; from MKS; www.mksinst.com), were bubbled through the buffer solution to adjust the desired concentrations of dissolved oxygen. All data were performed at constant temperature 25 °C.

Reproducibility tests and response curves were obtained by rapidly (within 1 s) moving a microsensor from one beaker to another, having different concentration of the analytes (pH; oxygen).

Photographic images of the sensor cocktails spread as thin films (Fig. 5.3) were acquired using a Leica DC 200 digital color camera mounted onto a Leica DMRE fluorescence microscope (www.leica-microsystems.com). The cocktails were coated on the polyester support to result in films after solvent evaporation. To avoid aggregation, the concentration of the beads in the films was reduced by a factor of 10 compared to the concentration in the microsensor. Photographic images of the sensor tip (Fig. 5.1) were obtained using a color Motic 1.3 Mpixel CCD-camera (type Moticom 1000; www.motic.com) mounted onto a Zeiss stereomicroscope (type STEMI 2000-C; www.zeiss.com).

5.2.5 Experimental Data Fitting

2D plots were fitted using Origin[®] vs. 6.1 (www.originlab.com). The equations were solved using Maple software (vs. 8; www.maplesoft.com).

5.3 Results and Discussion

5.3.1 Choice of Materials

The principle of designing the materials capable of simultaneous sensing of two analytes is straightforward: two probes are designed and then combined so that cross-sensitivity to the other analyte is avoided or minimized. That is best achieved by using microbeads that can be dispersed in a single polymer matrix that needs to be permeable, however, to both parameters.

For sensor materials such as for pO₂/pH, this approach also allows for an easy fine-tuning of the response range of a sensor.

The probes were chosen mainly by considering the criteria of (a) sensitivity (resolution over the range of interest); (b), photoexcitation with LEDs and – preferably – at one excitation wavelength only; (c) distinctly different decay times of luminescence; (d), readout via a commercial reader. The ranges of interest are as follows: 0-21 kPa oxygen, pH 6 – 8. As a reader, we envisioned the use of pH-1 micro.

The composite material of microsensor makes use of the two types of polymer microbeads – oxygen-sensitive and pH-sensitive ones. For the preparation of the oxygen-sensitive microbeads, the oxygen indicator Ru(dpp)₃²⁺ was entrapped into highly gas permeable organically modified silica (ormosil). Thus, optimal sensitivity to oxygen was achieved. Microbeads containing HPTS immobilized on the amino-modified p-HEMA were used as pH probes. The Ru(dpp)₃²⁺/ormosil and HPTS/pHEMA microbeads were dispersed in a biocompatible hydrogel matrix which is permeable to both oxygen and protons. Platinum(II) porphyrin complexes as well as various ruthenium(II)polypyridyl complexes are viable oxygen indicators and are widely in optical sensing and imaging of oxygen⁴⁰⁻⁴².

The size of the beads is critical for sensor properties, such as sensitivity and dynamic response, and even small inhomogeneities can produce significant deviation in case of microsensors. That is particularly true for the pH/O₂ microsensor, since fluorescence intensity of the pH indicator is a referenced parameter. Figure 5.3 shows images of the microbeads obtained with fluorescence microscopy. Sensor cocktails containing only single type of microbeads were coated on the polyester support and were allowed to dry to result in films. Typically, the size of the microbeads varies from 3 to 10 μm; in case of HPTS/pHEMA beads some bigger aggregates (up to 15 μm) are also visible. As will be shown the size of the beads is sufficient to obtain reproducible results.

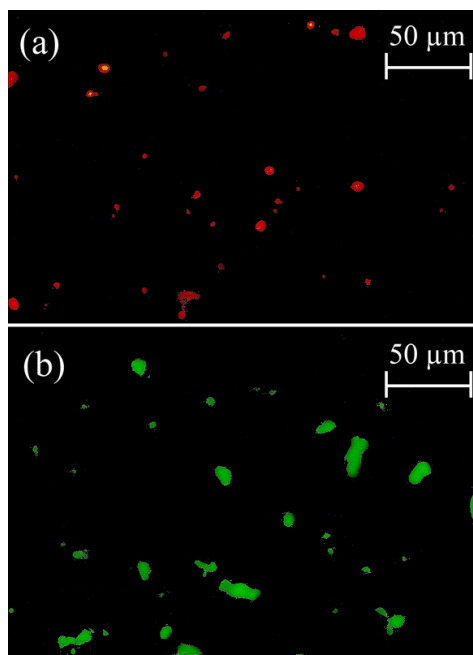


Figure 5.3 Photographic images (obtained with a fluorescence microscope) of the sensor materials: a, Ru(dpp)_3^{2+} /ormosil (oxygen sensitive) beads in hydrogel; b, HPTS/pHEMA (pH sensitive) beads in hydrogel.

5.3.2 Spectroscopy and Optoelectronic System

In the microsensor for pH and oxygen, a modified dual lifetime referencing method (m-DLR) was applied that was described in some detail previously⁴³. The pH probe (HPTS) with its excitation/emission maxima of 468/542 nm, respectively, and the oxygen probe (Ru(dpp)_3^{2+}) with its absorption/emission maxima of 468/608 nm, respectively, were simultaneously excited with a single LED. The overall phase shift of the luminescences at above 550 nm is detected at modulation frequencies of 30 and 60 kHz, respectively. This results in an information on the pH-dependent fluorescence intensity of the pH probe (see below), and on the oxygen-dependent luminescence decay time of the oxygen probe. Because the fluorescence intensity is actually referenced against the decay time, such sensors do not suffer from drifts of the opto-electronic system and variations in the optical properties of the sensor material (including probe concentration and layer thickness) and of the sample (including turbidity, intrinsic sample coloration, and refractive index) which are common drawbacks of intensity-based sensors.

5.3.3 Response of the Sensor

Figure 5.4 gives the experimental data. Measurement at two modulation frequencies (30 and 60 kHz) is adequate to end up with equations for the response of both analytes. The curves obtained with aqueous solutions of various pO_2 partial pressures can fit by the following equation ($r^2 > 0.997$):

$$\Phi = \frac{A_{\max} - A_{\min}}{1 + 10^{(pH - pK_a)/x}} + A_{\min}, \quad (5.1)$$

where Φ is overall phase shift, A_{\max} , A_{\min} and x are numerical coefficients. A_{\max} and A_{\min} are numerical values of the phase shift of the pH probe in fully protonated (A_{\min}) and fully deprotonated (A_{\max}) form, respectively.

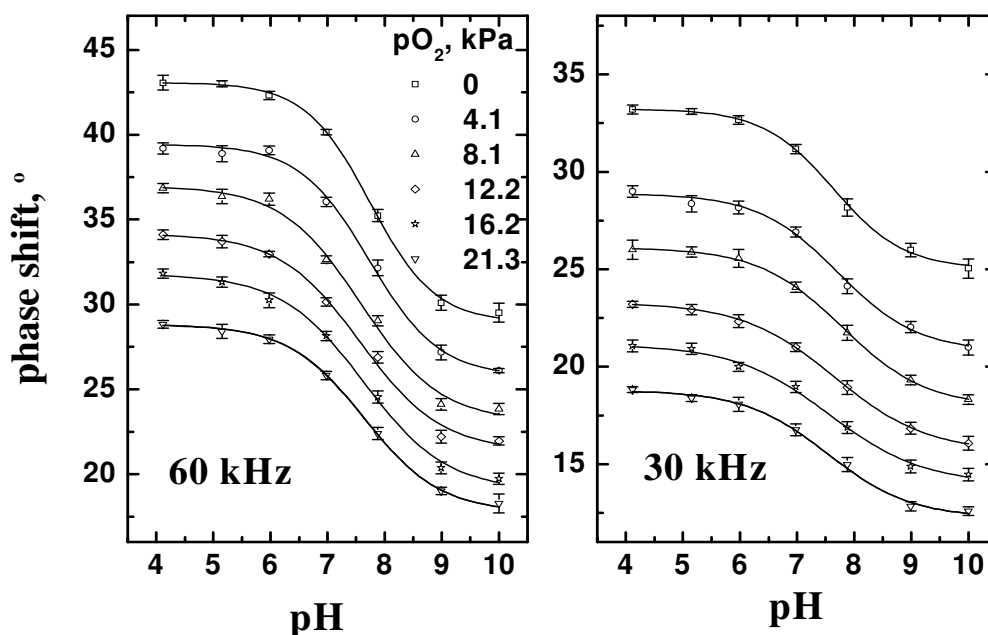


Figure 5.4 Response of the microsensor to pH at different oxygen partial pressures in buffered solutions (pO_2 , kPa). Lines represent a fit using eq. 5.1.

The pK_a is an intrinsic property of the (immobilized) probe and found to be independent of the pO_2 ($pK_a = 7.651 \pm 0.096$ and $pK_a = 7.651 \pm 0.07$; calculated for modulation frequencies of 30 and 60 kHz, respectively). The coefficient x does not depend on pO_2 either. It is slightly

affected, however, by the modulation frequency used ($x = 0.737 \pm 0.076$ and $x = 0.663 \pm 0.060$ at modulation frequencies of 30 and 60 kHz, respectively). On the other side, coefficients A_{\max} and A_{\min} reflect the contribution of the oxygen probe (which is quenched) to overall phase shift. They are plotted vs. pO_2 in Fig. 5.5.

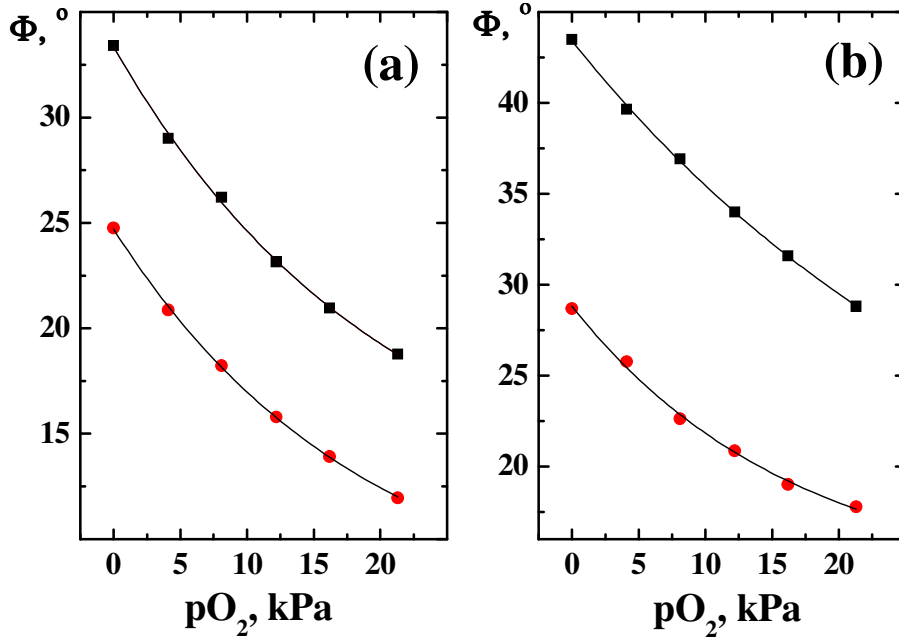


Figure 5.5 Dependence of the fitting parameters A_{\max} and A_{\min} on the oxygen partial pressure at modulation frequencies of 30 kHz (a) and at 60 kHz (b). Lines represent a fit using a monoexponential decay model.

The dependence of A_{\min} and A_{\max} on pO_2 is best described by a monoexponential decay model of the form

$$y = B \cdot \exp(-pO_2/C) + D \quad (5.2)$$

where $y = A_{\max}$ or A_{\min} ; B , C and D are fitting parameters. The respective numerical values are given in Table 5.1. If A_{\min} and A_{\max} are introduced into the equation of monoexponential decay model, the following equation for pH is obtained:

$$pH = 6.208 + \ln \left(\frac{(B_{\min} \cdot \exp(-pO_2/C_{\min}) + D_{\min}) - \Phi_{30kHz}}{\Phi_{30kHz} - (B_{\max} \cdot \exp(-pO_2/C_{\max}) + D_{\max})} \right) \cdot 0.8387 \quad (5.3)$$

Equation 5.3 can be applied for the calculation of pH both at 30 and 60 kHz.

Table 5.1 Numerical data for the fitting parameters of eq. 5.2 at various modulation frequencies.

<i>modulation frequency</i>	<i>B</i>	<i>C</i>	<i>D</i>
$A_{max} = 30 \text{ kHz}$	22.52	20.40	10.83
$A_{min} = 30 \text{ kHz}$	18.77	18.88	5.93
$A_{max} = 60 \text{ kHz}$	31.68	34.60	11.72
$A_{min} = 60 \text{ kHz}$	15.438	16.616	13.374

The fluorescence intensity of the pH probe is referenced against the phase shift of the oxygen probe in the m-DLR method. As a result, the resulting "initial" (first approximation) pH value calculated from these data depends on the oxygen partial pressure, which therefore needs to be calculated first in order to compensate for its effect on the initial pH value.

The response function of the oxygen probe can be described by the formula given in eq. 5.4. If the frequencies f_1 and f_2 are smaller than 100 kHz, this equation eliminates the contributions of both the pH probe (HPTS) with its decay time in the order of 5 ns, and of course also that of ns-lived background fluorescence. Our working frequencies are 30 and 60 kHz. The overall phase shift is determined at two different modulation frequencies as

$$\tau = \frac{1}{2\pi} \left(\frac{f_1^2 - f_2^2 \pm \sqrt{f_2^2 - f_1^2 - 4(\cot \Phi_2 \cdot f_2 \cdot f_1^2 - \cot \Phi_1 \cdot f_1 \cdot f_2^2)(\cot \Phi_2 \cdot f_2 - \cot \Phi_1 \cdot f_1)}}{2(\cot \Phi_2 \cdot f_2 \cdot f_1^2 - \cot \Phi_1 \cdot f_1 \cdot f_2^2)} \right), \quad (5.4)$$

where Φ_1 and Φ_2 are the measured phase shifts at modulation frequencies f_1 and f_2 . The response curves are shown in Fig. 5.6. For the sake of simplicity, only data for three different pH values are shown. It is evident that there is no cross-sensitivity to pH.

Averaged values obtained for each individual microsensor at all pH's tested (i.e., pH 10, 9, 8, 7, 6, 5 and 4) were used to generate an average response curve (Fig. 5.6b). Again, a fit employing a monoexponential decay model is adequate (r^2 is 0.998). The fit parameters B, C and D are $2.864 \cdot 10^{-6}$, 16.585 and $1.942 \cdot 10^{-6}$, respectively. Hence, the equation for calculating the pO_2 can be written as follows:

$$pO_2 = -16.585 \cdot \ln \left(\frac{\tau - 1.942 \cdot 10^{-6}}{2.864 \cdot 10^{-6}} \right) \quad (5.5)$$

where τ is the decay time calculated via eq. 5.4.

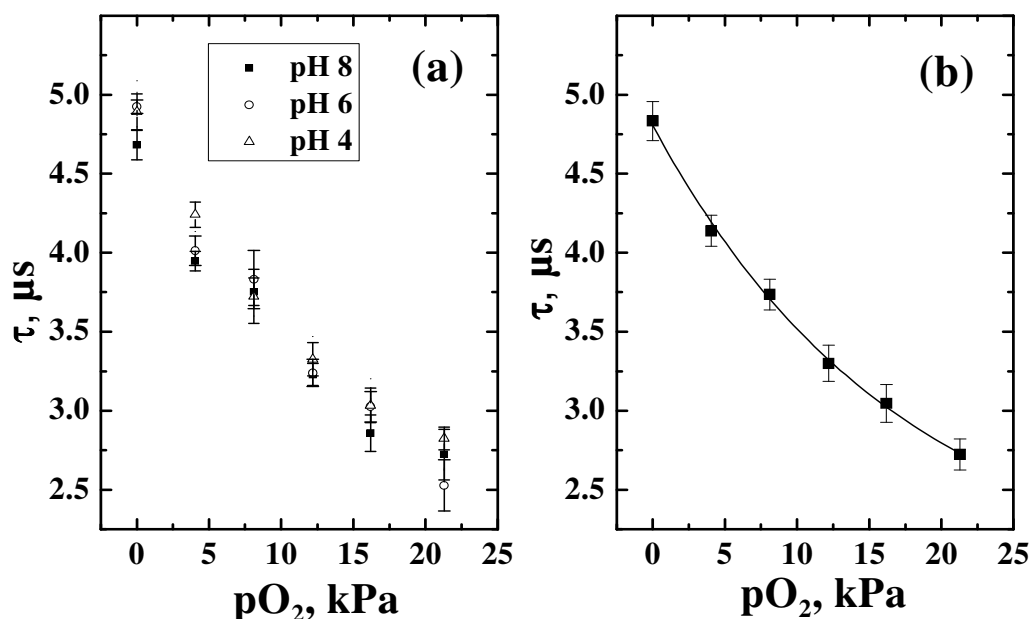


Figure 5.6 Response of the microsensor to dissolved oxygen: **a**, response at different pH of solution; **b**, medium curve, where points represent averaged values for all individual microsensors at all pH values; the curve represent a fit using monoexponential decay model.

5.3.4 Response Times

The response to oxygen of pH/O₂ microsensor took 30 s in average in both directions. The response of the pH/O₂ sensor to pH (t_{95}) varied from batch to batch but averaged 2 min when going from pH 4 to pH 9, and 3 min in the reverse direction. This is rather long and may be explained by diffusional barrier in the polymers and, possibly, electrostatic repulsion of protons in the pH beads.

5.3.5 Photostability

The dual microsensor makes use of highly photostable indicators, specifically Ru(dpp)₃²⁺ (O₂) and HPTS (pH). Since the light intensities used to induce their luminescence at the tip of the optical fibers significantly exceed those used in case of planar sensor foils, photodegradation can be a critical issue even for indicators that possess good photostability in other conditions.

Nevertheless, we have found that the microsensor exhibited surprisingly good photostability. The pH/O₂ microsensor was drift-free at pH 4 under 0 and 21.3 kPa O₂. No noticeable drift of phase shift was observed for the microsensor at pH 9 and oxygen-free condition. However, increases in the overall phase shift ($\sim 0.35^\circ$ per 500 data acquisition points) was observed at pH 9 under air saturation, which was accompanied by a decrease of luminescence intensity ($\sim 3\%$ per 500 measuring points). Assuming the acquisition of one data point per min (as is usual in practice), a drift of 0.35° will be found after an operation time of 8.3 h. The total phase shift at 60 kHz on going from pH 5 to pH 10 is typically $10 - 13^\circ$ (depending on pO_2). The increase in phase shift indicates decomposition of the pH indicator and is likely to be due to singlet oxygen generation by the oxygen-sensitive probe in the presence of molecular oxygen.

5.3.6 Validation

The performance of the microsensors was continuously tested at various conditions of pH and pO_2 . The experimentally determined phase shifts and the data calculated for pO_2 and pH are shown in Fig. 5.7. Equation 5.5 was used to determine pO_2 , and pH values were then calculated with the help of eq. 5.3.

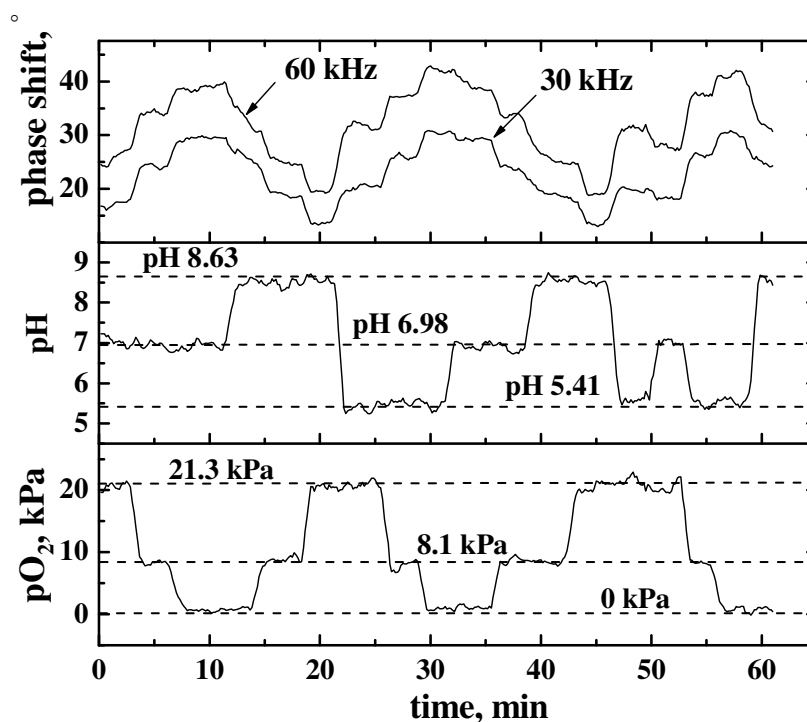


Figure 5.7 Performance of the pH/ pO_2 microsensor. Experimental phase shifts were

measured at 470-nm excitation at modulation frequencies of 30 and 60 kHz. pH values and oxygen partial pressures were calculated from eq. 5.3 and 5.5, respectively. All measurements were performed at 25 °C in aqueous solutions.

As can be seen from Fig. 5.7, continuous dual sensing is possible in a highly reproducible fashion over the whole period of the experiment, and the sensor responds fully reversibly to the changes of pH and oxygen partial pressure.

5.4 Conclusion

We have developed optical microsensor which is capable of simultaneous measurement of two important parameters such as pH and dissolved oxygen. The undesired cross-sensitivities to the other analyte are avoided by using analyte-sensitive microbeads, which are homogeneously dispersed in a sensor matrix. The microsensor relies on measurements of luminescence phase shift which is achieved by commercially available sensor reader devices. The sensors show good reproducibility, excellent photostability and full reversibility. They can be successfully applied for minimal-invasive measurements of high spatial resolution.

5.5 References

1. Canete F, Rios A, Luque de Castro M D, Valcarcel M **Determination of analytical parameters in drinking water by flow injection analysis. Part 1. Simultaneous determination of pH, alkalinity and total ionic concentration.** Analyst **1987**, 112, 263-266
2. Preininger C, Klimant I, Wolfbeis O S **Optical fiber sensor for biological oxygen demand.** Anal. Chem. **1994**, 66, 1841-1846
3. Schroeder C R, Weidgans B M, Klimant I **pH Fluorosensors for use in marine systems.** Analyst 2005, 130(6), 907-916
4. Klimant I, Meyer V, Kuhl M **Fiber-optic oxygen microsensors, a new tool in aquatic biology.** Limnol. Oceanogr. 1995, 40, 1159-1165
5. Marshall A J, Blyth J, Davidson C A B, Lowe C R **pH-sensitive holographic sensors.** Anal. Chem. **2003**, 75, 4423-4431

6. Young O A, Thomson R D, Merhtens V G, Loeffen M P F **Industrial application to cattle of a method for the early determination of meat ultimate pH.** Meat Sci. **2004**, 67, 107-112
7. O'Mahony F C, O'Riordan T C, Papkovskaya N, Kerry J P, Papkovsky D B **Non-destructive assessment of oxygen levels in industrial modified atmosphere packaged cheddar cheese.** Food Control. **2006**, 17, 286-292
8. Deshpande R R, Koch-Kirsch Y, Maas R, John G T, Krause C, Heinzle E **Microplates with integrated oxygen sensors for kinetic cell respiration measurement and cytotoxicity testing in primary and secondary cell lines.** Assay Drug Dev. Technol. **2005**, 3, 299-307
9. Alderman J, Hynes J, Floyd S M, Kruger J, O'Connor R, Papkovsky D B **A low-volume platform for cell-respirometric screening based on quenched-luminescence oxygen sensing.** Biosens. Bioelectron. **2004**, 19, 1529–1535
10. Zhang Z, Szita N, Boccazzi P, Sinskey A J, Jensen K F **A well-mixed, polymer-based microbioreactor with integrated optical measurements.** Biosens. Bioelectron. **2006**, 93, 286-296
11. Mekhail K, Khacho M, Gunaratnam L, Lee S **Oxygen sensing by H⁺. Implications for HIF and hypoxic cell memory.** Cell Cycle **2004**, 3, 1027-1029
12. Harms P, Kostov Y, French J A, Soliman M, Anjanappa M, Ram A, Rao G **Design and performance of a 24-station high throughput microbioreactor.** Biotech. Bioeng. **2006**, 93(1), 6-13
13. Borisov S M, Krause C, Arain S, Wolfbeis O S **Composite materials for simultaneous and contactless luminescent sensing and imaging of oxygen and carbon dioxide.** Adv. Mater. **2006**, 18, 1511-1516
14. Coyle L M, Gouterman M **Correcting lifetime measurements for temperature.** Sens. Actuators B **1999**, 61(1-3), 92-99
15. Mongey K F, Vos J G, MacCraith B D, McDonagh C M, Coates C, McGarvey J J **Photophysics of mixed-ligand polypyridyl ruthenium (II) complexes immobilized in silica sol-gel monoliths.** J. Mater.Chem. **1997**, 7, 1473–1479
16. Zelelow B, Khalil G E, Phelan G, Carlson B, Gouterman M, Callis J B, Dalton L R **Dual luminophor pressure sensitive paint II. Lifetime based measurement of pressure and temperature.** Sens. Actuators B **2003**, 96(1-2), 304-314
17. Borisov S M, Vasylevska A S, Krause C, Wolfbeis O S **Composite luminescent material for dual sensing of oxygen and temperature.** Adv. Funct. Mater. **2006**, 16(12), 1536-1542

18. Vasylevska G S, Borisov S M, Krause C, Wolfbeis O S **Indicator-loaded permeation-selective microbeads for use in fiber optic simultaneous sensing of pH and dissolved oxygen.** Chem. Mater. **2006**, 18(19), 4609-4616
19. Koese M E, Carrol B F, Schanze K S **Preparation and spectroscopic properties of multiluminophore luminescent oxygen and temperature sensor films.** Langmuir **2005**, 21, 9121-9129
20. Klimant I, Kuehl M, Glud R, Holst G **Optical measurement of oxygen and temperature in microscale: strategies and biological applications.** Sens. Actuators **1997**, 38, 29-37
21. Wolfbeis O S **Fiber-optic chemical sensors and biosensors.** Anal. Chem. **2006**, 78, 3859-3873; and previous biannual reviews
22. Rosenzweig, Z.; Kopelman, R. **Development of a submicrometer optical fiber oxygen sensor.** Anal. Chem. **1995**, 67, 2650-2654
23. McNamara K P, Li X, Stull A D, Rosenzweig Z **Fiber-optic oxygen sensor based on the fluorescence quenching of tris(5-acrylamido-1,10-phenanthroline)ruthenium chloride.** Anal. Chim. Acta **1998**, 361, 73-83
24. Park E J, Reid K R, Tang W, Kennedy R T, Kopelman R **Ratiometric fiber optic sensors for the detection of inter- and intra-cellular dissolved oxygen.** J. Mater. Chem. **2005**, 15, 2913-2919
25. Tan W, Shi Z Y, Kopelman R **Development of submicron chemical fiber optic sensors.** Anal. Chem. **1992**, 64, 2985-2990
26. Kosch U, Klimant I, Wolfbeis O S **Long-lifetime based pH micro-optodes without oxygen interference.** Fresenius J. Anal. Chem. **1999**, 364, 48-53
27. Song A, Parus S, Kopelman R **High-performance fiber-optic pH microsensors for practical physiological measurements using a dual-emission sensitive dye.** Anal. Chem. **1997**, 69, 863-867
28. Neurauter G, Klimant I, Wolfbeis O S **Fiber-optic microsensor for high resolution pCO₂ sensing in marine environment.** Fresenius J. Anal. Chem. **2000**, 366, 481-487
29. Ertekin K, Klimant I, Neurauter G, Wolfbeis O S **Characterization of a reservoir-type capillary optical microsensor for pCO₂ measurements.** Talanta **2003**, 59, 261-267
30. Werner T, Klimant I, Huber C, Krause C, Wolfbeis O S **Fiber optic ion-microsensors based on luminescence lifetime.** Mikrochim. Acta **1999**, 131, 25-28
31. Ji J, Rosenzweig Z **Fiber optic pH/Ca²⁺ fluorescence microsensor based on spectral processing of sensing signals.** Anal. Chim. Acta **1999**, 397, 93-102

32. Ferguson J A, Steemers F J, Walt D R **High-density fiber-optic DNA random microsphere array**. Anal. Chem. **2000**, 72, 5618-5624
33. Song L, Ahn S, Walt D R **Fiber-optic microsphere-based arrays for multiplexed biological warfare agent detection**. Anal. Chem. **2006**, 78, 1023-1033
34. Mock T, Dieckmann G S, Haas C, Krell A, Tison J L, Belem A L, Papadimitriou S, Thomas D N **Micro-optodes in sea ice: a new approach to investigate oxygen dynamics during sea ice formation**. Aqua. Microb. Ecol. **2002**, 29, 297-306
35. Klimant I, Ruckruh F, Liebsch G, Stangelmayer A, Wolfbeis O S **Fast response oxygen micro-optodes based on novel soluble ormosil glasses**. Mikrochim. Acta **1999**, 131, 35-46
36. Offenbacher H, Wolfbeis O S, Fuerlinger E **Fluorescence optical sensors for continuous determination of near-neutral pH values**. Sens. Actuators B **1986**, 9, 73-84
37. Klimant I **Verfahren und Vorrichtungen zur Referenzierung von Fluoreszenzintensitätssignalen**. Ger. Pat. Appl. **1997** DE 198 29 657
38. Klimant I, Wolfbeis O S **Oxygen-sensitive luminescent materials based on silicone-soluble ruthenium diimine complexes**. Anal. Chem. **1995**, 67, 3160 – 3166
39. Perrin, D. D.; Dempsey, B. *Laboratory Manuals*; Chapman & Hall: London, **1974**
40. Wolfbeis O S **Materials for fluorescence-based optical chemical sensors**. J. Mater. Chem. **2005**, 15, 2657-2669
41. Amao, Y. **Probes and polymers for optical sensing of oxygen**. Microchim. Acta **2003**, 143, 1-12
42. Wolfbeis O S, Leiner J P, Posch H E **A new sensing material for optical oxygen measurement, with the indicator embedded in an aqueous phase**. Microchim. Acta **1986**, 3, 359-366
43. Borisov S M, Neurauder G, Schroeder C, Klimant I, Wolfbeis O S **Modified dual lifetime referencing method for simultaneous optical determination and sensing of two analytes**. Appl. Spectrosc. 2006, 60(10), 1167-1173

Chapter 6

Simultaneous Non-invasive Monitoring of Dissolved Oxygen and pH During Bacterial Growth in 24-well Microplates

A new approach is proposed for non-invasive, simultaneous monitoring of oxygen and pH in 24-well microbioreactors. Sensor spots of a dually sensor material are placed on the bottom of a standard 24-well microplate while reading is performed by a 24-channel lifetime reader. The performance of the system is demonstrated by monitoring pH and oxygen kinetics during a cultivation of Pseudomonas putida and Escherichia coli. The results obtained for cultivation in the 3-mL microbioreactors and in 500-ml cultivation flasks are similar. The proposed approach is suitable for a variety of applications in high-throughput bioprocessing. (Biotechnol Bioeng 2007, submitted)

6.1 Introduction

In industrial biotechnology bacterial strains produce substances like fine chemicals, antibiotics, amino acids, vitamins, enzymes or biopolymers on a large scale. In this field there is a high demand for optimization of production processes and new applications. In medical and pharmaceutical biotechnology, tissue engineering for the renewal of injured body parts or transplantation of patient-own tissue opens new perspectives, as well as stem cell-based therapies offer new perspectives. Fast and reliable detection of diseases and genetic defects are other examples for the huge fields of application. In “green” biotechnology, properties of the plants are changed according to particular requirements, such as resistance to diseases or high productivity. For all these applications, microorganisms like bacteria, yeast or fungi, or higher cells like mammal or plant cells, need to be cultivated under controlled conditions, since biotechnological processes are extremely complex and often very sensitive to environmental changes. Assay optimization regarding different environmental parameters like temperature, pH value, oxygen concentration and media composition has to be performed for

ideal growth and expression.

Although standard systems like Petri dishes, T-flasks or shake flasks allow for a high number of screening experiments and optimization steps within a short time, only a few parameters (such as temperature or CO₂ concentration) can be controlled. On the other hand, bioreactors can monitor and control a variety of ambient conditions, like temperature, pH, dissolved oxygen (DO) and agitation, but are limited in their throughput. Furthermore, due to their large volume, they are not suitable for cells which are available only in limited amount.

Process development and optimization studies can be significantly intensified by using a high-throughput bioprocessing in simplified bioreactors like microplates wells which enable highly parallel and low-cost experiments. Optical sensing allows for easy miniaturization of the sensing element, non-invasiveness and disposability of the sensor. Several sensing elements enable simultaneous measurement of important parameters as DO and pH. Oxygen is a necessary substrate for most living beings, and its monitoring is of great importance in biotechnology to avoid oxygen limitation during cultivation, or for comparison of cell respiration under different conditions. Furthermore, optimal cell growth is significantly influenced by pH. Since many cells produce or consume acids during their metabolism, this parameter has to be monitored carefully as well. It is not only necessary to monitor and control these two parameters¹⁻⁶, but also to understand how they influence viability and productivity of a bioprocess. Although optical sensing of DO⁷⁻¹¹ and pH^{7,12} in microplates has recently been demonstrated, no realistic system for simultaneous monitoring of both parameters was proposed so far. In contrast to using two sensors for detection of one parameter each, simultaneous detection of several parameters with only one sensor gives information of both parameters at exactly the same location. This is especially important if these parameters are not homogeneously distributed within the sample. Several systems do allow for simultaneous measurements of dissolved oxygen and pH in a single microbioreactor, but can hardly be applied to high-throughput bioprocessing due to the complicity of the microbioreactor, sensing element or detection system. For example, an array sensor developed by Ferguson et al.¹³ was reported to be suitable for monitoring of O₂, pH and CO₂ simultaneously. The manufacturing of this sensor is however rather complicated and involves a low reproducible procedure including irradiation of different parts of the sensor to start photopolymerization and then soaking the spots with indicator solutions and buffers. Kostov et al.¹ have placed oxygen- and a pH-sensitive spots on the inner wall of a standard glass cuvette (2 ml vol.) while a fiber-optic detection system was located outside. A microbioreactor of Zanzotto et al.¹⁴ also contained two sensor spots combined with a

complicated detection system consisting of numerous excitation sources (LEDs), excitation filters and photodetectors. A similar approach was recently used by Zhang et al.¹⁵. Finally, Harms et al.¹⁶ have managed to monitor pH and oxygen in 24-microwells simultaneously. Obviously, the main disadvantage of all these systems is a significant effort needed to produce the sensing device and the disposable material (e.g. a 24-well microplate containing two indicator spots in each well), which significantly increases the cost of both components.

Recently, we developed a number of materials suitable for simultaneous optical sensing of two analytes: oxygen and temperature^{17,18}, carbon dioxide and oxygen^{19,20}, and pH and oxygen²¹. The sensor materials are composed of a polymer layer, in which two types of microbeads (each sensitive to one analyte) are dispersed. Such materials can be prepared as a planar sensor foil, but also directly in a microplate, by pipetting a sensor “cocktail” into the wells. The procedure, therefore, can be easily automatized. The sensors for simultaneous sensing of pH and DO²¹ and carbon dioxide and oxygen¹⁹ relied on the modified Dual Lifetime Referencing (m-DLR) measuring method. The method makes use of two indicators (a fluorescent pH indicator and an oxygen indicator with long-lived luminescence) contained in a polymer matrix and excited simultaneously by sinusoidally modulated light. The emission of both is registered by a single photodetector. The overall phase shift of luminescence, when measured at two different modulation frequencies f , provides information about the concentration of both analytes. Thus, the instrumentation is rather simple because only one excitation LED and once set of optical filters is required.

We showed previously¹⁹ that monitoring of carbon dioxide and oxygen in the gas phase during bacterial growth (*Pseudomonas putida*) in a single bioreactor can be successfully performed by using a dual sensor (requiring, however, two sets of excitation and emission filters, as well as LED sources). In this work we will demonstrate that non-invasive measurement of the two analytes (pH and DO) during a bioprocess (cultivation of *Pseudomonas putida* and *Escherichia coli*) becomes possible for 24-well microplates using a commercially available 24-channel lifetime reader (SensorDish[®]).

6.2 Experimental

6.2.1 Preparation of the Dually-Sensing Material

The material for simultaneous sensing of pH and oxygen was prepared analogously to the

procedure described previously²¹. In this work we used the pH-sensitive microbeads based on 8-hydroxy-pyrene-1,3,6-trisulphonate (HPTS). Absorption of HPTS is compatible with emission of the 470 nm-LED used in the 24-channel SensorDish[®] Reader. For the preparation of the dually-sensing material we used 20 mg of the pH-sensitive microbeads (HQ-N-1-HP1, obtained from PreSens GmbH, Germany), 10 mg of the oxygen-sensitive microbeads (Ru(dpp)₃(TMS)₂ in ormosil particles) and 300 mg of 5% solution of polyurethane hydrogel in ethanol:water (90:10 v/v). This "cocktail" was stirred overnight, knife-coated (K Control Coater, www.labomat.com) onto a 125 µm - polyester support, and dried at ambient air to obtain sensor film in a thickness of about 10 µm.

6.2.2 Instrumentation

Calibration of the sensor and bacterial growth experiments were performed in 24-well microplates (Roth, Germany, www.carl-roth.de). The plates were read out with the 24-channel SDR SensorDish[®] Reader (PreSens GmbH, Germany, www.presens.de). The general view of the SensorDish[®] Reader and the cross-section of a well of a microplate are shown in Fig. 6.1. The spots of the dually-sensing material were glued on the bottom of each well with silicone high vacuum grease and read out through the microplate bottom. The sensor spots are excited by a 470 nm LED and the fluorescence is detected for wavelength higher than 540 nm. The excitation light was modulated sinusoidally with subsequent frequencies of 45 kHz, and 22.5 kHz. Every sensor is read out by a separate channel. It takes only a few seconds per frequency to scan all 24 sensors, so that the oxygen or pH detections are performed almost simultaneously for all samples.

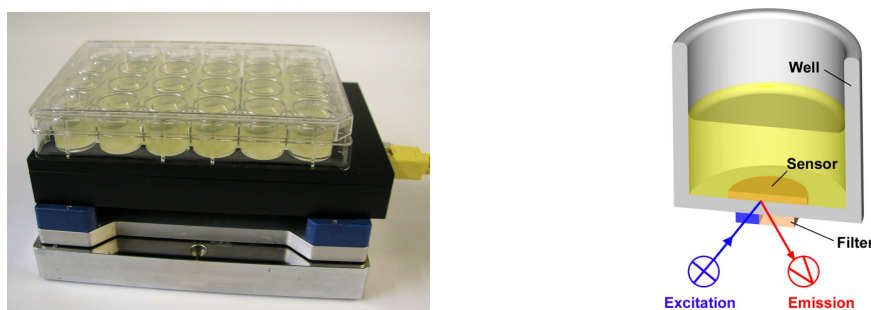


Figure 6.1 24-channel SensorDish[®] Reader on the shaker (left) and cross-section of a well of a microplate with included sensor at its bottom (right). Excitation and detection of the emission is performed through the bottom of the plate.

In a control experiment, monitoring of DO during bacterial growth was also performed by an oxygen meter Fibox 3 (PreSens, Germany) using spots of oxygen-sensing material glued to the inside wall of an Erlenmeyer flask (Fig. 6.2). The emission of the sensor spot is read out through the transparent bottom of the flask using a coaster (CFG, PreSens, Germany). The coaster contains a polymer optical fiber and redirects the light, thus enabling excitation of the sensor and detection of the signal from the bottom of the flask (Fig. 6.2, right).

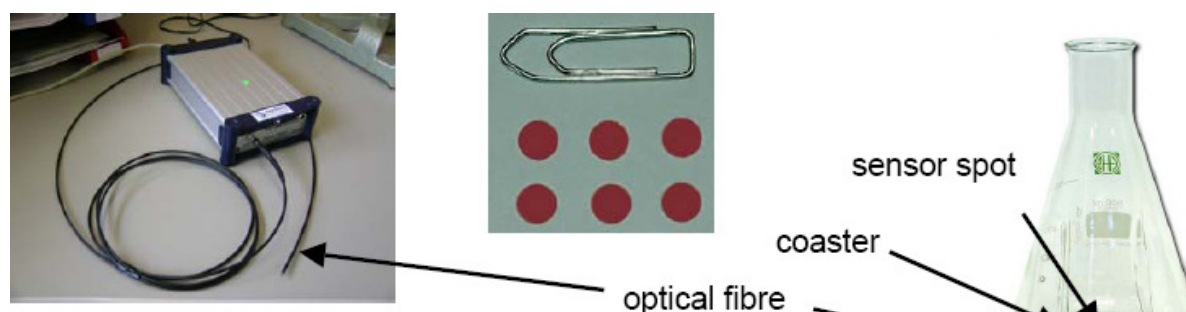


Figure 6.2 Oxygen meter Fibox 3 with polymer optical fiber (left); oxygen sensor spots (middle); a sensor spot glued to the bottom of an Erlenmeyer flask and read out by a coaster from below (right).

6.2.3 Calibration of the Dual Sensor

The spots of the dual optical sensor were glued with silicone high vacuum grease (Merck, Germany, www.merck.de) on the bottom of transparent glass vials (\varnothing 14 mm, h 45 mm, Chromatografie Zubehör Trott, Germany, www.czt.de). Calibration gases (nitrogen and oxygen, each of 99.999% purity, purchased from Linde, www.linde-gase.de) were prepared by a gas mixing device (MKS, Wilmington, www.mksinst.com). The gas mixtures were bubbled through the buffer solutions (3 ml in each vial) to adjust concentration of the DO. Doubly distilled water was used for the preparation of the MOPS buffer solutions (Roth, Germany). The pH was controlled with a digital pH meter (Knick, www.knick.de). All solutions were adjusted to constant ionic strength ($I = 140$ mM) using sodium chloride (Merck) as the background electrolyte. Calibration of the dual sensor was performed at 25 °C and 37 °C inside an incubator (Mettler GmbH, Germany, www.mettler.com).

6.2.4 Bacterial Cultivation – Preculture and Growth Experiments

Pseudomonas putida (*P. putida*) MIGULA, strain Berlin (DSM 50026) and *Escherichia coli* (*E. coli*), strain K12, both obtained from the German Collection of Microorganisms and Cell Cultures (DSMZ, Braunschweig, Germany, www.dsmz.de), were cultivated on standard agar S1 (Sigma-Aldrich) plates for at least 24 h at 25 °C (*P. putida*) and at 37 °C (*E. coli*). A preparatory culture with 100 ml of culture medium S1 (Sigma-Aldrich) was inoculated with a single colony of the respective bacteria. Prior to use, the inoculum was hand-shaken to until the solution was homogeneous. The same homogenized inoculum was used for experiments in the microbioreactors and in a shaking flask.

For monitoring of bacterial growth in a 24-well microplate, 1.5 ml of bacterial medium inoculated with bacteria was pipetted into each well and the microplate was closed with a microplate lid. Measurement of the luminescence phase shift was performed from the bottom using the SDR SensorDish® Reader. A microplate shaker (Variomag, Germany, www.variomag.com) was used at a shaker speed ~ 670 rpm to provide sufficient oxygen supply during cultivation. The cultivation experiments were performed in the incubator at 25 °C for *P. putida* and 37 °C for *E. coli*.

In a parallel control experiment, the oxygen decrease during bacterial cultivation was monitored using a shaking flask. 50 ml of inoculated bacterial medium were transferred into a 500 ml Erlenmeyer flask closed with an air-permeable cap. An oxygen sensor spot (Ø 5 mm, SP-PSt3-YOP-G-SUP-D5, PreSens GmbH) was glued onto the bottom of the flask with silicone rubber (prod. Nr. 692-542, RS Components GmbH, www.rsonline.de). Reading was performed from the bottom by a Fibox 3 oxygen meter using a coaster. The Erlenmeyer flask was fixed in the flask incubator-shaker (Stuart S150, Bibby Sterilin, United Kingdom, www.bibby-sterilin.co.uk) used at a shake speed of 250 rpm.

The pH value of bacteria solution before and after cultivation in microplate and in a flask was controlled with a digital pH meter (Knick). After cultivation, the biomass was determined by measurement of the optical density at 436 nm (OD₄₃₆) of a 1:100 dilution of the bacteria solution with a Hitachi U-3000 UV-VIS spectrophotometer (www.hitachi-hitec.com).

6.3 Results and Discussion

6.3.1 Calibration of Dual Sensor Membrane at 25 °C and at 37 °C

The calibration of the dual sensor was performed according to the protocol described previously²¹. Briefly, in the m-DLR method, measured overall phase shift (Φ) includes information about luminescent intensities of both long-lived and short-lived indicators, but also about phase shift of the long-lived indicator (Φ of the short-lived fluorescent indicator approaches zero at low modulation frequencies, which are in kHz range). All these three parameters (and therefore the overall Φ) depend on the concentration of both analytes. We have shown previously^{20,21}, that measurement of overall Φ at two different modulation frequencies is sufficient to obtain information about concentration of both analytes.

Temperature affects the properties of the dually-sensing material significantly. Not only the dissociation constant of the fluorescent pH indicator pK_a is temperature-dependent, but also decay time of the oxygen indicator. Decrease of the decay time (and thus Φ) and luminescence intensity of the oxygen sensor are attributed to a thermally activated non-radiative decay, and is often used in optical temperature sensing^{17,18,22,23}. Quenching of the long-lived luminescence by oxygen is increasingly efficient at higher temperatures due to faster diffusion of the quencher within the film, which is, in fact, the main reason for cross-sensitivity of the material to oxygen^{17,24}. All these effects are illustrated by Fig. 6.3, which shows the calibration plots for the dually-sensing material obtained at 25 °C and 37 °C for gas-equilibrated buffer solutions.

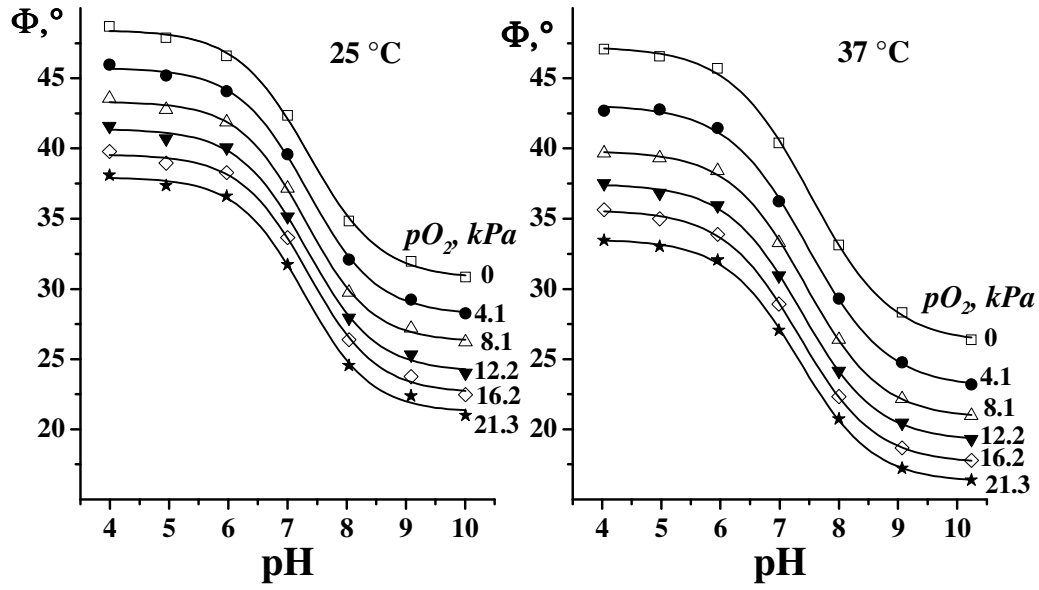


Figure 6.3 Calibration plots of the dually-sensing material (modulation frequency 45 kHz). Lines represent a fit via eq. 6.1.

As can be observed from Fig. 6.3, temperature only has a very minor effect on the form of the titration curves and the position of the inflection point. Overall phase shift, however, decreases significantly both in the absence of oxygen (due to thermal quenching only) and even more pronounced in presence of oxygen.

One also can observe that the titration curves are practically identical at different oxygen concentrations (pO_2 from 0 - 21.3 kPa). For given oxygen level the plots are well described by eq. 6.1^{21,25}:

$$I = \frac{A_{\max} - A_{\min}}{1 + 10^{(pH - pK_a)/x}} + A_{\min}, \quad (6.1)$$

where I is the fluorescence intensity, and A_{\max} , A_{\min} , x are numerical coefficients. A_{\max} and A_{\min} are numerical values of the fluorescence intensity of the pH indicator in fully protonated (A_{\min}) and fully deprotonated (A_{\max}) form, respectively. The fit parameters are identical at a given temperature and modulation frequency (45 kHz): pK_a is 7.33 and 7.41, x is 0.58 and 0.65 for 25 °C and 37 °C, respectively. The fit parameters A_{\min} and A_{\max} , on the other side, reflect contribution of the luminescence of the oxygen probe (which is quenched) to the overall phase shift.

The data could be well described by algorithms identified with the Table Curve 2D software. The resulting equations characterize the plots for the parameters A_{\max} and A_{\min} vs.

the oxygen partial pressure (Fig. 6.4) by a mono-exponential decay model (correlation coefficient $r^2 = 0.999$):

$$y = B \cdot e^{\left(\frac{pO_2}{C}\right)} + D, \quad (6.2)$$

where y is the phase shifts at deprotonated (A_{max}) and protonated (A_{min}) forms; and B , C and D are fit parameters.

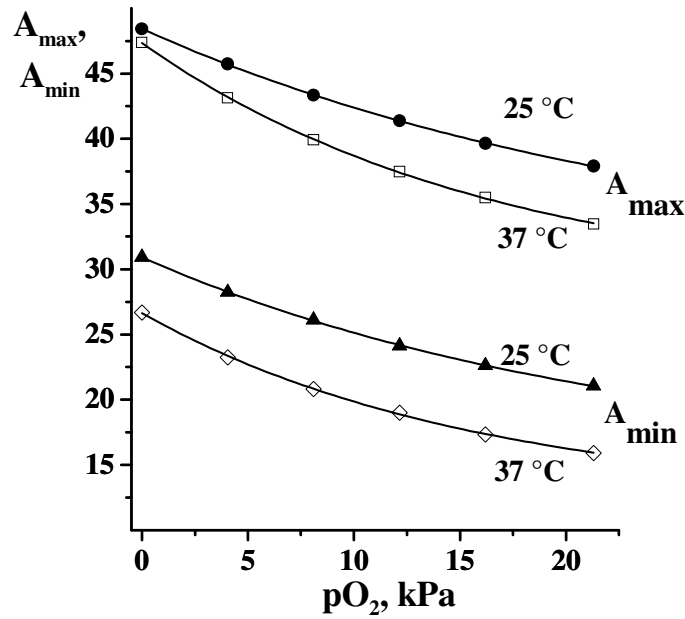


Figure 6.4 Dependence of the parameters A_{max} and A_{min} on the oxygen concentration at a modulation frequency of 45 kHz at 25 °C and 37 °C. Lines represent fits via eq. 6.2 (the mono-exponential decay model).

The following fit parameters were thus obtained from eq. 6.2 are presented in a table:

Table 6.1 Fit parameters for response to pH at the two working temperatures

fit parameters	25 °C		37 °C	
	A_{max}	A_{min}	A_{max}	A_{min}
B	18.600	16.117	19.113	14.372
C	25.465	22.441	16.590	15.659
D	29.830	14.800	28.224	12.259

After mathematical conversion one can obtain following equation for calculation of pH:

$$pH = pK_a + \ln \left(\frac{(B_{\min} \cdot \exp(-pO_2 / C_{\min}) + D_{\min}) - \Phi_{60kHz}}{\Phi_{60kHz} - (B_{\max} \cdot \exp(-pO_2 / C_{\max}) + D_{\max})} \right) \cdot x \quad (6.3)$$

As can be seen from eq. 6.3, pH is indeed referenced to oxygen content (pO_2), which, therefore, should be calculated first.

6.3.2 Calibration Function for Oxygen

By measuring the phase shift at the second modulation frequency (22.5 kHz) can be obtained that a calibration function for oxygen is independent on pH. The phase shifts Φ_1 and Φ_2 (measured at 45 and 22.5 kHz, respectively) were used to calculate the decay time of the long-lived indicator via eq. 6.4:

$$\tau = \frac{1}{2\pi} \left(\frac{f_1^2 - f_2^2 \pm \sqrt{f_2^2 - f_1^2 - 4(\cot \Phi_2 \cdot f_2 \cdot f_1^2 - \cot \Phi_1 \cdot f_1 \cdot f_2^2)(\cot \Phi_2 \cdot f_2 - \cot \Phi_1 \cdot f_1)}}{2(\cot \Phi_2 \cdot f_2 \cdot f_1^2 - \cot \Phi_1 \cdot f_1 \cdot f_2^2)} \right), \quad (6.4)$$

where Φ_1 and Φ_2 are the phase shifts at modulation frequencies f_1 and f_2 .

Although overall phase shifts measured at 22.5 and 45 kHz (Fig. 6.3) depend on pH, the decay time calculated for the oxygen indicator ($\tau_0 = 5.38 \pm 0.02 \mu s$ at 25 °C and $\tau_0 = 4.96 \pm 0.04$ at 37 °C in the absence of oxygen) remains constant from pH 4 to pH 10 and is dependent on oxygen concentration only (Fig. 6.5). As predicted, the temperature increase from 25 °C to 37°C results in a decrease in decay time from 5.38 μs to 4.96 μs . Equation 6.2 was used again to fit the response functions presented in Fig. 6.5 ($r^2 = 0.999$), and the following fit parameters were obtained: $B = 1.4923 \cdot 10^{-6}$, $C = 7.8895$ and $D = 3.4411 \cdot 10^{-6}$ at 25 °C; $B = 1.5905 \cdot 10^{-6}$, $C = 11.0036$ and $D = 3.789 \cdot 10^{-6}$ at 37 °C. The simple transformation results in the following equation for calculation of the oxygen concentration:

$$pO_2 = -C \cdot \ln \left(\frac{\tau - D}{B} \right), \quad (6.5)$$

where τ is the decay time calculated via eq. 6.4.

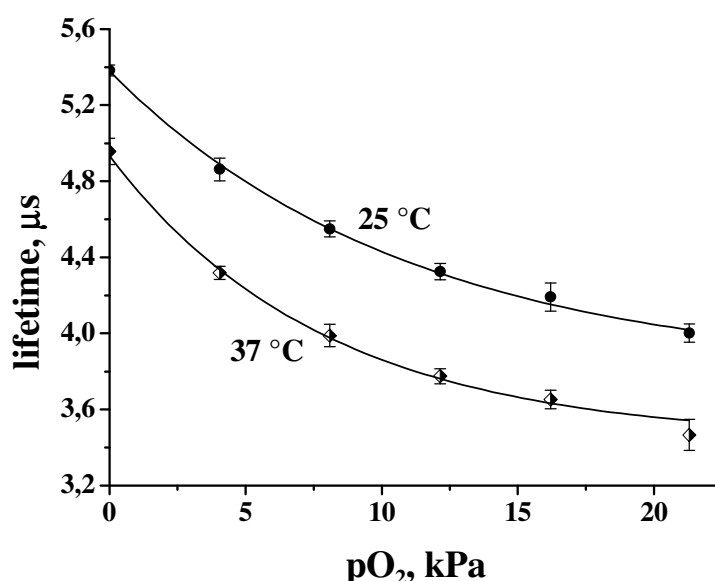


Figure 6.5 Response functions of the dual sensor to oxygen at pH 4, pH 5, pH 6, pH 7, pH 8, pH 9 and pH 10 at 25 °C and 37 °C; 21.3 kPa corresponded to 100 % air saturation. The data points are the average decay times as calculated via eq. 6.4 for all the pH used. The line represents a fit via eq. 6.2.

6.3.3 Bacteria Fermentation in Microbioreactors

The growth kinetics of *Pseudomonas putida* and *Escherichia coli* were investigated to demonstrate the feasibility of microbial cultivation in the microbioreactors. DO contents and pH values of the solutions were calculated according to eq. 6.5 and 6.3. Each data point represents the average value from 24 replicate experiments carried out in separate microbioreactors. The relatively small error bars for the observed pH and DO values within the microbioreactors (Fig. 6.6b and 6.7b) demonstrate the good reproducibility of the signals of the dual sensor during cell growth.

The oxygen consumption during the fermentation in the 24-well plate was compared with that obtained using a conventional bioreactor (shake flask). The oxygen kinetics in the microbioreactors shows typical behavior. The earlier oxygen decrease in the culture in the 24-well microplate compared to the culture in the shake flask indicates a lower oxygen transfer rate of the former set-up (Fig. 6.6a and Fig. 6.7a). The oxygen transfer rate depends on parameters as the geometry of the bioreactor²⁶⁻²⁸, the filling volume of the sample, the shaking frequency²⁹ and the sealing⁹. However, measurement of the optical density of 1:100 dilutions of the bacteria solutions after cultivation showed almost no difference between the bacteria

cultivated in the microbioreactors and those cultivated in Erlenmeyer flasks for *P. putida* as well as for *E. coli*. This indicates that the rather small difference in oxygen limitation (*P. putida*: $pO_2 = 0$ % air saturation after 5 h for the microbioreactor and after 7 h for the Erlenmeyer flask, see Fig. 6.6; *E. coli*: $pO_2 = 0$ % air saturation after 4 h for the microbioreactor and after 5 h for the Erlenmeyer flask, see Fig. 6.7) has only a small influence on the bacterial growth. Using smaller sample volumes in the microbioreactor will even reduce the deviations in oxygen transfer further.

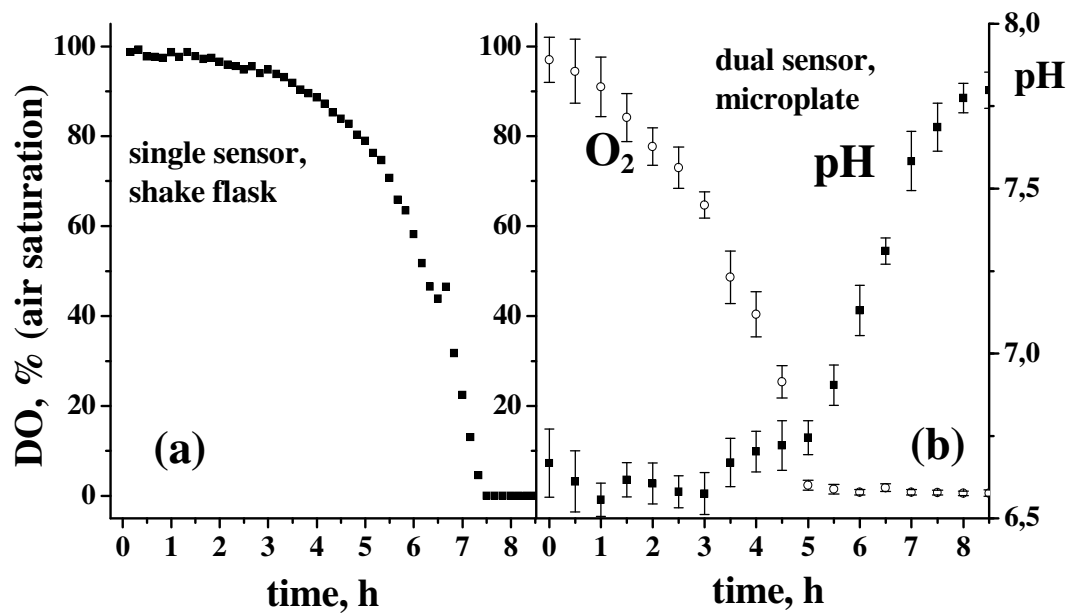


Figure 6.6 Fermentation of *P. putida* at 25 °C using standard S1 medium in a conventional bioreactor (shake flask) (a). Replicate fermentation of *P. Putida* in microbioreactors (n = 24) using medium S1 at 25 °C (b).

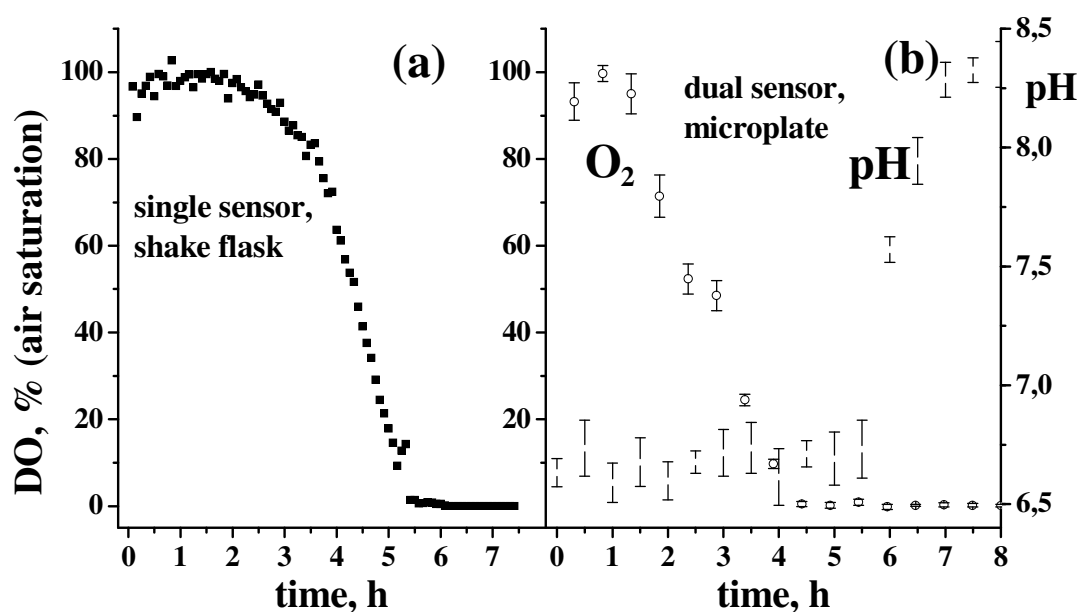


Figure 6.7 Fermentation of *E. coli* using medium S1 at 37 °C in conventional bioreactor (shake flask) (a); Replicate fermentation of *E. coli* in microbioreactors (n = 24) using medium S1 at 37 °C (b).

P. Putida and *E. coli* show reproducible behavior in all microbioreactors with respect to pH changes. The pH increases during cultivation, which indicates a consumption of acids and is a typical behavior for much fermentation. For *P. putida*, the pH increased from 6.67 to 7.8 (Fig. 6.6b), for *E. coli* it increased from 6.63 to 8.37 (Fig. 6.7b). With a control experiment using a standard pH meter a pH increase of the inoculum during fermentation from 6.58 to 7.7 and from 6.58 to 8.2 for *P. putida* and *E. coli* was obtained, respectively. This correlates very well with the data obtained by the dual sensor.

Similar dependences for DO and pH during fermentation of *E. coli* in a single microbioreactor were obtained by Kostov et al.¹.

6.4 Conclusion

In this work we described an optical sensing system for simultaneous and continuous measurements of the two key parameters pH and dissolved oxygen. The bioprocess was simultaneously realized in 24 microbioreactors using 1.5 ml working volume. The pH and DO kinetics during fermentation as well as the biomass after cultivation of two kinds of bacteria

(*P. putida* and *E. coli*) was found to be similar to that using a conventional 500 ml bioreactor (shake flask).

The new technique enables precise and reliable, non-invasive multi-parameter monitoring in 24 parallel experiments and can be used for high-throughput bioprocess optimization.

6.5 References

1. Kostov Y, Harms P, Randers-Eichhorn L, Rao G **Low-cost microbioreactor for high-throughput bioprocessing.** *Biotechnol. Bioeng.* **2001**, 72, 346-352
2. Lamping S R, Zhang H, Allen B, Shamlou P A **Design of a prototype miniature bioreactor for high throughput automated bioprocessing.** *Chem. Eng. Sci.* **2003**, 58, 747 – 758
3. Trummer E, Fauland K, Seidinger S, Schriebl K, Lattenmayer C, Kunert R, Vorauer-Uhl K, Weik R, Borth N, Katinger H, Müller D **Process parameter shifting: Part I. Effect of DO, pH, and temperature on the performance of Epo-Fc expressing CHO cells cultivated in controlled batch bioreactors.** *Biotechnol. Bioeng.* **2006**, 94, 1033-1044
4. Celik E, Calik P **Bioprocess parameters and oxygen transfer characteristics in β -lactamase production by *Bacillus* species.** *Biotechnol. Prog.* **2004**, 20, 491-499
5. Harms P, Kostov Y, Rao G **Bioprocess monitoring.** *Current opinion in Biotechnology*, **2002**, 13, 124-127
6. Maharbiz M M, Holtz W J, Howe R T, Keasling J D **Microbioreactor arrays with parametric control for high-throughput experimentation.** *Biotechnol. Bioeng.* **2004**, 85, 376-381
7. Arain S, John G T, Krause C, Gerlach J, Wolfbeis O S, Klimant I **Characterization of microtiterplates with integrated optical sensors for oxygen and pH, and their applications to enzyme activity screening, respirometry, and toxicological assays.** *Sens. Actuators* **2006**, B113(2), 639-648
8. Deshpande R R, Wittmann C, Heinzle E **Microplates with integrated oxygen sensing for medium optimization in animal cell culture.** *Cytotechnol.* **2004**, 46(1), 1-8
9. Arain S, Weiss S, Heinzle E, John G T, Krause C, Klimant I **Gas sensing in microplates with optodes: Influence of oxygen exchange between sample, air, and plate material.** *Biotechnol. Bioeng.* **2005**, 90(3), 271-280

10. Deshpande R R, Heinzle E **On-line oxygen uptake rate and culture viability measurement of animal cell culture using microplates with integrated oxygen sensors.** *Biotechnol. Lett.* **2004**, 26(9), 763-767
11. John G T, Klimant I, Wittmann C, Heinzle E **Integrated optical sensing of dissolved oxygen in microtiter plates: a novel tool for microbial cultivation.** *Biotechnol. Bioeng.* **2003**, 81, 829-833
12. John G T, Goelling D, Klimant I, Schneider H, Heinzle E **pH - Sensing 96-well microtitre plates for the characterization of acid production by dairy starter cultures.** *J. Dairy Research* **2003**, 70(3), 327-333
13. Ferguson J A, Healey B G, Bronk K S, Barnard S M, Walt D R **Simultaneous monitoring of pH, CO₂ and O₂ using an optical imaging fiber.** *Anal. Chim. Acta* **1997**, 340, 123-131
14. Zanzotto A, Szita N, Boccazzi P, Lessard P, Sinskey A J, Jensen K F **Membrane-aerated microbioreactor for high-throughput bioprocessing.** *Biotechnol. Bioeng.* **2004**, 87, 243-254
15. Zhang Z, Szita N, Boccazzi P, Sinskey A J, Jensen K F **A Well-mixed, polymer-based microbioreactor with integrated optical measurements.** *Biosens. Bioelectron.* **2006**, 93, 286-296
16. Harms P, Kostov Y, French J A, Soliman M, Anjanappa M, Ram A, Rao G **Design and performance of a 24-station high throughput microbioreactor.** *Biotechnol. Bioeng.* **2006**, 93, 6-13
17. Borisov S M, Vasylevska G S, Krause C, Wolfbeis O S **Composite luminescent material for dual sensing of oxygen and temperature.** *Adv. Funct. Mater.* **2006**, 16, 1536-1542
18. Borisov S M, Wolfbeis O S **Temperature-sensitive europium(III) probes and their use for simultaneous luminescent sensing of temperature and oxygen.** *Anal. Chem.* **2006**, 78(14), 5094-5101
19. Borisov S M, Krause C, Arain S, Wolfbeis O S **Composite materials for simultaneous and contactless luminescent sensing and imaging of oxygen and carbon dioxide.** *Adv. Mater.* **2006**, 18(12), 1511-1516
20. Borisov S M, Neurauder G, Klimant I, Wolfbeis O S **A modified dual lifetime referencing method for simultaneous optical determination and sensing of two analytes.** *Appl. Spectrosc.* **2006**, 60, 1167-1173

21. Vasylevska A S, Borisov S M, Krause C, Wolfbeis O S **Indicator-loaded and permeation-selective microparticles for use in fiber optic simultaneous sensing of pH and dissolved oxygen.** Chem. Mater. **2006**, 18(19), 4609-4616
22. Liebsch G, Klimant I, Wolfbeis O S **Luminescence lifetime temperature sensing based on sol-gels and poly(acrylonitrile)s dyed with ruthenium metal-ligand complexes.** Adv. Mater. **1999**, 11, 1296-1299
23. Coyle L M, Gouterman M **Correcting lifetime measurements for temperature.** Sens. Actuators B **1999**, 61, 92-99
24. Schanze K S, Carroll B F, Korotkevitch S, Morris M J **Temperature dependence of pressure sensitive paints.** Am. Inst. Aeron. Astron. J. **1997**, 35(2), 306-310
25. Liebsch G, Klimant I, Krause C, Wolfbeis O S **Fluorescent imaging of pH with optical sensors using time domain dual lifetime referencing.** Anal. Chem. **2001**, 73, 4354-4363
26. Kensy F, John G T, Hofmann B, Buechs J **Characterisation of operation conditions and online monitoring of physiological culture parameters in shaken 24-well microtiter plates.** Bioprocess Biosyst. Eng. **2005**, 28, 75-81
27. Kensy F, Zimmermann H F, Knabben I, Anderlei T, Trauthwein H, Dingerdissen U, Buechs J **Oxygen transfer phenomena in 48-Well microtiter plates: determination by optical monitoring of sulfite oxidation and verification by real-time measurement during microbial growth.** Biotechnol. Bioeng. **2005**, 89, 698-708
28. John G T, Klimant I, Wittmann C, Heinzle E **Integrated optical sensing of dissolved oxygen in microtiter plates: a novel tool for microbial cultivation.** Biotechnol. Bioeng. **2003**, 81, 829-836
29. Wittmann C, Kim H M, John G, Heinzle E **Characterization and application of an optical sensor for quantification of dissolved oxygen in shake-flasks.** Biotechnol. Lett. **2003**, 25, 377-380

Chapter 7

Summary

This thesis describes the development and characterization of novel, pH-sensitive, optical sensor materials. Special attention is given to the development of dual optical chemical sensors for non-invasive determination of pH and dissolved oxygen (DO) in biological systems. A new measurement scheme is introduced to evaluate and calculate the data for these two parameters via dual luminophore referencing (DLR). An application example for simultaneous monitoring of pH and DO in bioprocessing is given and discussed.

Chapter 1 gives an introduction to the importance of optical pH and DO sensors. Furthermore, the overview of existing planar dual sensor materials and dual microsensors was presented. Referencing methods for measurement with luminescent optical sensors were described.

Chapter 2 describes the application and spectral properties of a new type of fluorescent pH indicators with different dynamic pH ranges. The indicators used (ACIB, ACIDA and ACISA) are based on the luminescent dye iminocoumarin and were covalently immobilized on the surface of amino-modified polymer microbeads and incorporated into a hydrogel matrix to obtain novel pH-sensitive materials. Due to self-referencing of the ACISA-based microbeads, the ACISA-containing sensor membrane can be read out via ratiometric dual wavelength referencing. A membrane capable of optical pH sensing over a very wide pH range (pH 1 – pH 11) by using a mixture of two different microbeads was also developed.

In Chapter 3, pH-sensitive sensor membranes for the DLR scheme, based on carboxyfluorescein, dichlorocarboxyfluorescein and iminocoumarin are presented. The membranes are characterized with respect to their cross-sensitivity towards ionic strength at 25 and 140 mM. The sensor membrane based on iminocoumarin is found to possess no cross-sensitivity towards ionic strength at all, while for the other two a small effect is observed, which, however, was small compared to other pH indicators like HPTS. All three membranes showed an excellent photostability. The indicators immobilized on the microbeads are suitable for DLR measurements using polyacrylonitrile-derived nanoparticles incorporating Ru(dpp)_3^{2+} as reference standard. It was found that the variety of pH indicators in the DLR scheme results in pH sensors with pK_a values from 4 to 8.

In Chapter 4, a novel modified dual lifetime referencing method (m-DLR) for simultaneous sensing of pH and pO_2 with a single fiber-optic sensor is introduced. Three different dual sensor materials were investigated. The dual sensor membrane consisted of fluorescent indicators immobilized in different kinds of organic polymer microbeads, which in turn were contained in a single polyurethane-type hydrogel matrix. The phase-modulated light of an LED excites the luminescence of the indicators, and average decay times or phase shifts served as the analytical information. Data were evaluated by the m-DLR method which relates the phase shift (as measured at two different frequencies) to pH and to oxygen partial pressure. The working range of the dual sensor (pH 4 - pH 9 and 0 – 21.3 kPa pO_2) meets the requirements for application in biological systems.

A fiber-optic microsensor for minimal-invasive measurements is presented in Chapter 5. The tip of the optical fiber with a diameter of $\sim 140\ \mu\text{m}$ was covered with a sensor composition based on luminescent microbeads (HPTS/p-HEMA microbeads as pH-sensing system and Ru(dpp)_3^{2+} /ormosil microbeads as oxygen probe) dispersed in a hydrogel polymer matrix. Measurements and evaluation were performed according to the method introduced in chapter 4. The optimal working range of the sensor was from pH 5 to pH 10 and for pO_2 0 – 21.3 kPa. The sensor was characterized with respect to its photostability, reproducibility and reversibility.

Chapter 6 describes a new approach towards simultaneous, non-invasive and continuous measurements of pH and DO in 24-well microbioreactors. The performance of the system was demonstrated by monitoring pH and DO kinetics during cultivation of *Pseudomonas putida* and *Escherichia coli*. The results obtained in microbioreactors were compared with a conventional shake flask. The technique can be used for high-throughput bioprocess optimization.

Chapter 8

Zusammenfassung

In der vorliegenden Arbeit wurden die Entwicklung und Charakterisierung neuer, pH-sensitiver optischer Sensoren beschrieben. Der Schwerpunkt lag hierbei auf der Entwicklung von Dualsensoren für die nicht-invasive Messung von pH und Gelöstsauerstoff in biologischen Systemen. Ein neues Messschema zur Evaluierung und Kalkulation des pH-Werts und des Sauerstoffpartialdrucks aus den entsprechenden Daten mit Hilfe der Dual Lifetime Referencing (DLR)-Methode wurde vorgestellt. Ein Anwendungsbeispiel für das gleichzeitige Monitoring von Sauerstoff und pH in Bioprozessen wurde gezeigt und diskutiert.

Kapitel 1 gibt eine Einführung in die Bedeutung von optischen pH- und Sauerstoffsensoren. Ausserdem wurde eine Übersicht der existierenden Materialien für planare und Mikro-Dualsensoren präsentiert. Abschließend wurden Referenzierungsmethoden für die Messung mit optischen Lumineszenzsensoren beschrieben.

Kapitel 2 beinhaltet die Anwendung und die spektrellen Eigenschaften eines neuen Typs von fluoreszierenden pH-Indikatoren für verschiedene dynamische pH-Bereiche. Die Indikatoren (ACIB, ACIDA und ACISA) basieren auf dem Lumineszenzfarbstoff Iminocoumarin, das kovalent an die Oberfläche von amino-modifizierten Polymer-Mikropartikeln immobilisiert wurde. Der neuen, pH-sensitiven Sensormembrane erhielt man durch Einrühren dieser Mikropartikel in eine Hydrogel-Matrix. Aufgrund der Möglichkeit zur Selbstreferenzierung kann die ACISA-haltige Sensormembran mittels ratiometrischer Zweiwellenlängen-Referenzierung ausgelesen werden. Eine Membran für die Messung über einen extrem weiten pH-Bereich (pH 1 bis 11) erhält man durch Mischen zweier verschiedener Mikropartikel.

In Kapitel 3 wurden pH-sensitive Sensormembrane, die mit dem DLR-Schema ausgelesen werden können, vorgestellt. Diese Sensormembrane basieren auf den pH-Indikatoren Carboxyfluorescein, Dichlorcarboxyfluorescein und Iminocoumarin. Die Sensormembrane wurde auf ihre Querempfindlichkeit gegenüber Ionenstärke bei 25 mM und 140 mM untersucht. Während die Fluorescein-basierten Membrane eine, wenn auch im Vergleich zu anderen Indikatoren wie HPTS kleine, Querempfindlichkeit aufwiesen, ist die auf Iminocoumarin basierende Membran unabhängig von der Ionenstärke. Alle drei

Sensormembranen zeigen eine ausgezeichnete Photostabilität. Die in Mikropartikel immobilisierten Indikatoren waren für DLR-Messungen geeignet. Hierbei wurde $\text{Ru}(\text{dpp})_3^{2+}$, das in polyacryl-basierte Nanopartikel eingebettet wurde, als Referenzpartikel verwendet. Bei Variation des pH-Indikators entstehen so pH-Sensoren für das DLR-Schema mit pK_S -Werten von 4 bis 8.

In Kapitel 4 wurde eine neue, modifizierte Dual Lifetime Referencing (m-DLR)-Methode für die gleichzeitige Bestimmung von pH und pO_2 mit einem einzigen, faseroptischen Sensor vorgestellt. 3 verschiedene Dualsensor-Materialien wurden untersucht. Die Membran für die Dualsensoren besteht aus den Fluoreszenzindikatoren, die in verschiedenen organischen Polymerpartikeln immobilisiert sind, welche wiederum in einer Polyurethan-Hydrogelmatrix eingebettet sind. Das phasenmodulierte Anregungslicht einer LED regt die Lumineszenz der Indikatoren an, deren mittlere Abklingzeit oder Phasenverschiebung als analytische Information dienen. Die Daten wurden mit Hilfe der m-DLR-Methode evaluiert, die die bei zwei verschiedenen Frequenzen gemessenen Phasenverschiebungen in Beziehung zum pH-Wert bzw. Sauerstoffgehalt setzt. Der Messbereich der Dualsensoren ($\text{pH } 4 - 9$, $0 - 21,3 \text{ kPa } \text{pO}_2$) entspricht den Anforderungen für Anwendungen in biologischen Systemen.

Ein faseroptischer Mikrosensor für minimal invasive Messungen wird in Kapitel 5 vorgestellt. Die Spitze der optischen Faser, deren Durchmesser ca. $140 \mu\text{m}$ beträgt, wurde mit einem Sensorcocktail beschichtet, der aus lumineszierenden Mikropartikeln (HPTS/p-HEMA-Mikropartikel als pH-Sensor, $\text{Ru}(\text{dpp})_3^{2+}$ / Ormosil-Mikropartikel als Sauerstoffsensor) in einer Hydrogelmatrix besteht. Messung und Auswertung wurden wie in Kapitel 4 beschrieben durchgeführt. Der optimale Messbereich dieses Sensors ist $\text{pH } 5 - 10$ und $0 - 21,3 \text{ kPa}$ für Sauerstoff. Der Sensor wurde mit Hinblick auf Photostabilität, Reproduzierbarkeit der Signale und Reversibilität charakterisiert.

Kapitel 6 beschreibt eine neue Methode für gleichzeitige, nicht-invasive und kontinuierliche pH- und Sauerstoffmessung in 24-Well-Mikrobioreaktoren. Die Anwendbarkeit dieses Systems wurde anhand der pH- und Sauerstoffkinetiken während der Kultivierung von *Pseudomonas putida* und *Escherichia coli* demonstriert. Die Ergebnisse aus diesen Versuchen in den Mikrobioreaktoren wurden mit denen herkömmlicher Bioreaktoren (Schüttelkolben) verglichen. Die vorgeschlagene Technik kann für Bioprozess-Optimierungen mit hohem Durchsatz verwendet werden.

Chapter 9

Abbreviations, Acronyms and Symbols

λ_{abs}	Wavelength of the absorption maximum
λ_{em}	Wavelength of the emission maximum
QY	Quantum yields
ϵ	Molar absorption coefficient
τ	Luminescence lifetime or decay time
IS	Ionic strength
nm	Nanometer
Φ	Phase shift or phase angle of the modulated light
f_{mod}	Modulation frequency
I	Luminescence intensity
K_{sv}	Stern-Volmer constant
LED	Light emitting diode
pK_{a}	Negative decadic logarithm of an acidic dissociation constant
pO_2	Oxygen partial pressure
DO	Dissolved oxygen
pH	Negative decadic logarithm of a proton concentration
t_{95}	Response time (time required for a 95 % signal change)
CF	5(6)-carboxyfluorescein
DCCF	5(6)-dichlorocarboxyfluorescein
ImC	Iminocoumarin
ACIB	4-(9-diethylamino-5H-7-oxa-4b,6,13-triaza-indeno [2,1-a] anthracen-5-yl)-2-methoxy-6-nitro-phenol
ACIDA	4-(9-diethylamino-5H-7-oxa-4b,6,13-triaza-indeno [2,1-a] anthracen-5-yl)-benzene-1,3-diol
ACISA	5-(9-diethylamino-5H-7-oxa-4b,6,13-triaza-indeno [2,1-a] anthracen-5-yl)-benzene-1,3-diol
HPTS	8-hydroxypyrene-1,3,6-trisulfonate trisodium salt
D 4	polyurethane hydrogel

p-HEMA	Amino-modified poly(hydroxyethyl methacrylate)
AMC	Aminocellulose
AA-Q-N2	Modified poly(acrylamide)
P	Gas permeability
PAN	Poly(acrylonitrile)
PSAN	poly(styrene-co-acrylonitrile)
PtBuS	Poly(tretbutylstyrole)
ormosil	organically-modified sol-gel beads
EDC	N-(3-dimethylaminopropyl)-N'-ethylcarbodiimide hydrochloride
DCC	Dicyclohexylcarbodiimide
NHS	N-hydroxysuccinimide
Ru(dpp) ₃ ²⁺	tris-4,7-diphenyl-1,10-phenanthroline
PdTFPP	(5,10,15,20-tetrakis-(2,3,4,5,6-pentafluorophenyl)-21,23H-porphyrin-Pd-(II))
TMS	3-(trimethylsilyl)-1-propanesulfonate
DLR	(frequency domain) Dual lifetime referencing
m-DLR	Modified dual lifetime referencing
MS	Mass spectroscopy
NMR	Magnetic nuclear resonance
P. putida	Pseudomonas putida
E. coli	Escherichia coli

Chapter 10

Curriculum Vitae

Surname Kocincova (nee Vasylevska)

First Name Anna S.

Date of birth 02. January 1981

Place of birth Odessa (Ukraine)

Nationality Ukrainian

Education

09/1987 – 06/1992 Primary School, Odessa/Ukraine

09/1992 – 07/1997 Secondary School, Odessa/Ukraine

07/1997 Degree: Abitur

Studies

09/1997 – 06/2003 Chemistry at the National University of Odessa

06/2001 Bachelor Diploma

10/2002 – 06/2003 Master Work at the Institute of Analytical Chemistry at the National University of Odessa

Title: *“Sorption of Vanadium (V) and Radium (VII) with cation exchanger KU-2-8 and modified KU-2-8 by asparaginic acid.”*

06/2003 Degree: Master Diploma of Chemistry

02/2004 – 05/2007 PhD Work at the Institute of Analytical Chemistry, Chemo- and Biosensors (Prof. Wolfbeis) at the University of Regensburg

Title: *“New pH sensitive sensor materials. Luminescent fiber-optic dual sensors for non-invasive and simultaneous measurement of pH and pO₂ (dissolved oxygen) in biological systems.”*

Extracurricular Activities

07/2003 – 02/2004 Research staff at Institute of Analytical Chemistry at the National University of Odessa

02/2006 – 05/2007

Freelance work for Presens Precision GmbH

Chapter 11

List of Publications

Diploma Thesis

“Sorption of Vanadium (V) and Rhenium (VII) with cation exchanger KU-2-8 and KU-2-8 modified by asparaginic acid.” Institute of Analytical Chemistry, National University of Odessa (Ukraine)

Publications

1. Vasylevska G S, Borisov S M, Krause C, Wolfbeis O S **Indicator-loaded permeation-selective microbeads for use in fiber optic simultaneous sensing of pH and dissolved oxygen.** Chem. Mater. **2006**, 18(19), 4609-4616
2. Borisov S M, Vasylevska A S, Krause C, Wolfbeis O S **Composite luminescent material for dual sensing of oxygen and temperature.** Adv. Funct. Mater. **2006**, 16(12), 1536-1542
3. Vasylevska A S, Karasyov A A, Borisov S M, Krause C **Novel coumarin-based fluorescent pH indicators, probes and membranes covering a broad pH range.** Anal. Bioanal. Chem. **2007**, 387(6), 2131-2141
4. Borisov S M, Mayr T, Karasyov A A, Klimant I, Chojnacki P, Moser C, Nagl S, Schaeferling M, Stich M I, Vasylevska G S, Wolfbeis O S **New plastic microparticles and nanoparticles for fluorescent sensing and encoding.** Springer Series in Fluorescence **2006**, N. Berberan-Santos, ed.; in press
5. Vasylevska A, Arain S **Nicht-invasive Online-Sauerstoffmessung. Bakterien-Toxizitätstests für die pharmakologische Wirkstoffforschung.** GIT Labor-Fachzeitschrift **2006**, 11, 1012-1013

6. Vasylevska A S, Borisov S M, Krause C, Wolfbeis O S **Optical microsensors for simultaneous measurement of two analytes.** Anal. Chem. 2007, submitted
7. Vasylevska A S, Arain S, Krause C, Borisov S M, Arnold M, Wolfbeis O S **Simultaneous non-invasive monitoring of dissolved oxygen and pH during bacterial growth in 24-well microplates.** Biotechnol. Bioeng. 2007, submitted
8. Vasylevska A **Nichtinvasive und einfache Bestimmung des Sauerstoffverbrauchs bei Bakterien-Toxizitätstests.** Zeitschrift Labor & More 2007, accepted

Poster Presentations

1. Borisov S M, Vasylevska G S, Wolfbeis O S **Langzeitstabile und sterile fluoreszenz-optische Hybridsensoren zur räumlichen und zeitlich hochauflösenden in situ.** Bioprozess-Analyse, Biophotonica symposium, Jena, Germany **2005**
2. Vasylevska G S, Karasyov A, Krause C, Wolfbeis O S **Fluorescent two-step pH indicator involving both PET quenching and a protolytic equilibrium.** 9th Conference on Methods and Applications of Fluorescence (MAF), Lissabon, Portugal **2005**
3. Borisov S M, Vasylevska G, Krause C, Wolfbeis O S **Novel Materials for Simultaneous and Contactless Sensing and Imaging of two Analytes (pO₂/temperature, pO₂/pH and pO₂/pCO₂).** Europt(r)ode VIII, Tübingen, Germany **2006**
4. Vasylevska G, Karasyov A, Wolfbeis O S **Microparticles with Integrated Fluorescent Probes for Use in Optical Sensors for Simultaneous Measurements of pH and Oxygen.** Europt(r)ode VIII, Tübingen, Germany **2006**

5. Vasylevska G S, Borisov S M, Wolfbeis O S **Langzeitstabile und sterile fluoreszenz-optische Hybridsensoren zur räumlichen und zeitlich hochauflösenden in-situ Bioprozess-Analyse: Indikatorfarbstoffe für optische chemische Hybridsensoren.** 2nd Bioprozess-Analyse, Biophotonica symposium, München, Germany **2006**

6. Arain S, Krause C, Vasylevska A **Monitoring of pH and oxygen in 24 Well plates.** European BioPerspectives, Köln, Germany **2007**, abstract accept